5. Sam M. Austin, R. Madey, J.W. Watson, B.D. Anderson, A. Baldwin, B.S. Flanders, C. Lebo and C.C. Foster, Bull. Am. Phys. Soc. 27,731(1982).
6. L. Zamick and N. Auerbach, Phys. Rev. C26,2185(1982).

III.B.2.a. STUDIES OF EXOTIC NUCLEI WITH THE RPMS

W. Benenson, L.H. Harwood, E. Kashy, D. Mikolas, J.A. Nolen Jr.,
J. Stevenson, and B.A. Brown

Measurements of the properties of exotic nuclei test the ability of nuclear models to extrapolate to nuclei under extreme conditions of neutron or proton excess. Nuclear lifetime and mass measurements allow the matrix elements for beta decay to be determined. Furthermore studies of the masses and lifetimes of neutron rich isotopes can discover new regions of nuclear deformation[1].

1. Beta Lifetime Measurements

The Reaction Product Mass Separator (RPMS) is designed to separate heavy ion reaction products with energies in the range E/A=10-100 MeV. By eliminating interfering m/q species and concentrating the isotopes under investigation into small detectors, the RPMS provides a clean environment for decay studies.

Using a 30 MeV/A ^{18}O beam we made the first measurements[2] of the lifetimes of ^{14}Be and ^{17}C along with those previously determined of ^{9}Li,^{11}Li,^{12}Be,^{12}B,and ^{15}B during a single 48 hour run. Beta lifetimes were obtained by measuring the time interval between detection of a heavy ion and its subsequent beta decay. The focal plane detector consisted of a two-dimensional position sensitive proportional counter followed by a silicon ΔE-E telescope. Lifetime measurements were performed by turning the beam off whenever an ion with $Z \geq 3$ was detected in the telescope. The beam was left off for a preset time equal to several halflives of the longest lived isotope being collected. Isotope identification was accomplished by plotting (Fig. 1) the deflection in the RPMS (proportional to m/q) vs the silicon telescope particle identification function. The decay curves shown in Fig. 2 are the best fits to an exponential plus a constant background.

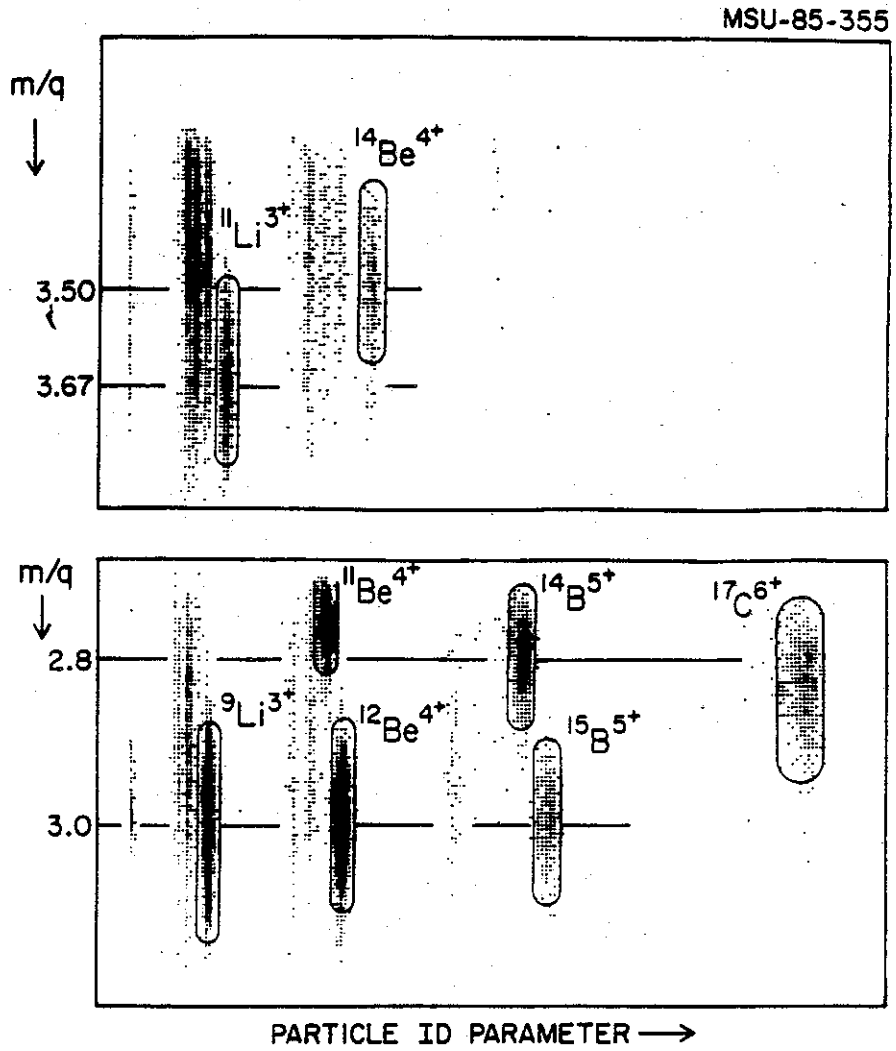

Fig. 1 Plot of m/q determined from deflection in the RPMS vs. silicon detector particle identification parameter.

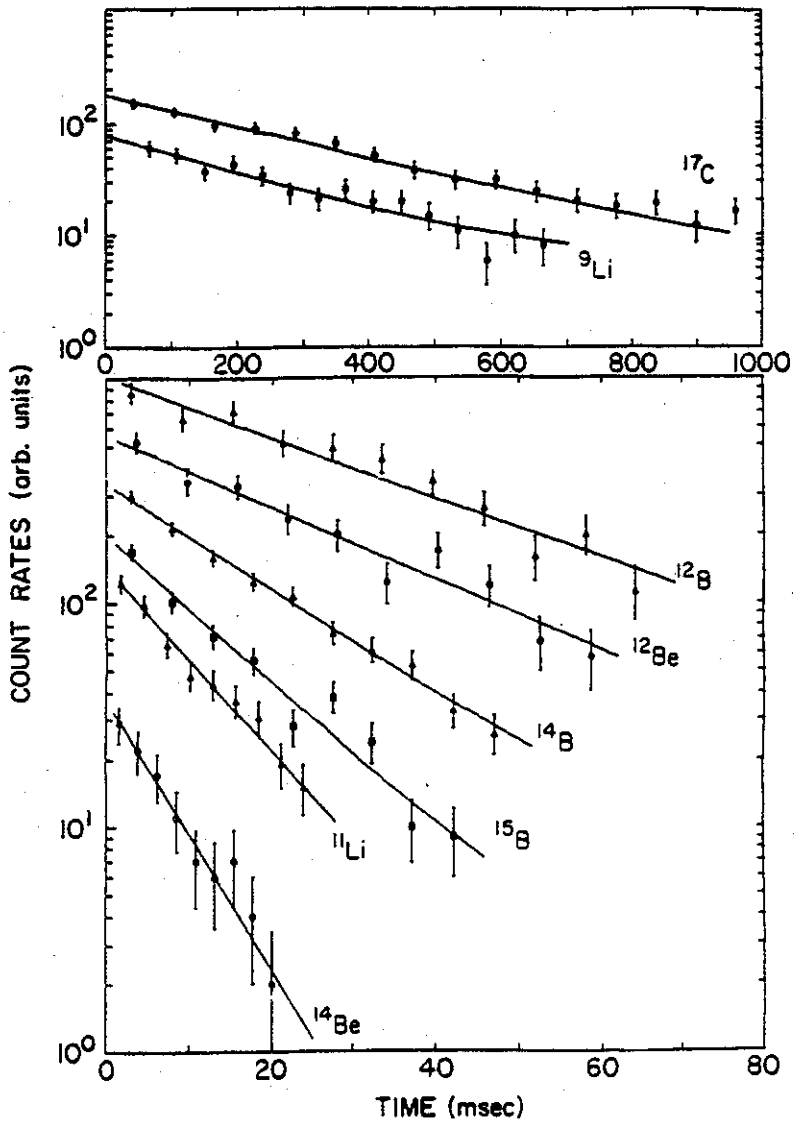

Fig. 2 Beta lifetime plots. The curves are best fits to an exponential plus constant background form.

The results of this experiment are compared with previous measurements[3-7] in table 1. There are two discrepancies larger than one standard deviation namely ^{14}B and ^{15}Be. There has been only one previous measurement of each lifetime and there is no obvious reason for the discrepancies.

For the nuclei studied in this experiment the dominant decay mode is Gamow-Teller beta decay. Partial Gamow-Teller beta decay halflives calculated in a spherical shell model formalism[8] are shown in Table 1. The calculated lifetimes are shorter than the measured lifetimes with one exception(^{17}C).

Table I Beta-decay half-lives for the neutron-rich isotopes measured in this experiment are compared with previous measurements when they exist. Theoretical predications for Gamow-Teller beta decay are also provided for comparison. The three theoretical half-lives for ^{17}C correspond to the assumption of ($1/2^+$, $3/2^+$, $5/2^+$) ground-state J^π values for ^{17}C in the calculation.

Isotope	This Measurement	Previous Measurement	Prediction[f]
^{9}Li	173±14 ms	175±1 ms[a]	76 ms
^{11}Li	7.7±0.6 ms	8.5±0.2 ms[a]	2.3 ms
^{12}Be	21.3±2.2 ms	24.4±3.0 ms[b]	8.8 ms
^{14}Be	4.2±0.7 ms	---	3.7 ms
^{12}B	20.0±1.5 ms	20.41±.06 ms[c]	13.6 ms
^{14}B	12.8±0.8 ms	16.1±1.2 ms[d]	11.1 ms
^{15}B	8.8±0.6 ms	11.0±1.0 ms[e]	6.2 ms
^{17}C	202±17 ms	---	(414,292,238)ms

a) Reference 13
b) Reference 14
c) Reference 15
d) Reference 16
e) Reference 17
f) Reference 8

With the ECR+K500 combination, high intensity beams of 40 MeV/A ions up to ^{40}Ar will be used to make a wide variety of extremely neutron rich nuclei whose lifetimes (and most other properties) are unknown. Using 30 MeV/A ^{18}O beams all neutron rich particle stable isotopes which were accessible by fragmentation (N≤10,Z≤8) had sufficient yield to measure lifetimes. In addition one isotope which required neutron pick up(^{17}C)was also measured. The principal limitation of these measurements is the present lack of high intensity beams of heavy nuclei.

This work will require the development of special beams of neutron rich isotopes as has been done with ^{18}O and ^{22}Ne. For example ^{26}Mg, ^{30}Si, and ^{48}Ca or ^{50}Ti beams will be important. High intensity(20 pna) beams of E/A=50 MeV ^{26}Mg from the K500 + ECR will make lifetime measurements possible for ^{17}B, ^{19}B, ^{18}C, ^{19}C, ^{20}C, ^{19}N, ^{20}N, and^{21}N for the first time. Similar beams of ^{48}Ca or ^{50}Ti will make ≈30 new lifetime measurements possible. Many of these lifetimes will be in the few ms range and provide a considerable challenge to shell model calculations.

2. Neutron and Proton Driplines

Projectile fragmentation has proven to be a very powerful means to study nuclei at the very limits of particle stability. Recent work at GANIL by Guillemaud-Mueller et.al.[8] using fragmentation of 44 MeV/A ^{40}Ar, 77 MeV/A ^{40}Ca and 35 MeV/A ^{86}Kr has resulted in the discovery of 27 new neutron rich isotopes. The limit of particle stability is however still not known for nuclei with Z≥5. The RPMS is ideally suited for this search. It seems probable that the limits of stability of nuclei with Z≤10 can be determined unambiguously by fragmentation of high intensity neutron rich beams, such as E/A=40 MeV ^{48}Ca or ^{50}Ti which will be available from the K500 + ECR combination.

3. Beta Delayed and Ground State Charged Particle Emission

We have recently measured the beta branching ratios of ^{9}C to levels in ^{9}B. This was accomplished by using the RPMS to separate ^{9}C projectile fragments and implant them in a silicon detector telescope. When a ^{9}C was

identified, the cyclotron was switched off (within 50 μs), and the ^{9}C decay was folllowed. Virtually all the energy deposited in the silicon detector was due to the subsequent decay of $^{9}B \rightarrow {}^{4}He + {}^{4}He + p$. Thus the energy deposited in the silicon detector by the entire decay appeared as lines corresponding to the excited states in ^{9}B populated by the ^{9}C decay. This is shown in figure 3. Note that even the branch to the ground state at 300 keV can be observed.

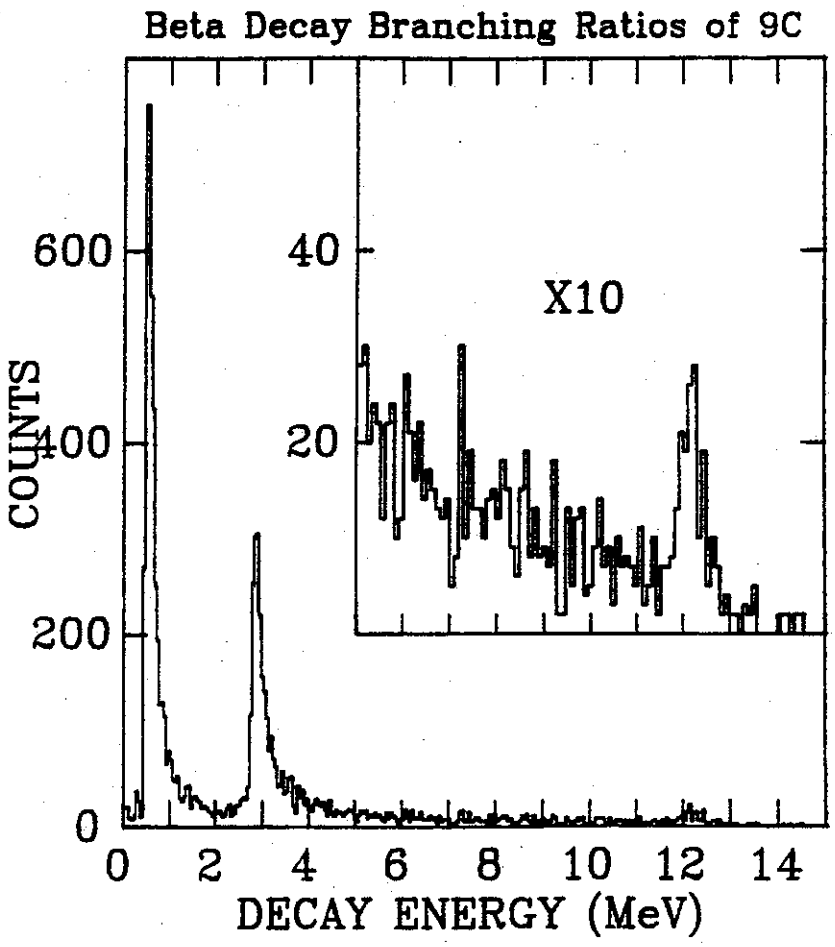

Fig. 3 Histogram of decay energies of ^{9}C implanted in a silicon detector. The decay to the ground state and at leasst three excited states of ^{9}B is observed. Note the broad state of atout 3 MeV underneath the narrow state at 2.7 MeV.

Fragmentation of E/A=40 MeV ^{40}Ca would allow observation of the known beta delayed proton emitters ^{27}P, ^{31}Cl, ^{36}Ca, and the beta delayed two proton emitters ^{22}Al and ^{26}P. Other proton emitters, at present unknown, could also be searched for by this technique. In addition we would be possible to study candidates for ground state two proton emitters such as ^{19}Mg or ^{31}Ar. The predicted halflives of these isotopes are less than 10 ms making recoil mass separators such as the RPMS far superior to gas transport techniques.

4. Fusion-evaporation processes.

Further possibilities for future experiments include investigations into alternative isotope production mechanisms, and more diverse decay properties. The fusion - evaporation residues from heavy beams on light targets may enhance the yield of proton rich nuclei, with respect to fragmentation yields. The reverse kinematics will ensure that the residues are still focused near 0°. For the low energy beams needed for fusion a further enhancement will come from the large increase in beam intensity expected from the K500 + ECR system.

New decay properties can be measured for nuclei whose half-life has already been determined. Masses of many nuclei might be measured from their beta end-point energy. Isomeric states in heavy nuclei far from stability with lifetimes greater than 200 nS (typical flight time through the RPMS) can be identified by their fast emision of gamma rays after stopping in a silicon detector. Sensitivity will be great since a sizeable fraction of the fragmentation products should be in bound excited states. Long lived isotopes can be implanted in a counter and removed for low background counting. When the spin-spectrometer (see Section C3(d)) is completed, beta-gamma and gamma-gamma coincidence experiments will be easily carried out using the 14 BGO detectors as the beta detectors. Angular correlations will be a biproduct of this experiment. An approved experiment (85042) proposes to measure the beta decay branching ratio's of ^{17}C. The delayed neutron activity will be identified by the ^{16}N activity following a ^{17}C

decay. Clean isotopic separation in 200 ns makes the RPMS an ideal device for all of these experiments.

References:

1. C. Thibault, R. Klapisch, C. Rigaud.A.M. Poskanser, R. Prieels, L. Lessard, and W. Reisdorf. Phys. Rev. C12 644 (1975).
2. M. Curtin, L.H. Harwood, J.A. Nolen, Jr., B. Sherrill, and Z.Q. Xie Submitted to Phys. Rev. Letters(1985).
3. E. Roeckl, P.F. Dittner, C. Detraz, R. Klapisch, C. Thibault, and C. Rigaud, Phys. Rev. C10, 1181(1974).
4. D.E. Alberger, and D.R. Goosman, Phys. Rev. C10, 912(1974).
5. F. Ajzenberg-Selove, Nucl. Phys. A248, 1(1975).
6. D.E. Alburger, et.al., Phys Rev. C17, 1525(1978).
7. J.P. Dufour et. al. Preprint CENBG 8430.
8. D. Guillemaud-Mueller, A.C. Mueller, D. Guerreau, F. Pougheon, R. Anne, M. Bernas, J. Galin ,J. C. Jacmart, M. Langevin, E. Quiniou,and C. Detraz GANIL Preprint P8508.

III.B.2.b. HIGHLY EXCITED PROTON AND NEUTRON PARTICLE STATES

J.E. Duffy, G.M. Crawley, H. van der Plicht, R.S. Tickle[a], S. Gales[b], E. Gerlic[b], C.P. Massolo[c], J.E. Finck[d].

The information obtained from the extensive[1] measurements of deep-lying hole states in nuclei is useful both for comparison with theoretical calculations and because the empirical values of position and width of particular hole states can be used as input for predictions of other nuclear phenomena such as giant resonances. However, until recently there has been little or no comparable information on highly excited particle states in medium and heavy nuclei. Measurements of the particle strength provide valuable information which is complementary to the hole strength already determined. Theoretical models have already been developed to explain the spreading of single particle strength by the mixing with both low-lying and high-lying phonon states[2-4]. While it is possible to obtain information on hole states from knockout reactions like (p,2p), there are no analogous reactions to populate particle states. Such states must be studied by transfer reactions of the kind discussed here. Understanding the potential of these reactions to provide information on high-lying particle states is therefore an additional important motivation of this work.

Some studies of particle states have recently been carried out at Orsay.[5,6] The present work is an extension to deformed nuclei. Since the spreading of the states is predicted to depend on the phonon structure, studies of deformed nuclei, to which the phonon structure is quite different from that in spherical nuclei, provide a useful test of the theory. We elected to use the even-even samarium isotopes as targets because they range from spherical to very deformed. The measurments were carried out with a 100 MeV α - beam from the K500 cyclotron, and both proton and neutron states were measured using the (α,t) and $(\alpha,{}^3He)$ reactions. The outgoing tritons and ^3He were detected cleanly in the focal plane of the S320 spectrograph.

differences in the $(\alpha,{}^3He)$ spectra as the targets increase in deformation. In these spectra we see the usual low-lying states and, at higher excitation, above 3 MeV one observes additional bound state peaks both in the (α,t) and $(\alpha,{}^3He)$ spectra. In the 8-16 MeV region of excitation energy, in the (α,t) spectra, we observe the development of a broad bump with increasing deformation. We do not observe this phenomenon in the $(\alpha,{}^3He)$ spectra.

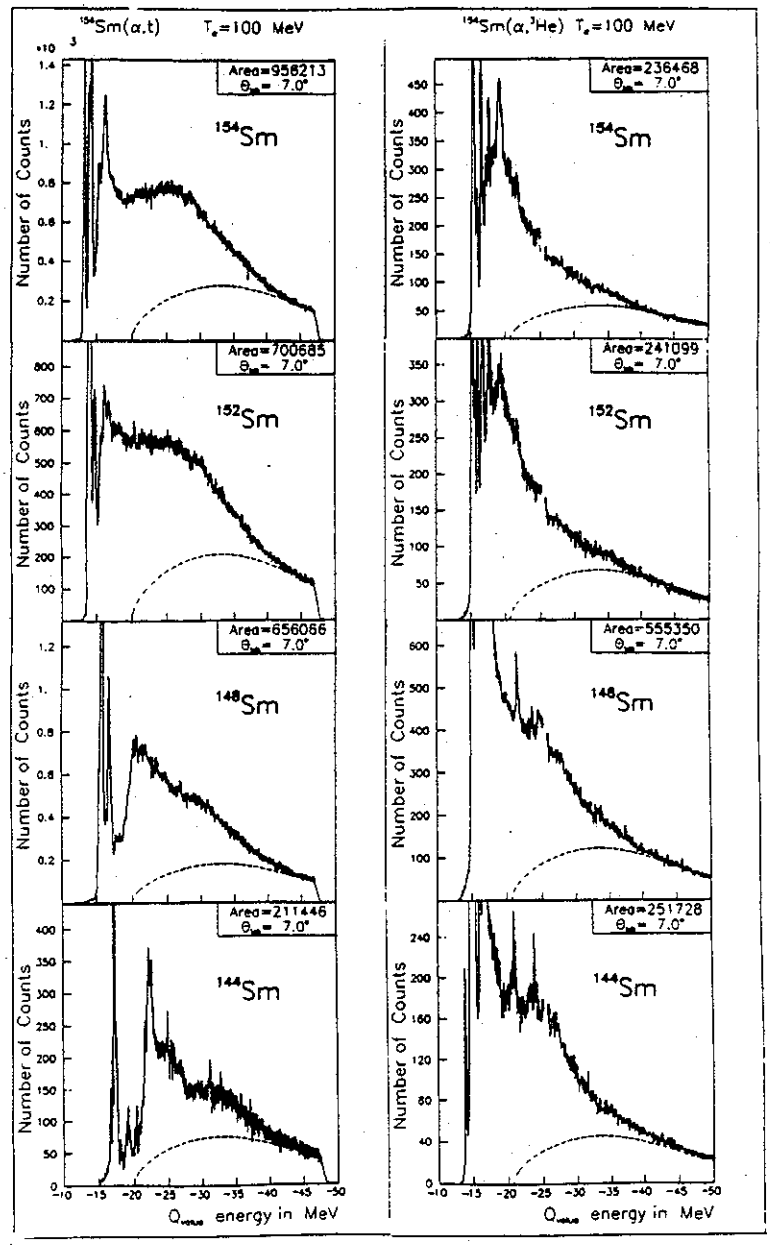

Figure 1.

Not all of the cross section at high excitation energy comes from single nucleon transfer. Some of the cross section comes from elastic break up. An elastic α break up calculation[7] is shown for the ^{148}Sm (α,t) case in Fig. 2. The calculation is normalized to the data at an excitation energy of 30 MeV. This cross section is subtracted from the spectra before further analysis of the data.

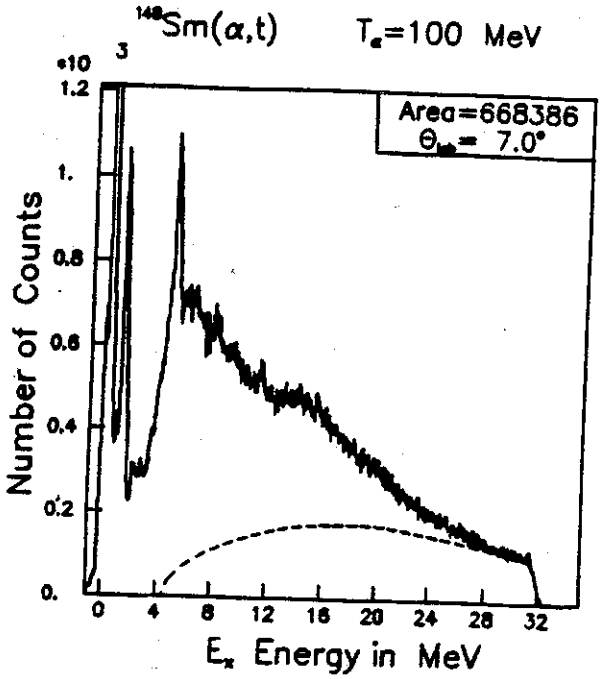

Fig. 2. Spectra of tritons from ^{148}Sm with the α-elastic break-up superimposed.

We have also tried to minimize arbitrary assumptions about the shape of the single-particle strength distribution. Therefore we "slice" the spectra into 280 keV bins and extract the angular distribution of the cross section for each bin. By comparing the angular distributions for each bin to DWBA calculations, the distributions of single-particle strength as a function of excitation energy can be obtained and compared with theoretical predictions.

At present, the data on the samarium isotopes is being analyzed and should shortly be ready for publication. Future work in this area will depend on how accurately the single particle strength functions can be determined by this technique. If accurate information can be obtained,

further measurements will be made to allow comparison with the hole state work and with theory over a wider range of nuclei.

Recent preliminary results with heavier projectiles (^{22}Ne) have shown large "bumps" at fairly high excitation energy in single particle transfer reactions (see Fig. 3). It would be interesting to see whether these correspond to known features observed with lighter projectiles or whether these represent new, perhaps higher angular momentum structure. More data is required to establish the properties of these bumps, including the angular momentum transfer needed to populate them.

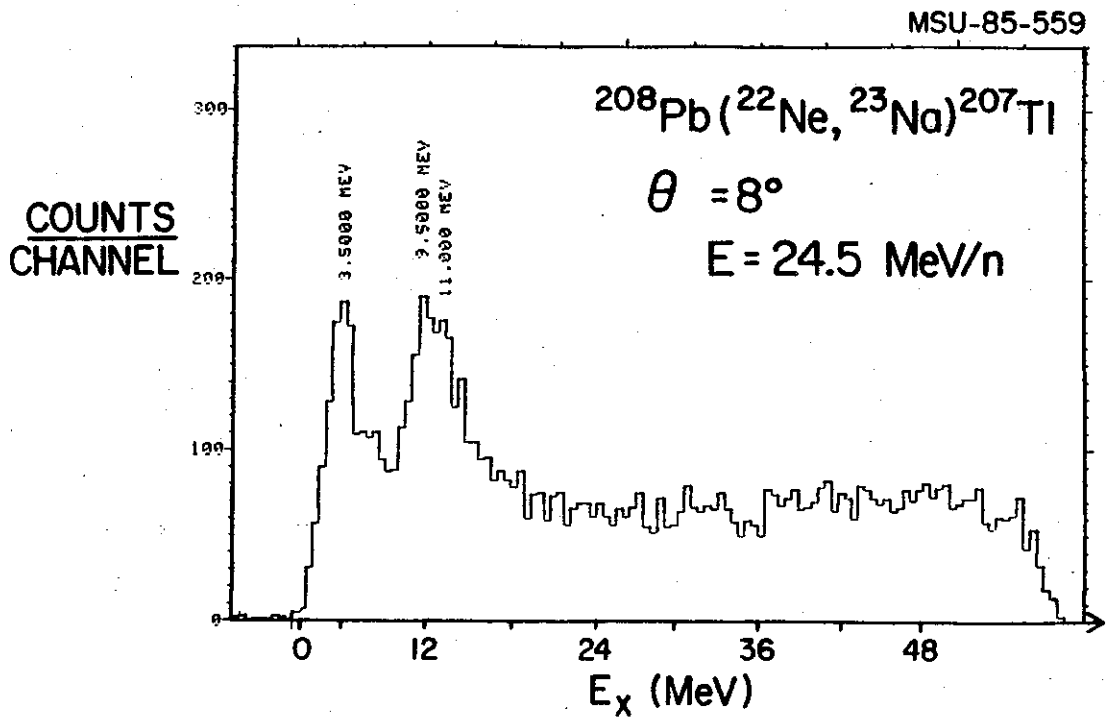

Fig. 3. One-proton transfer spectrum showing clear structure near E_x=10 MeV.

a. University of Michigan.
b. IPN, Orsay
c. IPN, Orsay and University of La Plata.
d Central Michigan University.

References:

1. G.M. Crawley. Proc. Int. Conf. on Structure of Medium-Heavy Nuclei, Osaka, Japan p590 (1980).
   S. Gales. Nuclear Physics A354,193c(1981)
2. V.G. Soloviev et al. Nuclear Physics A342,261(1980)
3. G. Bertsch et al. Physics Letters 80B,167(1969) and Rev. Mod. Phys. 55,287(1983)
4. O. Scholten, private communication
5. S. Gales et al. Phys. Rev. C 31,94(1985)
6. S. Gales, Int. School of Nuclear Structure, Alushta,USSR Oct 1985, IPN Report IPNO-DRE/85-31.
7. J.R. Wu et al. Phys. Rev. C 20,1284(1979)

III.B.2.c. SEARCH FOR STRUCTURES AT HIGH EXCITATION ENERGY IN HEAVY ION INELASTIC SCATTERING

S.M. Austin, W. Benenson, G.M. Crawley, H. van der Plicht, J.S. Winfield, S. Gales[a], S. Fortier[a]

In many ways the early optimism about the utility of heavy ions to explore giant resonances with large angular momentum has not been realized. Although the known giant resonances are observed quite clearly in the spectra of heavy ion scattering, little new information on them has been obtained from these studies. However there are a few measurements dating back to 1977 which apparently reveal structure at very high excitation energy in the reactions Ca + Ca and Cu + Cu.[1] The location of these structures appears to be independent of scattering angle and incident energy, which suggests that they correspond to real states in the residual nucleus. More recently, similar structures have been observed by the same group in the study of asymmetric systems with lighter projectiles viz., ^{36}Ar + ^{208}Pb and ^{20}Ne + ^{208}Pb.[2] The reported structures at energies of 73, 61, 52, 44, 38, 34, and 25 MeV have been interpreted in terms of multiphonon excitations built upon giant resonances. If such structures were real, they would represent an extremely interesting and novel phenomenon in nuclear science and would merit extensive study both experimentally and theoretically.

In an attempt to verify the existence of these structures, we have studied the ^{22}Ne + ^{208}Pb reaction using a 25 MeV/nucleon ^{22}Ne beam from the K500 cyclotron. The particles emerging from the reaction were detected in the S320 spectrograph. One advantage of the S320 spectrograph is that its broad range (20% in energy) allows a rather complete coverage of the region of interest in a single field setting. In order to identify the mass of the reaction product, time of flight through the S320 was measured with a parallel plate gas detector as a start detector and a plastic scintillator as a stop detector. Unfortunately during the first run the start detector did not prove 100% efficient at reasonable beam intensities. Therefore the absolute cross sections are uncertain at the 30% level. Nevertheless as can be seen in the data shown in Fig 1, we observe virtually no structures, and we can place upper limits almost five times smaller than the cross sections

reported in Ref. 1. The statistics of the data shown are so high that small imperfections in the apparatus, for example in the focal plane detector wires or ADC's, make a systematic modulation of the spectra at a very low level. The two spectra at 8° labelled "1" and "2" were taken for different times and different fields. The comparison shows that the periodic modulation is spurious, and in any case it is much smaller than the previously reported structures. Since our experiment began, we have learned of two other similar spectrograph measurements, one at Grenoble[3] and one at Oak Ridge.[4] These experiments also do not find structures like the ones reported earlier.[1]

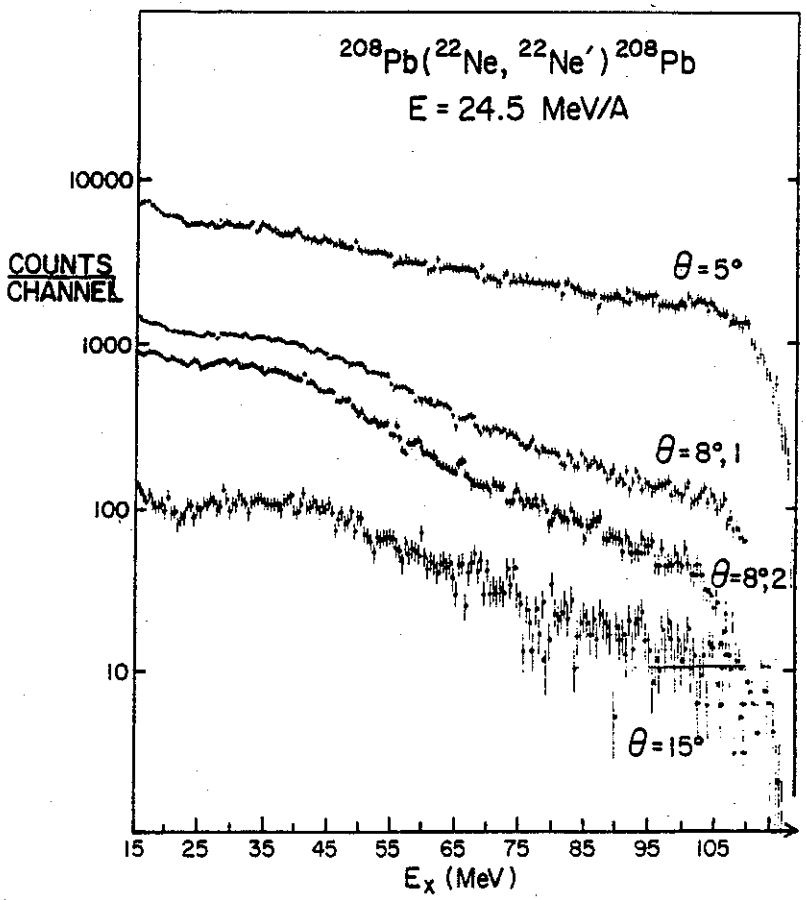

Figure 1.

We are building a more efficient start detector in order to obtain more reliable absolute cross sections. The K500 cyclotron with the ECR source will permit measurements for all the cases studied in Refs 1 and 2. Transfer reactions will be studied at the same time since the spectra

already obtained appear to be rich in structure at excitation energies near 10 MeV. (See Section B3(a)).

a. IPN Orsay, France.

References:

1. N. Frascaria et al., Phys. Rev. Lett. 39,918(1977).
2. Ph. Chomaz et al., Z. Phys. A318,41(1984).
3. M. Buenerd et al. preprint.
4. F. Bertrand et al., preprint.

III.B.2.d. HIGHER ORDER NUCLEAR DEFORMATIONS FROM INELASTIC SCATTERING.

R.M. Ronningen, G.M. Crawley, and N. Anantaraman

For some time there has been a systematic program in this laboratory to determine the deformation parameters of the nuclear matter distribution of deformed nuclei in the rare-earth and actinide regions.[1,2,3] The recent emphasis has been to extend our knowledge to higher orders in deformation and to make detailed comparisons to previous studies,[6] which used different probes or different incident energies.

More recently, this program has been extended using polarized protons[4,5] at 134 MeV at IUCF, where we studied inelastic scattering from ^{154}Sm, ^{166}Er, ^{176}Yb, and ^{182}W. These data were analyzed using coupled channels calculations from which the parameters of a deformed official model potential (DOMP) were determined. Using a theorem due to Satchler[7] we deduced the multipole moments of the matter distributions of these nuclei. In all four cases the quadrupole moments of the DOMP were in reasonable agreement with those determined by Coulomb excitation. For Sm and Er the same was true for the hexadecapole moments, but for Yb and W significant disagreements between different studies were observed, even from those using protons but with differing incident energies.

In ^{154}Sm, the energy dependence of the quadrupole moment of the DOMP (due to energy and density dependence of the microscopic nucleon-nucleon interaction) which we observed agreed with the prediction of Brieva and Georgiev.[8] This was not the case for the hexadecapole moment. Ichihara, et al.,[9] have also studied (p,p') on nuclei in the middle of the rare-earth region and have also performed folding model calculations including density-dependence. They observe similar effects. We conclude that density-dependent effects are certainly observed, but we still are unable to calculate them accurately for higher order moments.

There are no systematic predictions for the hexacontatetrapole moment although Nilsson, et al. have, predicted the trend for β_6 in the rare-earth region.[10] This result can also be obtained by an extention of a simple picture due to Bertsch.[11] In Fig. 1 we show a summary of what is currently known about β_6 in the rare-earth region. The trend of the experimental results is in fair agreement with the theoretical predictions. Similar

effects should be present in the actinide region. In nuclei such as ^{248}Cm, even the β_4 values from Coulomb excitation studies have large uncertainties. Therefore, we plan to extend our systematic studies to this region at IUCF using the new high resolution spectrograph.

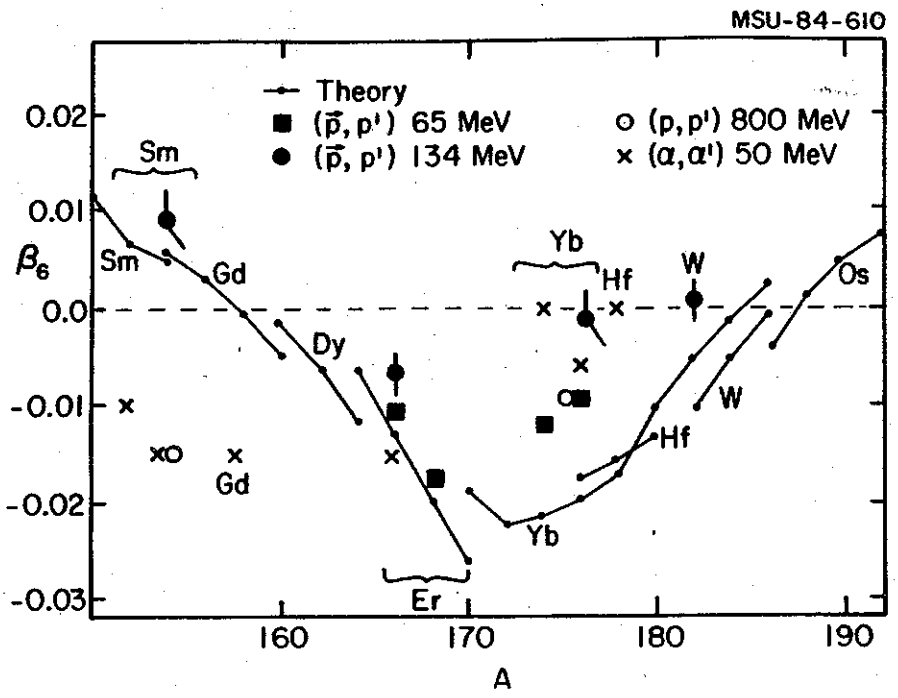

Fig. 1 Comparisons of measured and theoretically calculated hexacontatetrapole deformation parameters(β6) in the rare-earth region. The theoretical values are from Ref. 10. The experimental values are from Ref. 4-6, 8, 12.

Another fascinating topic of current interest is the effect of higher order deformations in heavy-ion reactions. Specifically, it is suspected that to minimize the Coulomb potential part of the heavy ion-heavy ion interaction potential, deformed nuclei become spacially oriented. Because of the mutual Coulomb excitation to quite high spin, a highly aligned system results. Oberacker and Rhoades-Brown have shown that hexadecapole deformations play a profound role in the cross section for fusion of two deformed nuclei, or even a deformed target and a spherical projectile.[12] Experimental studies are underway to verify this.[13] Oberacker has very recently pointed out that the alignment of very heavy deformed systems has been neglected in the theoretical treatments of spontaneous QED vacuum

decay, and that these may increase the predicted cross section for a long-lived resonant system (with enough charge to cause the vacuum to spontaneously decay).[14]

We propose to perform studies with deformed beams from the K500 plus ECR source at the NSCL. In particular in the mass 70 region, there are permanently deformed nuclei where the hexadecapole deformation parameter[15] apparently changes sign. Specifically, β_4 changes sign in the heavy stable selenium nuclei. Selenium and germanium, whose low-lying level structures are very similar to Se, should be relatively easy beams to obtain from the ECR source. The appropriate target fusion cross sections will be measured for different values of β_4. The theoretical picture for fusion of oriented deformed systems can then be tested without having to accelerate very heavy beams, such as rare-earth or actinide nuclei. To test the theory of vacuum decay (positron production) very heavy beams at energies available from the K800 are necessary.

References:

1. C.H. King, J.E. Finck, G.M. Crawley, J.A. Nolen, Jr., and R.M. Ronningen, Phys. Rev. C 20,2084(1979).
2. R.M. Ronningen, R.C. Melin, J.A. Nolen, Jr., G.M. Crawley, and C.E. Bemis, Jr., Phys. Rev. Lett. 47,635(1981).
3. P.T. Deason, C.H. King, R.M. Ronningen, T.L Khoo, F.M. Bernthal, and J.A. Nolen, Jr., Phys. Rev. C 23,1414(1981).
4. R.M. Ronningen, G.M. Crawley, N. Anantaraman, S.M. Banks, B.M. Spicer, G.G. Shute, V.C. Officer, J.M.R. Wastell, D.W. Devins, and D.L. Friesel, Phys. Rev. C 28,123(1983).
5. B.G. Lay, S.M. Banks, B.M. Spicer, G.G. Shute, V.C. Officer, R.M. Ronningen, G.M. Crawley, N. Anantaraman, and R.P. DeVito, Phys. Rev. C 32,440(1985).
6. D.L. Hendrie, N.K. Glendenning, B.G. Harvey, O.W. Jarvis, H.H. Duhm, J. Saudinas, and J. Mahoney, Phys. Lett. 26B,127(1968).
7. G.R. Satchler, J. Math. Phys. 13,1118(1976).
8. F.A. Brieva and B.Z. Georgiev, Nucl. Phys. A308,27(1978).
9. T. Ichihara, H. Sakaguchi, N. Nakamura, T. Noro, F. Ohtani, H. Sakamato, H. Ogawa, M. Yosoi, M. Ieiri, N. Isshiki, and S. Kobayashi, Phys. Rev. C 29,1228(1984).
10. S.G. Nilsson, Chin Fu Tsang, A. Sobiczewski, Z. Syzmanski, S. Wycech, C. Gustafson, I.-L. Lamm, P. Moller, and B. Nilsson, Nucl. Phys. A131,1(1969).
11. G.F. Bertsch, Phys. Lett. 26B,130(1968).
12. V.E. Oberacker and M.J. Rhoades-Brown, Phys. Rev. Lett. 50,1435(1983).
13. H.J. Kim, C.E. Bemis Jr., F.K. McGowan, R.L. Robinson, S.G. Steadman, F. Plasil, R.L. Ferguson, T.C. Awes, F.E. Obenshain, J.R. Beene, and V. Rauch, Oak Ridge National Laboratory Physics Division Progress Report ORNL-6004(1983-1984), p.136.

14. H. Ogawa, H. Sakaguchi, M. Nakamura, T. Noro, H. Sakamoto, T. Ichihara, M. Yosoi, M. Ieiri, N. Isshiki, Y. Takeuchi, and S. Kobayashi, Research Center for Nuclear Physics, Osaka University, Annual Report(1984), p.38.
15. Volker E. Oberacker, Phys. Rev. C 32,1793(1985).

III.B.2.e. ALPHA CLUSTERING AT THE NUCLEAR SURFACE

N.S. Chant[a], P.G. Roos[a], G.M. Crawley and C. Djalali

One of the interesting quantities that can be obtained from cluster knockout reactions like (p,pα) and (α,2α) is the alpha-particle spectroscopic factor. Quite extensive results have been reported[1-6] for (p,pα) and for (α,2α).[7-9] The first issue is whether the clean quasi-free ejection of an extended cluster from a nucleus is possible and whether a DWIA description is adequate. For the 140 MeV (α,2α) reaction, agreement between the shape of the measured angular distributions and those predicted using the free α-α scattering data is excellent, presumably owing to the strong surface localization of the reaction. For the 100 MeV (p,pα) reaction, the case is not quite so convincing. Thus, either the reaction mechanism is more complicated than assumed or, for this less well-localized reaction, an analysis which avoids the factorization approximation is needed.

For heavier targets DWIA predictions agree fairly well with the experimental data so one is encouraged to use the (p,pα) reaction to extract α-cluster spectroscopic factors in these cases. Results are shown in Fig. 1 for (p,pα).

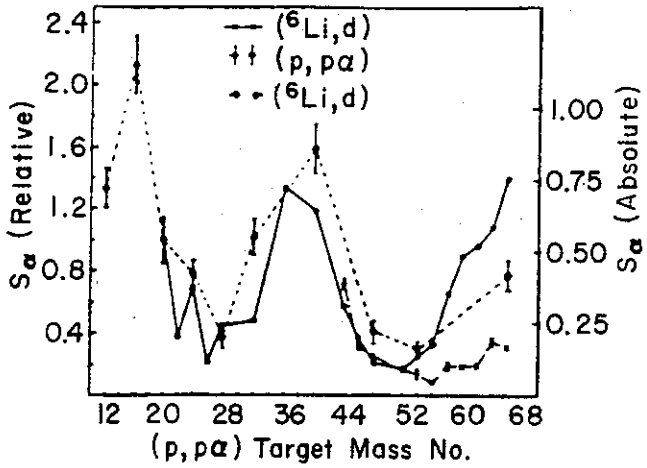

Fig.1. Extracted spectroscopic factors for ground state transitions as a function of target mass. The left scale indicates the relative value and the right scale the absolute value extracted in (p,pα).

For the ground state transitions studied, the results are largely consistent with (^{6}Li,d) studies carried out at Rochester.[11,12] However, the (p,pα) results are probably more stable with respect to uncertainties in the optical potentials than are the transfer reaction. Since this

reaction is mismatched by about four units of angular momentum for the ℓ=0 ground state transitions. In contrast, the (p,pα) reaction is, of course, exactly matched and involves optical potentials somewhat less subject to uncertainty. The absolute values obtained in the (p,pα) study are in agreement with shell model predictions for the 1p shell targets. In the sd shell the experimental values start at around three times shell model predictions, increasing to around 20 times for ^{40}Ca. Alpha-clustering has been predicted in this mass region by some models.[13]

For the (α,2α) reaction the extracted relative spectroscopic factors have much the same behavior as the (p,pα) results. However, the absolute values are around 100 times larger than the (p,pα) values.[7,8] Since essentially the same approximations are involved in the DWIA calculations for both reactions, this discrepancy is hard to dismiss. The problem does not seem to arise from a poor choice of distorting potentials. It can be remedied by a rather unphysical increase in the rms radius of the α-cluster wave function. However, in this case agreement with the (p,pα) data is lost. As shown in Fig. 2, the (α,2α) reaction is much more strongly surface localized than the (p,pα) case.

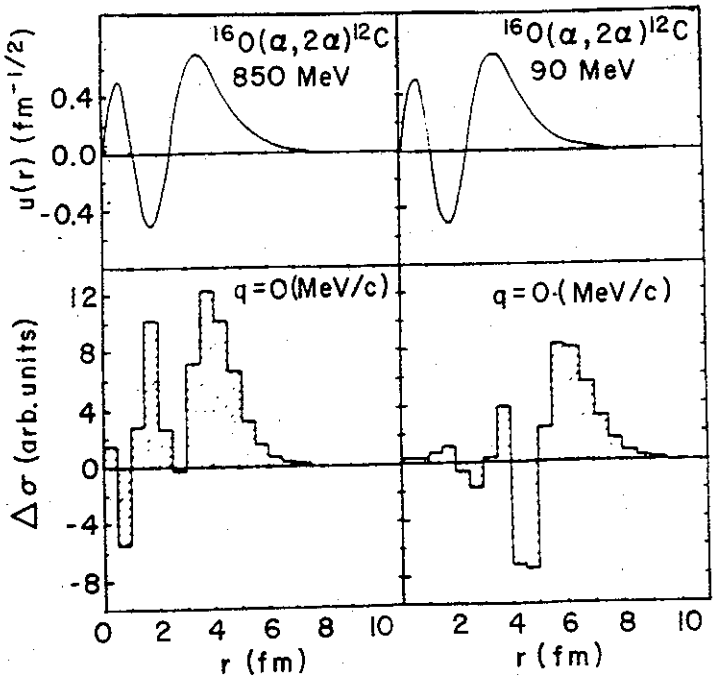

Fig.2. Radial localization of the ^{16}O(α,2α)^{12}C reaction at 90 and 850 MeV.

Thus it seems reasonable to conclude either:

a) The incident projectile itself induces clustering in the surface region, and this effect is much more severe for the more massive alpha-projectile. In slightly different language this implies a two-step process involving significant excitation of the target to levels having large alpha width prior to the actual knockout process. Or:

b) In the extreme surface region (around 0.1% of central density) probed in $(\alpha,2\alpha)$ the extent of alpha clustering is around 100 times that predicted in a "simple" shell model.

A calculation of the two-step process has yet to be carried out. However, in view of the good factorization of the $(\alpha,2\alpha)$ reaction this possibility seems less likely, since some broadening of the angular distribution would be expected in a multi-step process. Clearly more extensive comparisons of α-transfer $(p,p\alpha)$ and $(\alpha,2\alpha)$ reactions would be of interest. It is worth noting that the $^{16}O(\alpha,2\alpha)$ reaction at 800 MeV does not exhibit the large discrepancy cited above.[14] Rather the measurement is essentially in agreement with the $(p,p\alpha)$ spectroscopic factors. This behavior is consistent with the fact that, at the higher alpha energy, the $(\alpha,2\alpha)$ reaction is no longer highly surface-localized and samples the nuclear volume much like $(p,p\alpha)$ at around 200 MeV. It would therefore be interesting to study the $(\alpha,2\alpha)$ reaction as a function of bombarding energy.

We plan to investigate the $(\alpha,2\alpha)$ reaction from 200 to 800 MeV. The higher energy α beams will only be available with the K-800 cyclotron. In addition these experiments are probably best done with at least one of the two detector arms being a magnetic spectrometer. The S800 spectrograph, with its solid angle of 20 msteradian, would be ideal. Measurements could be started using NaI detectors since comparatively modest detector sizes and resolution would be needed.

a University of Maryland

References:

1. P.G. Roos et al., Phys. Rev. C 15,69(1977).
2. T.A. Carey et al., Phys. Rev. C 23,576(1981).
3. T.A. Carey et al., Phys. Rev. C 29,1273(1984).
4. A. Nadasen et al., Phys. Rev. C 22,1394(1980).
5. A. Nadasen et al., Phys. Rev. C 23,2353(1981).
6. C.W. Wang et al., Phys. Rev. C 31,1662(1985).

7. N.S. Chant et al., Phys. Rev. C 17,8(1978).
8. C.W. Wang et al., Phys. Rev. C 21,1705(1980).
9. J.D. Sherman et al., Phys. Rev. C 13,20(1976).
10. N.S. Chant and P.G. Roos, Phys. Rev. C 15,57(1977).
11. N. Anantaraman et al., Phys. Rev. Lett. 35,1131(1975).
12. H. Fulbright et al., Nucl. Phys. A284,329(1977).
13. T. Tomoda and A. Arima Nuclear Phys. A303,217(1978).
14. N. Chirapatpimol et al., Nucl. Phys. A264,379(1976).

III.B.3.a. EXPERIMENTS USING A GAMMA-RAY SPIN SPECTOMETER

R. Blue, R. Ronningen, R. Aryaeinejad, J. Saladin,[a]
I.Y. Lee,[b] and C. Baktash[b]

Much of the work on the spectroscopy of high-spin states of nuclei has involved the formation of highly-excited nuclei via fusion-evaporation reactions. It was recognized some time ago that heavy-ion-induced multiparticle-transfer reactions, known variously as partial fusion, massive transfer, or break-up fusion reactions, may also serve to populate states of interest in high-spin spectroscopy.[1-3] In fact, reactions of this type appear to offer greater experimental flexibility so that nuclei not previously accessible may be studied. The primary disadvantage of the use of transfer reactions is that, in general, many residual nuclei will be populated and contribute to the observed gamma-ray spectra. In work initiated at NSCL by Utsunomiya, et al.,[4] the feasibility of selecting specific reaction channels via particle-gamma coincidences has been demonstrated, and this technique was employed to investigate the reaction mechanisms involved in multiparticle transfers.

We are now proposing to employ transfer reactions and the same particle-gamma techniques for the purposes of gamma-ray spectroscopy at high excitation energy. The gamma-rays will be detected in Ge detectors surrounded by Bismuth Germanate (BGO) shields for Compton suppression. The proposed investigations will be conducted in collaboration with Professor J.X. Saladin of the University of Pittsburgh and co-workers and will employ elements of a spin-spectrometer system developed by this group for use at NSCL. This system will ultimately include six Ge detectors equipped with Bismuth Germanate anti-Compton shields and an array of 14 BGO elements to serve as an energy-sum and multiplicity filter (see Section V4(f)). For the particle-gamma investigations these gamma detectors will operate in coincidence with silicon surface barrier telescopes as the detectors of projectile-like fragments (PLF). Isotopic identification of the PLF thus serves to tag coincident gamma-ray spectra with sufficient specificity to restrict the identity of the residual target-like fragment (TLF) to within a range allowed by the variation in the number of neutrons (or perhaps alphas) emitted in the de-excitation process. The provision for Compton suppression

is particularly advantageous for this type of experiment in that it will reduce the underlying background which tends to obscure low-intensity spectral lines and the continuum gamma-ray spectrum.

For an initial experiment we have selected the reaction $^{22}Ne + ^{170}Er$ at a bombarding energy of 10 MeV per nucleon. This experiment has been approved by the NSCL PAC (#85023; spokesperson, J. Saladin). We expect to obtain spectra for a number of nuclei in the vicinity of the target mass and to map the general range of spin and excitation energy that is reached by the transfer of one or more nucleons to or from the target. In addition to providing spectroscopic information, this experiment will also allow an investigation of the mechanism of these multiparticle transfer reactions. The improved quality of the gamma-ray spectra obtained via the use of Compton suppression should make it possible to identify more of the low-intensity components of the spectra and thus better evaluate which portions of the reaction cross sections are associated with the less probable processes. The measurement of the total gamma-ray energy and the multiplicity will bring important additional information to these studies as well.

a. University of Pittsburgh.

b. Oak Ridge National Lab.

References:

1. T. Inamura, M. Ishihara, T. Fukuda, T. Shimoda, and H. H. Hiruti, Phys. Lett. 68B,51(1977).
2. H. Yamada, C.F. Maguire, J.H. Hamilton, A.V. Ramayya, D.C. Hensley, M.L. Halbert, R.L. Robinson, F.E. Bertrand, and R. Woodward, Phys. Rev. C24,2565(1981).
3. D.R. Haenni, T.T. Sugihara, R.P. Schmitt, G. Mouchaty, and U. Garg, Phys. Rev. C25,1699(1982).
4. H. Utsunomiya, E.C. Deci, R.A. Blue, L.H. Harwood, R.M. Ronningen, K. Siwek-Wilczynska, J. Wilczyski, and D.J. Morrissey, Phys. Rev. (to be published).

III.B.3.b. HIGH-SPIN BEHAVIOR USING NEUTRON-GAMMA COINCIDENCE TECHNIQUES

R.M. Ronningen,[a] F. Haas,[a,b] J. Kasagi,[a,c] P. Chowdhury,[d,e] W. Henning,[d] R. Holzmann,[d] R.V.F. Janssens,[d] T.L. Khoo,[d] K.T. Lesko,[d] D.C. Radford,[d,f] G. Rossner,[d,g] A. van den Berg, and W. Kühn.[d,h]

Until recently, the high-spin behavior of nuclei has been studied by discrete-line and continuum gamma-spectroscopy using modest numbers of detectors. New arrays of Compton event-suppressed Ge detectors, "crystal balls" of lower-resolution, high efficiency scintillators, and mass or velocity filters are revolutionizing the field of high-spin studies. New applications of older experimental techniques are also finding use, often coupled with these sophisticated devices.

An example is current work on the high-spin states of rare-earth nuclei. Studies of Yb nuclei at ORNL using a spin spectrometer have shown that dipole radiation dominates in a narrow spin region of ~35-45 ħ.[1] Subsequent work at the University of Rochester, using a recoil mass separator has shown the same result for Er nuclei by observing internal-conversion[2] which strongly suggests that the gamma radiation from this intermediate spin region is mainly M1. Quadrupole radiation dominates above and below this spin region.

Dipole radiation at high spin is indicative of non-collective behavior such as single-particle spin alignment about an oblate shape. But the sudden reappearance of quadrupole radiation at a relatively low spin of 50 ħ implies that the traditional picture of an oblate shape having modest deformation, which persists to very high spin is not complete. Another explanation is that superdeformed shapes exist at these relatively low spins, around 50 ħ. This has been a subject of study by our Argonne National Laboratory-NSCL collaboration during the past three years.

The collaboration is studying several projectile-target combinations which lead to the same compound nucleus. Our first experiment used 3.6 MeV/nucleon ^{64}Ni on a target of ^{92}Zr.[3] By detecting neutrons in coincidence with the summed gamma-ray energies, we could determine compound nuclear temperatures as a function of excitation energy. By identifying the residual nuclei (after neutron emission) by their discrete gammas, the

neutron multiplicity distribution was obtained. This distribution did not agree with statistical model predictions. As seen in Fig.1 the 2n-to-3n ratio is underpredicted by a factor of 20. It would appear that the emission of the third neutron is impeded by a lack of available energy; the excitation energy above the compound nuclear yrast line is less than half the neutron binding energy. When an yrast line corresponding to a superdeformed shape is used in the statistical model calculations, the neutron multiplicity distribution is better reproduced, as shown in the figure. A subsequent experiment using the reaction $^{12}C+^{144}Sm$ showed that the statistical model predicts the multiplicity distribution for this system very well. Analysis of these data as well as those from the symmetric systems $^{78}Se+^{78}Se$ and $^{82}Se+^{82}Se$ are in progress. The latter was chosen because theoretical expectations[4] for this system are that the superdeformed minimum does not exist.

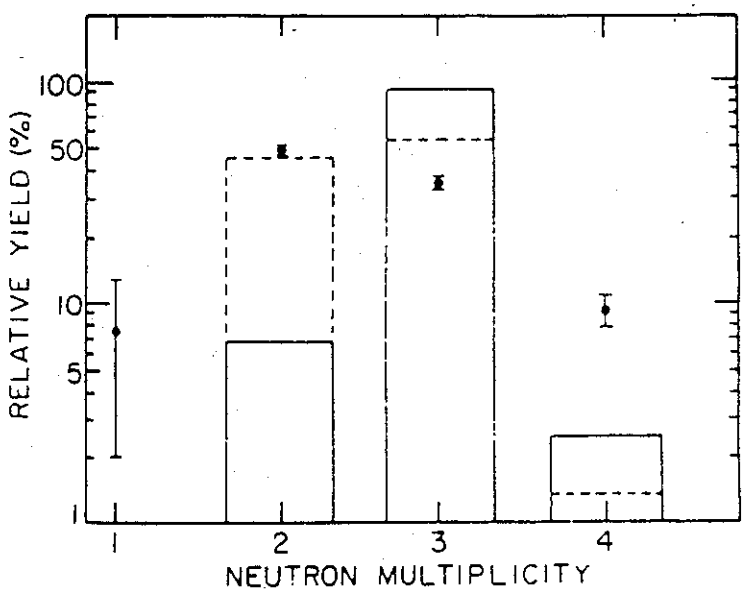

Fig. 1 Comparison of experimental (circles) neutron multiplicity distribution with those for statistical model calculations using the normal (solid bars) and elevated (dashed bars) yrast lines.

More work on fusion below and near the barrier needs to be done; the concept of a superdeformed shape is not experimentally well established. Comparisons to simple models of fusion must be critically examined because it appears[5] that coupled-channel effects in the entrance channel must also be considered.

Neutron-gamma coincidence techniques will be very useful in high-spin and fusion studies by helping to identify reaction products, especially those with low cross sections, when sophisticated devices such as velocity filters and mass separators are also employed. The use of a recoil-mass spectrometer in conjunction with high resolution gamma detectors[6] has provided particle-gamma data whose quality is comparable to gamma-gamma coincidence data. Even higher quality data will be obtainable with the use of Compton-suppressed gamma detectors to provide gamma-gamma-particle concidences. Furthermore, when nuclei far from the stability line are studied, and when charged particle emission competes with neutron emission, the addition of neutron multiplicity information will further enhance the ability to identify low cross section events. Such experiments are currently in progress.[7] Similar experiments are planned at NSCL using the K500 plus ECR combination. The RPMS, Compton-supressed detectors such as are present in the gamma ray spin spectrometer and existing neutron detectors will be employed. The gamma and neutron counter arrays will be placed at the target position to tag events by mass so as to study prompt events. Alternately, the arrays will be set up in the RPMS focal plane to study longer-lived species in a relatively background-free environment.

a. NSCL
b. Present address: CRN-PNIN Strasbourg
c. Present address: Tokyo Institute of Technology
d. ANL
e. Present address: Material Science Laboratory, Reactor Research Center, Kalpakkan, India
f. Present address: AECL-Chalk River
g. Technical University-Munich
h. University of Geissen

References:

1. M. Jääskelainen, D.G. Sarantites, F.A. Dilmanian, R. Woodward, H. Puchta, J.R. Beene, J. Hattula, M.L. Halbert, and D.C. Hensley, Phys. Lett 119B, 65(1982).
2. T.M. Cormier, P.M. Stwertka, M. Herman, and N.G. Nicolis, Phys. Rev. C30, 1953(1984).
3. W. Kühn, P. Chowdhury, R.V.F. Janssens, T.L. Khoo, F. Haas, J. Kasagi, and R.M. Ronningen, Phys. Rev. Lett. 51, 1858(1983).
4. S. Aberg, Phys. Scr. 25, 23(1982), and private communication.
5. M. Beckerman, Phys. Rep. 129 (1985), and references therein.
6. S.J. Robinson, A.V. Ramayya, M.A. Herath-Banda, W.C. Ma, C.F. Maguire, S. Wen, X. Zhao, T.M. Cormier, P.M. Stwerka, J.D. Cole, E.F. Zganjar, and R.B. Piercey, Bull. Am. Phys. Soc. 29, 1035(1984).
7. R.B. Piercey, private communication.

III.B.3.c. IN-BEAM GAMMA-RAY SPECTROSCOPY OF ODD-ODD NUCLEI

Wm. C. McHarris, R. Aryaeinejad, W-T. Chou, and W.A. Olivier

Until recently in-beam γ-ray spectroscopy of odd-odd nuclei was thought to be unrewardingly cumbersome. Spectra were very complicated and it was difficult to assign quantum numbers, much less meaningful configurations to the states. During the last several years, however, a number of experimental groups have discovered that, under certain conditions, in-beam γ-ray studies of odd-odd nuclei produce far simpler spectra than expected, with the resulting level schemes yielding a considerable amount of worthwhile information about details of nuclear structure. The necessary conditions appear to be deformed nuclei and/or high-spin states.

In Fig. 1 we show the level scheme produced by the $^{181}Ta(\alpha,3n\gamma)^{182}Re$ reaction.[1] This reaction brings in only a moderate amount of angular momentum; yet most of the de-excitation proceeds through only two high-spin rotational bands, the remainder through two additional low-spin but high-Ω bands. All four bands show considerable distortion -- in particular, a compressed A-term and a non-negligible positive B-term when their energies are fitted to the standard equation,

$$E_J = E_0 + AJ(J+1) + BJ^2(J+1)^2.$$

This type of distortion is characteristic of Coriolis coupling.

Thus, a perturbation expansion results in a negative A-term (effectively increasing the moment of inertia) and a positive B-term. If we examine the single-particle states involved in these bands, we find that the neutron state for all of them is the $9/2^+[624]$ Nilsson state, which originates from the $i_{13/2}$ spherical state and has very large Coriolis matrix elements; also, three of the four proton states originate from the $h_{11/2}$ or $h_{9/2}$ spherical states and have large Coriolis matrix elements. It is these states that decouple and align their spins with that of the rotating core to produce "backbending".[2] In other words, an efficient mechanism for carrying large amounts of angular momentum is for it to be shared between $\vec{R}$ of the core and $\vec{j}$ of the single nucleons. In even-even nuclei this requires the

uncoupling of a pair, but in odd-odd nuclei it merely requires the selective population of aligned single-particle states. Once such states are populated in the highly-excited nucleus, normal γ-ray selection rules tend to keep the de-excitation locked into related states, the result being that only a small subset of the possible states are seen. This mechanism means that a great deal of angular momentum is tied up in the single-particle modes. For example, in the ^{182}Re level scheme the largest value of $\vec{R}$ is only 10 (in the K = 2 band), not enough to produce any drastic shifts in the moments of inertia.

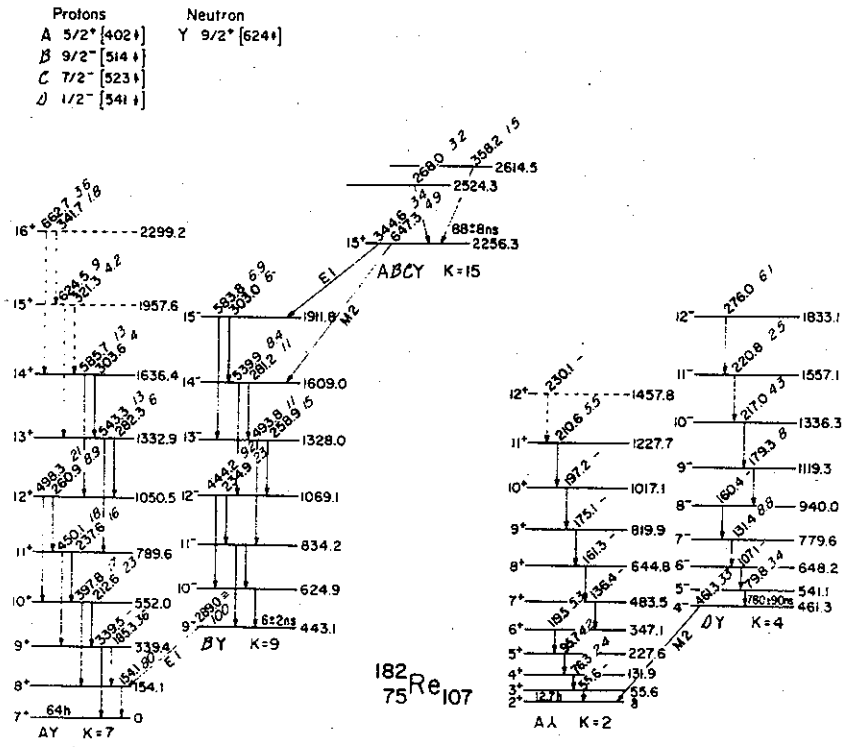

Figure 1.

Because so much angular momentum is tied up in single-particle motion, heavier beams are needed to extend the studies. ^{182}Re is difficult to produce by heavier beams, but the lighter Re nuclei can easily be produced by beams such as ^{14}N on Er targets. Preliminary results[4] for ^{180}Re are shown in Fig. 2, and an example[5] of a γ-ray spectrum for ^{178}Re is shown in Fig. 3. Both are somewhat more complex than ^{182}Re; yet they indicate the same sort of behavior: most of the de-excitation occurs through a select few bands, which are composed of highly-aligned odd-odd states.

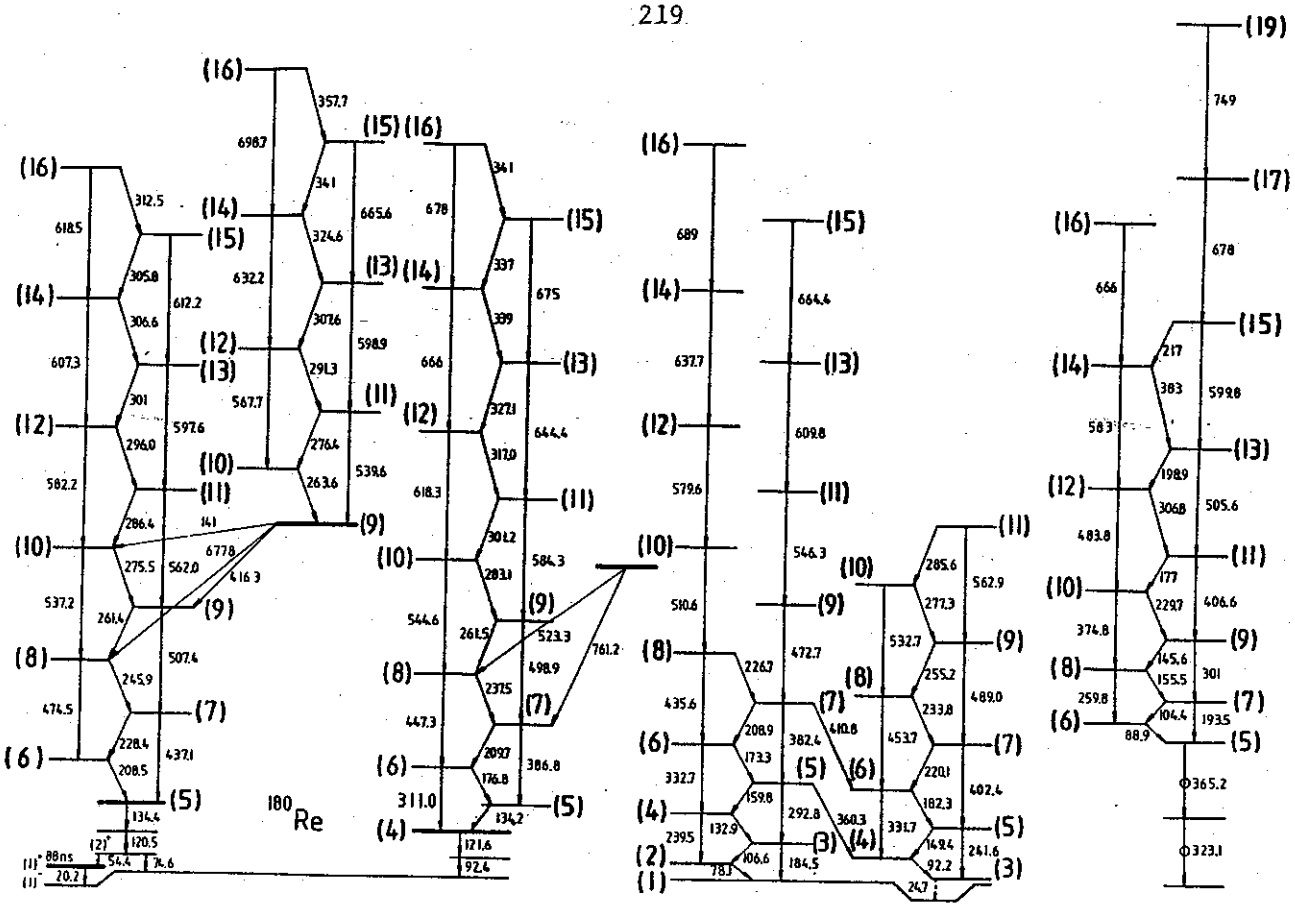

Figure 2.

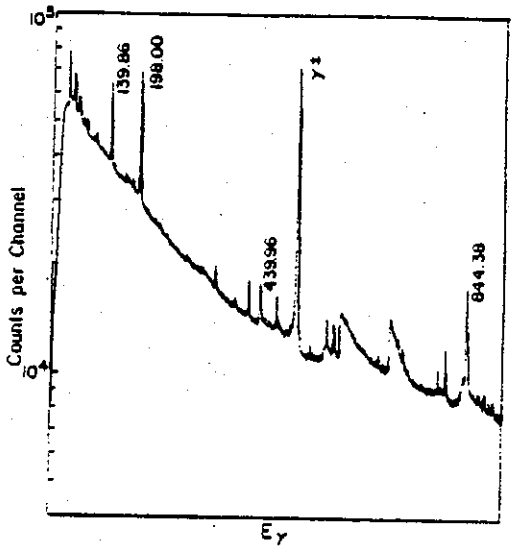

Figure 3.

Although odd-odd rotational bands are best understood in well-deformed nuclei, for quite some time they have also been known to exist,

based on excited states, in nuclei very close to closed shells.[6] Rather intriguing examples of this occur in many of the odd-odd Sb isotopes. The high-spin level scheme of ^{116}Sb, resulting from the ^{115}In(α,3nγ) reaction,[7] is shown in Fig. 4. Calculations reproduce the observed spacings[8] remarkably well. That these rotational bands figure prominently in the de-excitation pattern is again consistent with our proposed mechanism of selectively populating aligned single-particle states. Less can be said about the most prominent high-spin de-excitation pattern (at the left side of Fig. 4), for there are too many possible constructs. However, oblate-| | pseudo-rotation and rotationally aligned particles could certainly play major roles. And the other odd-odd Sb show remarkably parallel behavior.

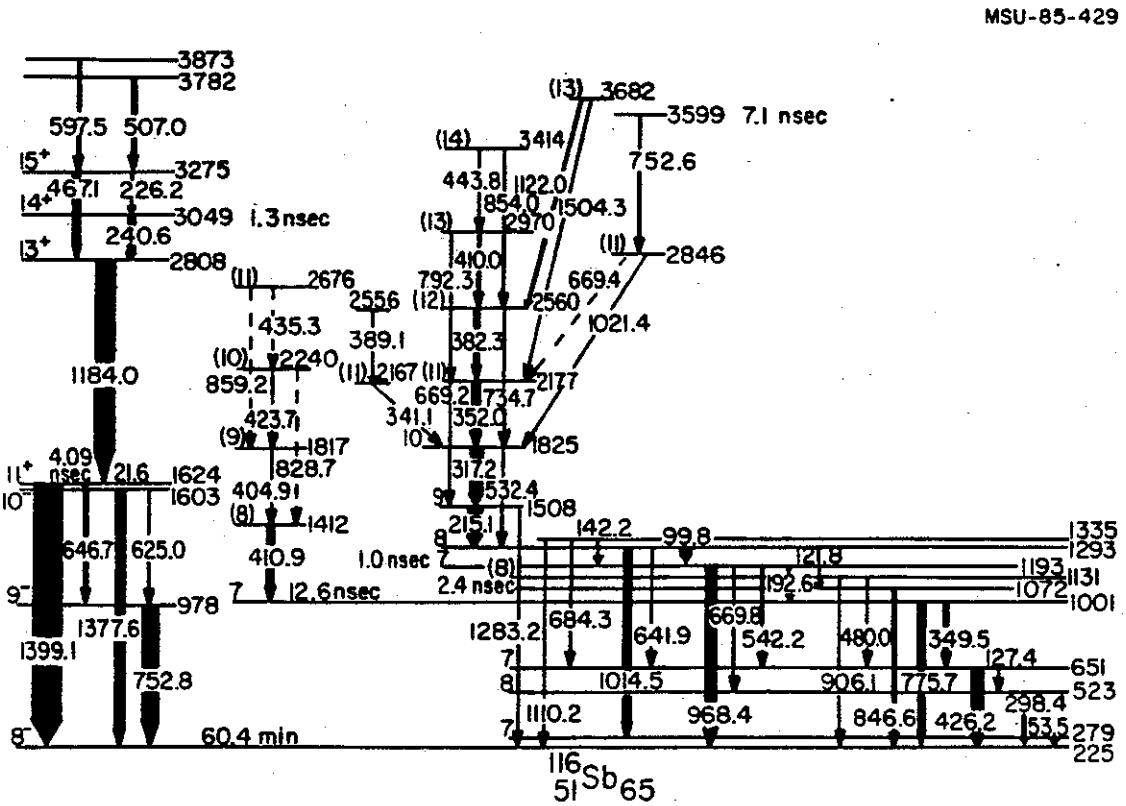

Figure 4.

In addition to using the above physical models, we have been performing calculations using the Interacting Boson-Fermion Approximation.[9] One of our aims is to compare the results from such calculations with the physical models and perhaps to obtain better insight into the IBA and IBFA models. We have performed IBA-1 calculations on even-even nuclei in both the ^{180}Os region and on some of the even-even members of the N=80 isotones, using the PHINT code.[10] We have also performed IBFA calculations on the odd-mass Re isotopes adjacent to the even-even Os nuclei and on odd-mass members of the N=80 isotones, using the ODDA code.[11] Examples of preliminary results are shown in Figs. 5 and 6.

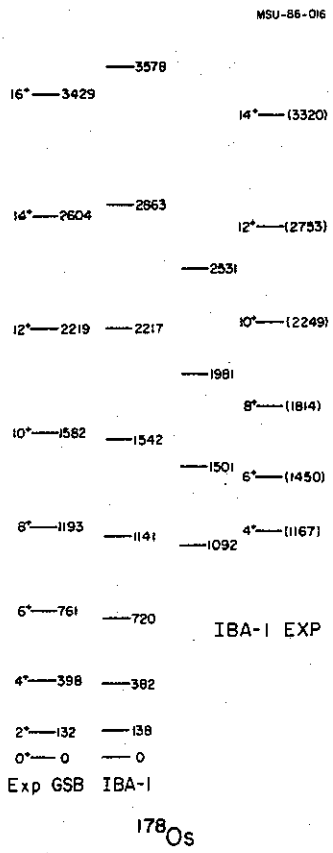

Figure 5.

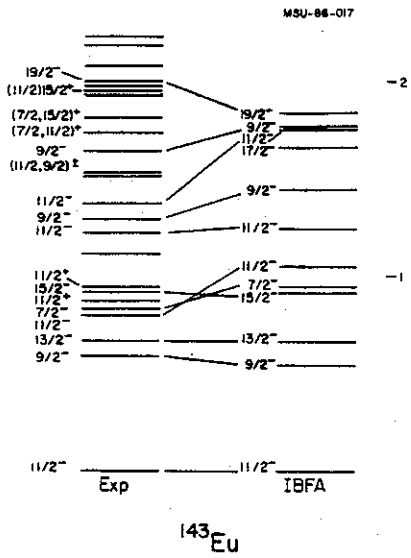

Figure 6.

Calculations for the odd-mass systems involved a coupling of the odd particle to the even-even core. Parameters used to change the effective interaction between the core bosons and the fermion included a quadrupole

interaction strength, an exchange interaction strength, occupation probabilities for plausible orbits of the fermion, and single-particle energy factors.

The calculations for the even-even Os isotopes have yielded seemingly consistent results and fitted the experimental energies within 10% for levels up to J = 16. The calculations for the odd-mass N = 80 isotones failed to duplicate the experimental energies thus far. Calculations for the odd-mass Re isotopes, while not complete at this time, have yielded promising results. A difficulty in these calculations is the extremely large basis sets, for both ^{181}Re and ^{177}Re which are 13-boson systems. Results from the initial ^{181}Re calculations showed very little mixing between the possible valence states for the odd fermion, which allowed us to reduce the basis set initially.

Once we have become proficient and in the odd-mass calculations we plan to progress to odd-odd calculations. The first odd-odd calculations will be "hand-fitted" combinations of odd-proton and odd-neutron calculations; then we plan full-fledged odd-odd calculations. Odd-odd calculations should prove a very stringent test of the IBFA model(s), for systematics and extrapolations do not work very well in such nuclei.

Experimentally, we are now working on the neutron-deficient Re isotopes, using ^{170}Er(^{14}N,xn)$^{184-x}$Re reactions produced by the ^{14}N beam at the NSCL K500 cyclotron. We have obtained excitation functions (including those for many individual γ-rays), γ-γ coincidence spectra, and limited angular distributions. So far we have been working primarily on ^{180,178,176}Re and their odd-mass neighbors (necessary both for input into the analyses and to keep track of contaminants). It would be more exciting to work on the most-neutron-deficient isotopes possible (say, ^{170}Re, perhaps even lower), but it is much safer to work our way down to these. We plan to do so as quickly as possible. In addition, depending on manpower, we hope to progress to odd-odd nuclei in the "transition" (between spherical and deformed) region below N=82.

References:

1. M. F. Slaughter, R. A. Warner, T. L. Khoo, W. H. Kelly, and Wm. C. McHarris, Phys. Rev. C 29, 114 (1984).
2. F. S. Stephens and R. Simon, Nucl. Phys. A183, 257 (1972).
3. A. Bohr and B. R. Mottelson, Nuclear Structure (Benjamin, Reading, Mass, 1975), Vol. II, pp. 43ff, 72ff.
4. R. M. Lieder, XXIII International Winter Meeting on Nuclear Physics, Bormio, Italy, Proceedings, p. 276 (1985).
5. W. A. Olivier, W.-T. Chou, R. Aryaeinejad, and Wm. C. McHarris, work in progress (1986); an invited paper reporting our preliminary results was presented at the Symposium on Modern Techniques for the Study of Nuclei Off the Line of Stability, American Chemical Society Chicago Meeting, 12 Sept. 1985, and will appear in the published proceedings.
6. L. E. Samuelson, W. H. Bentley, W. H. Kelly, R. A. Warner, F. M. Bernthal, and Wm. C. McHarris, Phys. Rev. C 15, 821 (1977).
7. W. H. Bentley, R. A. Warner, Wm. C. McHarris, and W. H. Kelly, submitted to Phys. Rev. C (1985).
8. H. Toki, H. L. Yadav, and A. Faessler, Phys. Lett. 71B, 1 (1977).
9. A. Arima and F. Iachello, Ann. Phys. 99, 253 (1976); 111, 201 (1978); 123, 468 (1979).
10. O. Scholten, "The Program Package PHINT," KVI report #63 (1979).
11. O. Scholten, "The Program Package ODDA," KVI report #252 (1980).

III.B.4.a. NUCLEAR STRUCTURE THEORY

B. A. Brown

1. INTRODUCTION

The effective nucleon-nucleon interaction and its relationship to the shell-model space truncation is the most basic aspect of our work, and this will be the first topic discussed. In the remaining sections recent and proposed work on the tests and applications of the shell model are summarized. Sec. 3 covers the results for isospin and parity nonconserving nucleon-nucleon interactions which are of fundamental importance in formulating a complete and consistent theory of the strong and weak interactions. Elastic and inelastic scattering and electromagnetic decay properties are covered in Secs. 4 and 5. Magnetic dipole and Gamow-Teller type excitations are the most important of these and are discussed together with the topic of double beta decay in Sec. 4. Direct reactions with an emphasis on those involving pions are covered in Sec. 6.

2. SHELL-MODEL EFFECTIVE INTERACTIONS AND COMPUTATIONAL TECHNIQUES

Our research in the area of formulating new shell-model wave functions emphasizes the incorporation of as many active configurations as possible and as many nuclei as possible into the calculation. The results should be validated by comparison with experiment for as great a range of states and for as many different types of phenomena as feasible. We think that only in this context is it possible to seriously consider either the "normality" or the "aberrancy" of an observed effect relative to theoretical expectations.

The prototype of this global analysis was initiated at MSU by B. H. Wildenthal for the 1s-0d shell. These sd shell wave functions have been used extensively to test our understanding of many types of phenomena in this mass region: initially with the Chung-Wildenthal interaction [1]-[2] and more recently with the "Universal" sd shell (USD) interaction [3]-[13]. The best results for the sd shell have been obtained by using an unconstrained two-body interaction. The USD interaction was obtained by allowing essentially all two-body matrix elements (63 for the sd shell) and single-particle energies (3 for the sd shell) to be free parameters in a fit to experimental binding energies and excitation energies (440 data). In

necessary to assume an $A^{-0.3}$ mass dependence in the two-body matrix elements; this mass dependence is close to that expected for a G-matrix type interaction.[14]

For shell-model spaces larger than that of the sd shell, where the number of two-body matrix elements are much larger, it is a much more difficult process to extract an unconstrained empirical Hamiltonian from a fit to experimental data. We are investigating whether it is possible to base the empirical Hamiltonian on G-matrix elements, derived from a realistic nucleon-nucleon interaction, plus correction terms for core polarization. For the G-matrix interaction we propose to start with the radial-dependent "M3Y" type parameterization pioneered at MSU[15] and more recently adopted to the Paris potential.[14] Those elements of the G-matrix which are most important in determining shell-model eigenvalues would be adjusted to their optimum values relative to experimental energies, and those elements to which the shell-model values are quite insensitive would be held fixed. The adjustments obtained in such fits would yield the optimal core-polarization corrections as well as corrections for errors introduced by approximations made in calculating the G matrix.

Essential to this approach is the representation of the Hamiltonian in a scheme which efficiently separates "important" from "unimportant" terms. Work has been initiated on this project in collaboration with W. Richter of Stellenbosch University. We have decomposed the jj-coupled sd shell two-body matrix elements into central, tensor, spin-orbit and antisymmetric spin-orbit components, and within this scheme we have compared empirical interactions with various G-matrix and renormalized G-matrix calculations.[16]

We have initiated projects which make use of this new approach for the sd shell[17] and the fp shell.[18] Our immediate goal is to understand the constrained Hamiltonian for the sd shell and apply this understanding to obtaining an improved description for the fp shell nuclei. Also, it will be important to apply this approach to other situations of current interest (see below) such as the properties of exotic neutron-rich nuclei, the excited states of oxygen and calcium isotopes and the nuclei involved in double beta decay.

We are also interested in density-dependent interactions which can be used for the valence interactions as well as in Hartree-Fock calculations

for the closed-shell configurations and for RPA calculations of particle-hole configurations. We have used the SGII interaction of Sagawa and van Giai[19] for the calculation of the the $\Delta N>0$ ($N=2n+\ell$) core-polarization contribution to the E2 and E4[20] transition densities in the sd shell. The results of the calculation were in good agreement with experiment. These results were used to estimate the E2 effective charges for the states outside of an A=88 closed shell[21] where it was found that most of the core polarization comes from the low-lying ($\Delta N=0$) states of the closed ^{88}Sr core. Calculations which include both $\Delta N=0$ and $\Delta N=2$ excitations of the core have also been performed for the A=132 mass region;[22] in this case calculated E2 effective charges turn out to be systematically smaller than experiment and futher work needs to be done to understand the reason for this.

We recently discovered that the SGII interaction gives a qualitatively good description of the valence spectra.[23] This was surprising because such calculations with other Skryme interactions work very poorly for the valence spectra, and some even give an "anti-pairing".[23] The SGII interaction has a relatively weak $\rho^{1/6}$ density dependence as compared to the usual linear density dependence. This may be reason for the better agreement. Thus far all of the parameters of the SGII interaction have been based on the properties of the ground and excited states of closed-shell nuclei. However, there remains an ambiguity in some of the parameters. We plan to try to remove this ambiguity and further improve the interaction by making least squares fits to the sd shell binding energies and excitation energies.

The attempts to improve upon the shell-model wave functions by enlarging the model space require a continual improvement in the computational techniques. We have extensively used the MSU versions of the Rochester-Oak-Ridge code and OXBASH, the Oxford-Buenos-Aires code. With the help of E. Ormand and J. Winfield, many improvements have been made in OXBASH to make it faster, more comprehensive and more useful. A manual for OXBASH has been updated,[24] and the program has been sent to about 20 people who have made requests for it. At present OXBASH is very much oriented to the file handling facilities available with the VAX software. In the near future we plan to convert the programs to a more general form which can be used on the FPS164 array processor as well as on the supercomputers which are now becoming more easily available to the physics community. We have also used OXBASH to examine the statistical properties of the shell-model

wave functions which are important for the random matrix theory approach to nuclear excited states and nuclear reactions.[25]

(iii) ISOSPIN AND PARITY NON-CONSERVING INTERACTIONS

The nucleon-nucleon interactions discussed in the previous section conserve both isospin and parity; a typical two-body matrix element in the sd shell has a magnitude of several MeV. The size of the isospin non-conserving (INC) component is several hundred keV, and the size of the parity-non-conserving (PNC) component is about 1 eV. Thus, for most purposes the calculations of the INC and PNC components can be simplified by using perturbation theory. We have worked out the shell-model formalism for evaluating the two-body transition densities needed for these calculations and have written computer programs to evaluate the matrix elements.[24]

We were one of the first[26] to use these procedures to make a fully microscopic calculation for parity violation in light nuclei (^{10}B, ^{16}O, ^{18}F, ^{19}F and ^{21}Ne) using the DDH interaction.[27] This has led to some interesting constraints on the PNC interaction.[28] We have also made calculations for other cases of interest in ^{6}Li[29] and ^{14}N.[30] However, it turns out that the matrix elements of the PNC interaction are quite sensitive to the nuclear structure,[31] and we feel that major progress in this area relies on the improvements in the shell-model wave functions which will come out of the research proposed in the previous section.

Our initial work on the effects of isospin non-conservation (INC) included a comprehensive study of analogue-state displacement energies and forbidden Fermi decays in the $f_{7/2}$ shell,[32] and a survey and interpretation of displacement energies (the Nolen-Schiffer anomaly) in mirror nuclei.[33] For the mirror nuclei we found that the "core-compression" effect proposed[34] accounts remarkably well for all displacement energies between A=17 and 55, except for those states which are very loosely bound. This work has been extended to include the new results for the A=57[35] and A=59[36] mirror nuclei obtained by the MSU group. The "core-compression" effect is, however, just a phenomenological interpretation of the Nolen-Schiffer anomaly, and we believe that more work needs to be done in order to understand the relative importance of higher-order nuclear-structure effects and charge-asymmetric interactions.

More recently we have calculated INC in light nuclei within the framework of the large-basis shell model, and Erich Ormand has just finished his Ph.D. thesis work on this subject.[37] The basis of this work is to find a unified empirical interaction which can describe all aspects of the INC. The empirical interaction has been determined by making least square fits of the b and c coefficients of the isobaric mass multiplet equation ($M = a + b\,T_z + c\,T_z^2$) to forms of the INC interaction, which include charge-dependent and charge-asymmetric strong interaction terms as well as the usual Coulomb interaction.[37, 38] We find clear evidence for a charge-dependent proton-neutron interaction which is about 2% stronger than the average of the proton-proton and neutron-neutron interactions.[38] The charge-asymmetric interaction must be treated carefully in order to take into account the isovector potential in the Hartree-Fock mean field induced by the Coulomb potential. After making a correction for this induced isovector potential we find evidence for a charge-asymmetric interaction where the neutron-neutron interaction is 1-1.5% stronger than the proton-proton interaction.[37]

We have used these new potentials to calculate the INC correction to allowed ($0^+ \rightarrow 0^+$) Fermi decay. The ft value for these decays have been measured to an accuracy of about 0.05%,[39] and they provide the most accurate souce of information on the weak-interaction vector coupling constant for the nucleon. Comparison with the vector coupling constant deduced for the decay of the muon provides an important test for the weak interaction theory, in particular for the universality of the Cabbibo angle and the calculations of the radiative corrections.[40,41]

Calculations have been made for the "isospin-mixing" correction as well as for the "radial-overlap" correction. The radial-overlap correction was based on radial wave functions obtained from self-consistent Hartree-Fock calculations for the parent and daughter nuclei. The Fermi decay of ^{34}Cl was the subject of our first study[38] where we found a large difference between the INC correction compared to previous calculations.[42] The calculations have been extended to include all cases of interest.[37] Isospin-forbidden Fermi decays have also been considered, including those for ^{24}Al,[43] ^{28}Si,[44] and ^{42}Sc.[45]

Another aspect of INC in light nuclei concerns the isospin-forbidden proton and neutron decays. The $T=3/2 \rightarrow T=0$ decays have been systematically studied for many nuclei. The experimental reduced widths for the decay of

the lowest T=3/2 states show a $\Delta A=8$ periodicity which has led to much interest in the origin of this effect.[46,47] Recently we have used our empirical INC interaction together with Wildenthal's isospin-conserving interaction in the full sd shell-model space, to calculate these INC nucleon decays for the sd shell nuclei.[48] Our calculation accounts for the observed magnitude and size of the state-to-state variation of the reduced widths. We also find that the mixing with the T=1/2 states, which lie within a few hundred keV of the T=3/2 state, are important and that the calculated state-to-state variation is due to the more-or-less random or statistical properties of the positions, allowed widths, and isospin mixing matrix elements for these states. The variation that we find does not show a $\Delta A=8$ periodicity but is of a statistical nature. We propose to look further for more favorable situations where the INC decay is not dominated by mixing with the nearby states. In particular, we plan to make calculations for $T=2\rightarrow T=1/2$ and $T=5/2\rightarrow T=0$ proton and neutron decays and for $T=2\rightarrow T=0$ alpha decays.

(iv) M1 AND GT EXCITATIONS AND DOUBLE BETA DECAY

The study of the M1 gamma decay, magnetic moments, and Gamow-Teller (GT) beta decay provides a relatively direct test of the multi-particle structure of the nuclear wave functions and of the nature of the electromagnetic and weak interactions. We have emphasized a unified study which encompasses essentially all relevant data in a wide variety of nuclei.

Concerning the spin part of these operators, three important conclusions were obtained[3] by considering the isoscalar and isovector magnetic moments for mirror pairs of sd-shell nuclei and the Gamow-Teller decay between them: (1) A large quenching [$\langle\sigma\rangle$(effective)=0.7$\langle\sigma\rangle$(free)] for the matrix elements deduced from the isoscalar moments was found. This can be attributed only to higher-order configuration mixing.[49] (2) Large quenching [$\langle\sigma\tau\rangle$(GT-effective) = 0.73$\langle\sigma\tau\rangle$(GT-free)] for the matrix element deduced from GT beta decay was found. Comparison with other the calculations,[49] together with the fact that higher-order configuration mixing was found to be important for the $\langle\sigma\rangle$ matrix elements, indicates that about two-thirds of the Gamow-Teller quenching comes from higher-order configuration mixing and about one-third of it comes from exchange currents due to delta-isobar admixtures. Thus, we favor those models in which the

higher-order configuration mixing dominates[49,50] over those in which the delta-isobar admixtures dominates.[51] (3) Relatively less quenching [$\langle\sigma\tau\rangle$(M1-effective)=0.9$\langle\sigma\tau\rangle$(M1-free)] was found for the matrix elements deduced from the isovector magnetic moments. This shows the effect of enhancement from the pionic exchange currents, which are important for the (vector) M1 operator but not for the (axial-vector) GT operator.

We also deduced the properties of the effective orbital and spin-tensor ($[Y^2 \otimes \sigma]^1$) parts of the effective operators.[3] The magnitude of the spin-tensor term was also isolated in an analysis[52] of the ℓ-forbidden $3/2^+ \rightarrow 1/2^+$ GT and M1 decays in ^{39}Ca and ^{39}K. The large quenching for the isoscalar M1 spin operator was recently confirmed in a (p,p') experiment on ^{28}Si.[5]

It has been pointed out that the main correction to the isoscalar orbital operator is inversely proportional to the renormalization of the nucleon mass in the nucleus.[53] Recent calculations in a relativistic meson field theory indicate as much as a 20% decrease in the nucleon mass.[54] Our empirical result[3] of [$\langle\ell\rangle$(effective)=1.04$\langle\ell\rangle$(free)] thus shows that the conventional nonrelativistic treatment is more appropriate.

The previous analysis[3] has recently been extended to include essentially all GT beta decays in the sd shell[6] and all M1 moments and transitions.[55] In addition, we have used our wave functions and effective operators to predict the lifetimes and decay properties of the very neutron-rich nuclei in the sd shell.[7] Similar calculations have also recently been carried out for the neutron-rich p-shell nuclei and compared to new experimental results obtained with the RPMS at the NSCL.[56] In addition, we have made calculations for neutron-rich fp-shell nuclei which have been studied in beta decay[57] and with exotic transfer reactions[58] at Brookhaven.

The experimental sd-shell beta-decay strengths are uniformly quenched, relative to theory, by a factor of about 60%. The GT beta decays have recently been supplemented by information on the "giant" GT strength as a function of excitation energy which can be extracted from forward-angle (p,n) and (p,p') cross sections with E_p = 100-200 MeV.[59] The 60% quenching is qualitatively consistent with the results of a number of (p,n) experiments in the sd shell,[60] as well as in the fp shell.[61,62]

However, we have recently found evidence for a systematic difference between GT beta decay and the strength extracted from (p,n) reactions.[59]

This difference is strongly evident in the $p_{1/2} \rightarrow p_{1/2}$ $^{15}N(p,n)^{15}O(gs)$ transition at E_p=135 MeV. It appears to be associated with the spin-tensor component of the transition operator, thus indicating that the tensor component of the nucleon-nucleus interaction may be at fault. We have joined in experimental proposals at the IUCF[63] and TRIUMF[64] to study this anomaly over the 100-400 MeV energy range.

It is also important to compare the GT strengths obtained in (p,n), (p,p') and (n,p) from the same target nucleus. On a neutron-rich nucleus with isospin T_0, the (p,n) reaction can reach all three components (T_0-1, T_0 and T_0+1) of the GT resonance. However, the strength is dominated by the T_0-1 component and the upper components usually cannot be isolated (although near N=Z there is evidence in a few cases for the T_0+1 component in (p,n) reactions).[65] The T_0 component can be isolated in the (p,p') reaction and the T_0+1 component can be isolated in the (n,p) reaction.

For A>40 it is rather surprising to find in (p,p') reactions only about 30% of the expected strength in the T_0 component.[62-66] On the experimental side, the T_0 strength is most concentrated in $^{48}Ca(p,p')$,[66] and this case will be studied with higher resolution on the new K600 spectrometer at the IUCF.[67] On the theoretical side, we note that the shell-model wave functions used for A>40 are very truncated relative, for example, to our sd-shell wave functions, and we have pointed out that the total strength in the T_0 component can be greatly reduced by allowing for more configuration mixing in the initial state.[62] The strength in the T_0-1 state is reduced even more by this mechanism, and this is one of the reasons we have advocated (n,p) reaction studies.[68]

The (e,e') and (p,p') reactions to the same final states can be compared in order to extract information on the relative spin and orbit contribution to the 1^+ transition. Recent comparisons for nuclei in the $f_{7/2}$ shell and the rare-earth region[69] have shown that some of the low-lying 1^+ states are dominated by the orbital contribution. For the $f_{7/2}$ region we had predicted relatively large M1 strengths to the lowest 1^+ states[70] in ^{46}Ti, ^{48}Ti and ^{50}Cr, and these indeed turn out to have about equal orbital and spin contributions for the (e,e')[71] in this simple model. When more fp shell configurations are admixed, the orbital contribution is not changed much, while the spin contribution is slightly reduced.[72] Similar low-lying 1^+ states built upon the $d_{5/2}$ configuration can be found in the lower sd

shell,[55] for example in ^{20}Ne.[73] Theoretically, the properties of the 1^+ states in the rare-earth nuclei were first discussed in the context of the Nilsson model.[74] Together with O. Scholten and A. Kuliev, we have made new calculations in the Nilsson model for many nuclei, which include a pairing interaction, a residual Q·Q interaction, and a $\sigma\cdot\sigma$ interaction. The results of these calculations show that the orbital strength is spread out over the entire spectrum, 2-9 MeV, and that the spin strength is small for the low-lying states and concentrated in the 7-9 MeV region.

M1 and GT strength in LS closed-shell nuclei such as ^{16}O and ^{40}Ca are indicative of the non-closed shell admixtures into the ground states of these nuclei. A relatively large amount of strength has been found experimentally in the lowest few 1^+ T=1 states, and we have made several shell-model calculations which can qualitatively account for this.[75-76] However, on a quantitative level, we find the strength distribution to be quite sensitive to the model-space and interaction assumed for the ground state correlation,[75] and we hope to find more reliable methods and better interactions for doing these calculations. We are in close collaboration with several groups analyzing the (p,p') and (p,n) cross sections to these states. In addition, we note that double-gamma decay experiments in LS closed-shell nuclei can be related to these M1 strengths,[77] and we have made shell-model calculations for the $0_2^+ \rightarrow 0_1^+$ (gs) transition in ^{16}O which are in good agreement with experiment.[78] Further calculations are planned for the double-gamma decay of sd-shell nuclei.

The M1 and GT properties of nuclei are important for the interpretation of various experiments and models needed for neutrino studies and astrophysics. For example, the Gamow-Teller strength from the ground state of ^{71}Ga to excited states in ^{71}Ge is needed for the calibration of proposed solar neutrino experiments.[79-80] One of the most important issues concerns the GT strength to the first excited $5/2^-$ state at 0.175 MeV. With 35 MeV protons the first excited state was excited with a (p,n) cross-section almost equal to that of the ground state.[81] However, we have shown that the transition to the excited state is dominated by the terms with $\Delta J>1$ at this energy and that the GT part alone is probably small.[82] The $\Delta J>1$ terms should be less important at higher proton energies, and this seems to be borne out by experiment at 120 MeV.[79] Another important question concerns the contribution of the analogue transition to the 0^+ state. Up to now this

has not been included in the solar-neutrino calculations because it is above the neutron decay threshold and it is assumed that it particle decays. However, gamma decay may compete since the neutron decay is isospin forbidden; we plan to make calculations for the decay modes of this state.

Finally, we conclude this section with a summary of our present and proposed work on double beta decay. With some approximations, double beta decay can be regarded as a coherent summation over intermediate 1^+ states of the β^- GT strength from the ground state of the initial nucleus times the β^+ GT strength from the ground state of the final nucleus. Because of the very different phase-space factors for two-neutrino and neutrinoless double-beta decay, this decay in nuclei is very sensitive to the properties of the neutrino such as its mass.[83] The degree to which this sensitivity can be exploited depends upon the accuracy with which the nuclear two-body density can be calculated.

We have examined the case for the $^{48}Ca \rightarrow {}^{48}Ti$ double-beta decay[84] to investigate: (1) the validity of some of the approximations often used,[83] (2) the sensitivity to the model-space truncation, and (3) the sensitivity to the effective two-body interaction used. Due to large cancellations in the summation over intermediate states, the usual approximations of taking the excitation energy out of the summation for two-neutrino decay and the (1/r) factor out of the integral for neutrinoless decay are not very good. The model-space sensitivity was explored by making calculations for the analogous case in the sd shell, $^{22}O \rightarrow {}^{22}Ne$, where the full configuration space could be used. We plan to continue the study of ^{48}Ca as well as for heavier nuclei such as ^{76}Ge, by making use of the above-mentioned improvements in the shell-model effective interactions and computational techniques. On the experimental side, we have encouraged the study of the $^{48}Ti(n,p)$ reaction at TRIUMF[85] in order to test this aspect of the calculation.

(v) OTHER ASPECTS OF ELASTIC AND INELASTIC EXCITATION

One of the most fundamental and well-determined properties of a nucleus is its spatial extension. We have had a long interest in combining the Hartree-Fock mean field theory with the techniques of the large-basis shell model in order to understand nuclear shapes and sizes.[84-89] Also we have collaborated with others in using these nuclear densities in folding-model

calculations of α, ^{6}Li, ^{7}Li, and ^{12}C elastic and inelastic scattering.[92] In our most recent work[91] we compared essentially all measured rms charge radii with the droplet-model, with global harmonic-oscillator and Woods-Saxon potential models, and with the spherical Hartree-Fock model based on the SIII and SGII Skyrme interactions.[19] The B(E2) values to the low-lying 2^+ states were considered in order to account for zero-point vibrations[93] and for deviations from a spherical intrinsic shape. The SGII model was found to be most successful in reproducing the trends of the experiment.

In the sd shell we have made extensive calculations for the low-lying E2 and E4 excitations. Experimental information is most plentiful on the E2 mode from both gamma decay and electron scattering. There is also some data available on the E4 mode from electron scattering.[8-10] Theoretically, the E2 and E4 transitions are dominated by the isoscalar component. The experimental matrix elements are uniformly larger than theory by a factor of 1.7 for E2 and 2.0 for E4.[8] These large isoscalar effective charges can be understood in a microscopic theory by a coupling of the valence sd shell configurations to the "giant" E2 and E4 states near $2\hbar\omega$ in excitation.[20]

In comparisons with the deformed model-calculation of Zamick, the E4 mode has proved particularly interesting. The shell model predicts about equally strong E4 transitions for all sd shell nuclei,[8] whereas the deformed model predicts very small E4 strength in the upper part of the sd shell.[94] Experimental data for ^{32}S support the shell-model prediction.[10]

The isovector component in the low-lying E2 transitions is weak compared to the isoscalar component and for this reason has proved difficult to analyze empirically.[2] Also it turns out that the isovector component is in some cases sensitive to the difference between the wave functions obtained with the Chung-Wildenthal interaction[2] and those obtained with the new USD interaction.[55,95] One of the consequences of the isovector component is an asymmetry between the B(E2) values in mirror transitions. It can also be studied by inelastic hadron scattering on the stable neutron-rich nuclei.[9] Results from these types of experiments have been recently summarized by Alexander.[95] Experiment is in reasonable agreement with theory except for the $2_2^+ \rightarrow 0_1^+(gs)$ (T=1→T=1) transition in A=34.

Electron scattering usually provides the cleanest and most model independent method for studying nuclear transition densities. Over the past few years we have made extensive calculations for electron scattering to

low-lying states in the p and sd shell nuclei. A summary of the theoretical methods used in the plane-wave impulse approximation is presented.[13] Detailed studies include those for E2 and E4 excitations for the stable even-even sd shell nuclei;[8] elastic magnetic excitation (M1, M3 and M5) for the ground states of the stable odd-even and odd-odd p and sd shell nuclei;[11] excitation to all states in ^{19}F;[13] and excitation to all states in ^{27}Al.[11]

Some data exists for E0 matrix elements which connect excited 0^+ states to the ground state and new electron scattering data out to a momentum transfer of 3 fm^{-1} are available.[96] From our experience, the E0 excitations prove difficult to understand, and more work needs to be done.

Several projects are of current and future interest. We have found that there are significant concentrations of the strength of the transverse E4 operator which should be excited in the inelastic scattering from 0^+ targets to higher-lying 4^+ states. These concentrations correspond to excitations of stretched $0d_{5/2}$ hole-$0d_{3/2}$ particle configurations which are analogous to the stretched $0d_{5/2}$ hole-$0f_{7/2}$ particle 6^- configurations already identified in inelastic electron and proton scattering.[97] We are collaborating with the group at NIKHEF for an experiment to look for the predicted E4 strength in ^{26}Mg.[98]

Available evidence[99] suggests that the strength of the M3 (unique first-forbidden beta decay) operator is dramatically quenched in sd-shell nuclei. More electron scattering experiments, both inelastic and elastic, are needed to clarify this issue. We are calculating the M3 form factors for cases of practical experimental interest. Concurrently, we are calculating M5 form factors and have found significant concentrations of M5 strength in low-lying states. We are conferring with various experimental groups, such as the one at Saskatoon which has data from Mainz and Darmstadt on ^{20}Ne.[100] Complementary (p,n) data on these higher multipole transitions is being analyzed in collaboration with the Kent state group for sd-shell[101] as well as fp-shell[102] nuclei.

Finally, we mention the need in future work to go beyond the plane-wave impulse approximation for the electron scattering calculations. It is clear from our analysis of M1 and GT excitation discussed above that mesonic-exchange currents as well as higher-order configuration mixing are

important. For the most part, the nature of the effective operator at zero-momentum transfer is understood. However, this understanding cannot be trivially extended to finite momentum transfer. P. Blunden has calculated these corrections as a function of momentum transfer for the single-particle and single-hole states,[103] and we have started collaborations in order to combine these with the multi-particle wave functions.

(vi) TRANSFER REACTIONS

For the $f_{7/2}$ shell (p,π^-) reactions, we were the first to show[104] that the detailed selectivity for populating high-spin states[105] follows from the $f_{7/2}$ structure of these states together with some simple assumptions about the reaction mechanism. The $^{48}Ca(p,\pi^-)^{49}Ti$ data is particularly striking with the spectra dominated by two strong peaks. Two-nucleon transfer in the $f_{7/2}$ shell is of course more familiar and better understood.[106,107] The expected structure of these states has been confirmed in a recent experiment and calculation for the $^{51}V(d,\alpha)^{49}Ti$ reaction.[108]

Recent results for the relative strengths and angular distributions for the states seen in the $^{88}Sr(p,\pi^-)$ reaction are in remarkably good agreement with our calculations in the $g_{9/2}$ shell.[109] Experiments have been carried out to look for similar concentrations of strength for the $h_{11/2}$ orbit in ^{144}Sm and for the $i_{13/2}$ orbit in ^{208}Pb.[110] However, the results for these heavier nuclei are more difficult to interpret since they appear to have unresolved multiplets of states.

To extend these calculations we propose to extend the one-orbit formalism[104] to include many shell-model orbits. This will be important for the interpretation of new experiments which have been carried out or proposed for p and sd shell targets at IUCF with the (p,π^-) reaction[111] and at LAMPF with the (π^-,p) reactions.[112]

Finally, we mention that we are involved in collaborations to study the microscopic models for pion double-charge exchange. Work which considers the nuclear structure effects in the $T=0 \rightarrow T=2,0^+ \rightarrow 0^+$ nonanalog transitions is in progress[113] and other studies are planned.

References:

1. B. A. Brown and B. H. Wildenthal, Phys. Rev. C21, 2107 (1980); B. A. Brown, W. Chung and B. H. Wildenthal, Phys. Rev. C21, 2600 (1980); B.

A. Brown, W. Chung and B. H. Wildenthal; Phys. Rev. C22, 774 (1980); B. A. Brown, W. Chung, B. H. Wildenthal and T. A. Shibata, Phys. Rev. C22, 842 (1980); B. A. Brown, J. Phys. G8, 679 (1982).
2. B. A. Brown, B. H. Wildenthal, W. Chung, S. E. Massen, M. Bernas, A.M. Bernstein, R. Miskimen, V. R. Brown and V. A. Madsen, Phys. Rev. C26, 2247 (1982).
3. B. A. Brown and B. H. Wildenthal, Phys. Rev. C27, 1296 (1983).
4. B. A. Brown and B. H. Wildenthal, Phys. Rev. C28, 2397 (1983), and B.A. Brown, in the proceedings of the 1985 Kikuchi Summer School.
5. N. Anantaraman, B. A. Brown, G. M. Crawley, A. Galonsky, B. H. Wildenthal, C. Djalali, N. Marty, M. Morlet, A. Willis and J. C. Jourdain, Phys. Rev. Lett. 52, 1409 (1984).
6. B. A. Brown and B. H. Wildenthal, Atomic Data and Nuclear Data Tables, November 1985.
7. B. H. Wildenthal, M. S. Curtin and B. A. Brown, Phys. Rev. C28, 1343 (1983).
8. B. A. Brown, R. Radhi and B. H. Wildenthal, Physics Reports C101, 313 (1983).
9. R. Alarcon, J. Rapaport, R. T. Kouzes, W. H. Moore and B. A. Brown, Phys. Rev. C31, 697 (1985).
10. B. H. Wildenthal, B. A. Brown, and I. Sick, Phys. Rev. C32, 2185 (1985).
11. R. Radhi, Ph.D. thesis MSU, 1983 and R. Radhi, B. A. Brown and B. H. Wildenthal, unpublished.
12. B. A. Brown, R. Radhi and B. H. Wildenthal, Phys. Lett. B133, 5 (1983).
13. B. A. Brown, B. H. Wildenthal, C. F. Williamson, F. N. Rad, S. Kowalski, J. Heisenberg, H. Crannell and J. T. O'Brien, Phys. Rev. C32, 1127 (1985).
14. A. Hosaka, K. I. Kubo and H. Toki, Nucl. Phys. A444, 76 (1985); N. Anantaraman, H. Toki and G. F. Bertsch, Nucl. Phys. A398, 269 (1983).
15. G. F. Bertsch, J. Borysowicz, H. McManus and W. G. Love, Nucl. Phys. A284, 399 (1977).
16. B. A. Brown, W. A. Richter and B. H. Wildenthal, Jour. Phys. G11, 1191 (1985).
17. B. A. Brown, W. A. Richter and R. Julies, unpublished.
18. W. A. Richter, M. van der Merwe and B. A. Brown, unpublished.
19. Nguyen van Giai and H. Sagawa, Phys. Lett. 106B, 379 (1981) and Nucl. Phys. A371, 1 (1981).
20. H. Sagawa and B. A. Brown, Nucl. Phys. A430, 84 (1984), and Phys. Lett. 150B, 247 (1985).
21. P. Raghavan, M. Senba, Z. Z. Ding, A. Lopez-Garcia, B. A. Brown and R. S. Raghavan, Phys. Rev. Lett. 54, 2592 (1985).
22. H. Sagawa, O. Scholten and B. A. Brown, in the proceedings of the Workshop on Interacting Boson-Boson and Boson-Fermion Systems, ed. by O. Scholten (World Scientific, 1984), p. 276.
23. H. Sagawa, B. A. Brown and O. Scholten, Phys. Lett. 159B, 228 (1985).
24. B. A. Brown, A. Etchegoyen, W. M. D. Rae and N. S. Godwin, MSUCL report number 524, OXBASH, the Oxford-Buenos-Aires-MSU Shell Model Code.
25. B. A. Brown and G. F. Bertsch, Phys. Lett. 148B, 5 (1984).
26. B. A. Brown, W. A. Richter and N. S. Godwin, Phys. Rev. Lett. 45, 1681 (1980).

27. B. Desplanques, J. F. Donoghue and B. R. Holstein, Ann. Phys. 124, 449 (1980).
28. J. F. Donoghue and B. R. Holstein, Phys. Rev. Lett. 46, 1603 (1981).
29. R. G. H. Robertson and B. A. Brown, Phys. Rev. C28 443 (1983).
30. E. G. Adelberger, P. Hoodbhoy and B. A. Brown, Phys. Rev. C30, 456 (1984).
31. E. G. Adelberger, M. M. Hindi, C. D. Hoyle, H. E. Swanson, R. D. Von Lintig and W. C. Haxton, Phys. Rev. 27, 2833 (1983).
32. B. A. Brown and R. Sherr, Nucl Phys. A322, 61 (1979).
33. B. A. Brown and L. Meyer-Shutzmeister, Relationships Between Displacement Energies and Rms Radii, unpublished.
34. S. Shlomo and E. Friedman, Phys. Rev. Lett. 39, 1180 (1977) and E. Friedman and S. Shlomo, Z. Physik A238, 67 (1977).
35. B. Sherrill, K. Beard, W. Benenson, C. Bloch, B. A. Brown, E. Kashy, J. A. Nolen Jr, A. D. Panagiotou, J. vanderPlicht, and J. S. Winfield, Phys. Rev. C31, 875 (1985).
36. B. Sherrill, K. Beard, B. A. Brown, W. Benenson, E. Kashy, W. E. Ormand, H. Nann, J. J. Keheyias, A. D. Bacher and T. E. Ward, Phys. Rev. C28, 1712 (1983).
37. W. E. Ormand, Ph.D. Thesis, MSU, Dec. 1985.
38. W. E. Ormand and B. A. Brown, Nucl. Phys. A440, 274 (1985).
39. V. T. Koslowsky et al., in the proceedings of the Atomic Mass and Fundamental Constants conference (AMCO-7), Darmstadt Germnany, 1985, p. 60.
40. I. S. Towner and J. C. Hardy, in the proceedings of the Atomic Mass and Fundamental Constants conference (AMCO-7), Darmstadt Germany, 1985, p. 564.
41. D. H. Wilkinson in Les Houches, Session XXX, ed. by R. Balian (North-Holland, 1978), p. 879.
42. I. S. Towner and J. C. Hardy, Phys. Lett. 74B, 20 (1978).
43. C. D. Hoyle, E. C. Adelberger, J. S. Blair, K. A. Snover, H. E. Swanson and R. D. Von Lintig, Phys. Rev. C27, 27 (1983).
44. D. E. Alburger and E. K. Warburton, Phys. Rev. C20, 793 (1979).
45. W. W. Daehnick and R. D. Rosa, Phys. Rev. C31, 1499 (1985).
46. J. F. Wilkerson, R. E. Anderson, T. B. Clegg, E. J. Ludwig, and W. J. Thompson, Phys. Rev. Lett. 51, 2269 (1983).
47. A. B. McDonald and E. G. Adelberger, Phys. Rev. Lett. 40, 1692 (1978).
48. W. E. Ormand and B. A. Brown, submitted to Phys. Rev. Lett., Dec. 1985.
49. I. S. Towner and F. C. Khanna, Nucl. Phys. A399, 334 (1983).
50. A. Arima, H. Hyuga and K. Shimizu, in Mesons in Nuclei, ed. by D. H. Wilkinson and M. Rho (North Holland, Amsterdam, 1979).
51. E. Oset and M. Rho, Phys. Rev. Lett. 42, 47 (1979), and A. Bohr and B. R. Mottelson, Phys. Lett. 100B, 10 (1981).
52. E. G. Adelberger, J. L. Osborne, H. E. Swanson and B. A. Brown, Nucl. Phys. A417, 269 (1984).
53. T. Yamazaki, Phys. Lett. 160B, 227 (1985).
54. J. D. Walecka, Ann. Phys. (NY) 83, 491 (1974); L. D. Miller, Ann. Phys. (NY) 91, 91 (1975); and L. S. Celenza, A. Rosenthal and C. M. Shakin, Phys. Rev. C31, 232 (1985).
55. B. A. Brown and B. H. Wildenthal, unpublished.
56. M. S. Curtin, L. H. Harwood, J. A. Nolen, B. Sherrill, Z. Q. Xie and B. A. Brown, to be published in Phys. Rev. Lett.
57. D. E. Alburger, E. K. Warburton and B. A. Brown, Phys. Rev. C30, 1005 (1984).

58. W. Benenson, K. Beard, C. Bloch, B. Sherrill, B. A. Brown, A. D. Panagiotou, J. van der Plicht, J. S. Winfield and C. E. Thorn, Phys. Lett. 162B, 87 (1985).
59. C. D. Goodman, C. A. Goulding, M. B. Greenfield, J. Rapaport, D. E. Bainum, C. C. Foster, W. G. Love, and F. Petrovich, Phys. Rev. Lett. 44, 1755 (1980).
60. J. W. Watson, W. Pairsuwan, B. D. Anderson, A. R. Baldwin, B. S. Flanders, R. Madey, R. J. McCarthy, B. A. Brown, B. H. Wildenthal and C. C. Foster, Phys. Rev. Lett. 55, 1369 (1985).
61. B. D. Anderson, T. Chittrakarn, A. R. Baldwin, C. Lebo, R. Madey, J. W. Watson, B. A. Brown and C. C. Foster, Phys. Rev. C31, 1161 (1985).
62. J. Rapaport, R. Alarcon, B. A. Brown, C. Gaarde, J. Larsen, C. D. Goodman, C. C. Foster, D. Horen, T. Masterson, E. Sugarbaker and T. N. Taddeucci, Nucl Phys. A427, 332 (1984).
63. J. W. Watson, B. D. Anderson, R. Madey, A. R. Baldwin, B. A. Brown, B. H. Wildenthal and C. C. Foster, Research Proposal submitted to the IUCF, Nov. 1985.
64. W. P. Alford, R. Helmer, K. P. Jackson, S. Yen, K. Hicks, O. Hausser, C. A. Miller, A. Celler, D. Frekers, B. A. Brown, C. D. Zafriratos, J. Watson, and R. Henderson, Research Proposal submitted to TRIUMF, Nov. 1985.
65. R. Madey, B. D. Anderson, J. W. Watson, A. R. Baldwin, B. S. Flanders, C. Lebo, C. C. Foster, S. M. Austin, A. Galonsky and B. H. Wildenthal, Bull. Am. Phys. Soc. 27, 731 (1982); and N. Anantaraman, S. M. Austin, G. M. Crawley, A. Galonsky, H. Toki, B. D. Anderson, A. R. Baldwin, B. S. Flanders, C. Lebo, R. Madey, J. W. Watson, C. C. Foster and A. G. M. van Hees, NSCL preprint 1985.
66. C. Djalali, N. Marty, M. Morlet, A. Willis, J. C. Jourdain, N. Anantaraman, G. M. Crawley, A. Galonsky, and P. Kitching, Nucl. Phys. A388, 1 (1982).
67. G. M. Crawley, A. Galonsky, C. Djalali, B. A. Brown, V. Rotberg, N. Marty, M. Morlet and A. Willis, Research Proposal accepted at the IUCF, June 1985.
68. W. P. Alford, R. E. Azuma, B. A. Brown, A. Celler, D. Frekers, G. T. Ewan, O. F. Hausser, R. L. Helmer, K. Hicks, K. P. Jackson, C. A. Miller, B. H. Wildenthal, and S. Yen, Research Proposal submitted to TRIUMF, 1985.
69. C. Djalali, N. Marty, M. Morlet, A. Willis, J. C. Jourdain, D. Bohle, U. Hartmann, G. Kuchler, A. Richter, G. Caskey, G. M. Crawley and A. Galonsky, to be published in Phys. Rev. Lett.
70. W. Kutschera, B. A. Brown and K. Ogawa, La Rivista del Nuovo Cimento 11, (1978).
71. L. Zamick, Phys. Rev. C31, 1955 (1985).
72. B. A. Brown, unpublished.
73. W. Knupfer and B. C. Metsch, Phys. Rev. C27, 2487 (1983).
74. S. I. Gabrakov, A. A. Kuliev, N. I. Pyatov, D. I. Salomov and H. Schulz, Nucl. Phys. A182, 625 (1972).
75. K. A. Snover, E. G. Adelberger, P. G. Ikossi and B. A. Brown, Phys. Rev. C27, 1837 (1983).
76. B. A. Brown, B. Castel, D. Horen and H. Toki, Phys. Lett. 127B, 151 (1983).
77. J. Schirmer, D. Habs, R. Kroth, N. kwong, D. Schwalm, M. Zirnbauer and C. Broude, Phys. Rev. Lett. 53, 1897 (1984).
78. J. Kramp, Diplomarbeit, Heidelberg 1985.

79. D. Krofcheck, E. Sugarbaker, J. Rapaport, D. Wang, J. N. Bachall, R. C. Byrd, C. C. Foster, C. D. Goodman, I. J. Van Heerden, C. Gaarde, J. S. Larsen, D. J. Horen, and T. N. Taddeucci, Phys. Rev. Lett. 55, 1051 (1985).
80. G. J. Mathews, S. D. Bloom, G. M. Fuller and J. N. Bachall, Phys. Rev. C32, 796 (1985).
81. H. Orihara, C. D. Zafiratos, S. Nishimura, K. Furukawa, M. Kabasawa, K. Maeda, K. Miura and H. Ohnuma, Phys. Rev. Lett. 51, 1328 (1983).
82. T. Baltz, J. Weneser, B. A. Brown, J. Rapaport, Phys. Rev. Lett. 53, 2078 (1984).
83. W. C. Haxton in Progress in Particle and Nuclear Physics, ed. by D. Wilkinson (Pergamon Press, 1984), Vol. 12, p. 409.
84. B. A. Brown in Nuclear Shell Models, ed. by M. Valliers and B. H. Wildenthal (World Scientific Publishing, Singapore, 1985), p. 42.
85. W. P. Alford, R. Helmer, K. P. Jackson, S. Yen, K. Hicks, O. Hausser, C. A. Miller, A. Celler, D. Frekers, B. A. Brown and C. D. Zafriratos, Research Proposal submitted to TRIUMF, Nov. 1985.
86. B. A. Brown, S. E. Massen and P. E. Hodgson, J. Phys. G5, 1655 (1979); Phys. Lett. 85B, 167 (1979); and in the Proceedings of the Karlsruhe International Discussion Meeting on "What do we Know About the Radial Shape of Nuclei in the Ca Region?", Karlsruhe 1979, p. 377.
87. A. S. Owen, B. A. Brown and P. E. Hodgson, J Phys. G7, 1051 (1981); and J. Streets, B. A. Brown and P. E. Hodgson, J. Phys. G8, 839 (1982).
88. J. B. McGrory and B. A. Brown, in the Conference Proceedings of Lasers in Nuclear Physics (ed. by C. E. Bemis and H K Carter, Harwood Academic Publishers, 1982) p. 455.
89. R. C. Thompson, M. Anselment, K. Bekk, S. Goring, A. Hanser, G. Meisel, H. Rebel, G. Schatz and B. A. Brown, Jour. Phys. G9, 443 (1983).
90. B. A. Brown, S. E. Massen, J. I. Escudero, P. E. Hodgson, G. Madurga and J. Vinas, Jour. Phys. G9, 423 (1983).
91. B. A. Brown, C. Bronk and P. E. Hodgson, Jour. Phys. G10, 1683 (1984).
92. A. M. Kobos, B. A. Brown, P. E. Hodgson, G. R. Satchler and A. Budzanowski, Nucl. Phys. A384, 65 (1982); C. J. Woods, B. A. Brown and N. A. Jelley, Jour. Phys. G8, 1699 (1982); R. H. Bassel, B. A. Brown, R. Lindsay and N. Rowley, Jour. Phys. G8, 1215 (1982); and A. M. Kobos, B. A. Brown, R. Lindsay and G. R. Satchler, Nucl. Phys. A425 (1984).
93. H. Esbensen and G. F. Bertsch, Phys. Rev. C28, 355 (1983).
94. H. R. Jaqaman and L. Zamick, Phys. Rev. C30, 1719 (1984).
95. T. K. Alexander, G. C. Ball, D. Horn, J. S. Forster, I. V. Mitchell and H. B. Mak, Nucl. Phys. A444, 285 (1985).
96. P. Harihar, K. K. Seth, D. Barlow, S. Iverson, M. Kaletka, A. Saha, C. F. Williamson, J. W. Wong, M. Deady and W. J. Gerace, Phys. Rev. Lett. 53, 152 (1984); H. Blok, H. P. Blok, J. F. A. van Hienen, G. van der Steenhoven, C. W. de Jager, H. de Vries, A. Saha and K. K. Seth, Phys. Lett. 149B, 441 (1984).
97. R. A. Lindgren, W. J. Gerace, A. D. Bacher, W. G. Love and F. Petrovich, Phys. Rev. Lett. 42, 1524 (1979); and G. S. Adams, A. D. Bacher, G. T. Emery, W. P. Jones, R. T. Kouzes, D. W. Miller, A. Picklesiemer and G. E. Walker, Phys. Rev. Lett. 38, 1387 (1979).
98. NIKHEF proposal 84-E6 (1984).
99. M. V. Hynes, et al., Phys. Rev. Lett. 42, 1444 (1979); and E. K. Warburton, G. T. Garvey and I. S. Towner, Annals of Physics, 57, 174 (1970).

100. J. C. Bergstrom, R. Neuhausen, C. Rangacharyulu, E. J. Ansaldo and A. Richter, unpublished.
101. B. D. Anderson, T. Chittrakarn, A. R. Baldwin, C. Lebo, R. Madey, R. J. McCarthy, J. W. Watson and B. A. Brown, unpublished.
102. B. D. Anderson, T. Chittrakarn, A. R. Baldwin, C. Lebo, R. Madey, R. J. McCarthy, J. W. Watson, B. A. Brown and C. C. Foster, Phys. Rev. C31, 1147 (1985).
103. P. G. Blunden and B. Castel, preprint February 1985; and P. Blunden, preprint June 1985.
104. B. A. Brown, O. Scholten and H. Toki, Phys. Rev. Lett. 21, 1952 (1983).
105. S. E. Vigdor, T. G.Throwe, M. C. Green, W. W. Jacobs, R. D. Bent, J. J. Kehayias, W. K. Pitts and T. E. Ward, Phys. Rev. Lett. 49, 1314 (1982).
106. B. A. Brown in the proceedings of the Symposium on Shell Model Calculations for Light and Medium Weight Nuclei, Tokyo 1977, p. 13; P. Decowski, W. Benenson, B. A. Brown and H. Nann, Nucl. Phys. A302, 186 (1978).
107. A. Saha, K. K. Seth, H. Nann and B. A. Brown, Phys. Lett. 130B, 152 (1983).
108. R. Sherr, R. T. Kouzes, H. Nann and B. A. Brown, Phys. Lett. B146, 25 (1984); and H. Nann, W. W. Jacobs, A. D. Bacher, J. D. Brown, G. D. Cravens, G. T. Emery, W. P. Jones, E. J. Stephenson and B. A. Brown, Phys. Rev. C30, 1509 (1984).
109. M. C. Greene, J. D. Brown, W. W. Jacobs, E. Korkmas, T. G. Throwe, S. E. Vigdor, T. E. Ward, P. L. Jolivette and B. A. Brown, Phys. Rev. Lett. 53, 1893 (1984).
110. S. E. Vigdor, in the proceedings of the International Symposium on Nuclear Spectroscopy and Nuclear Interactions, Osaka, Japan, March 21-24 1984; and W. W. Jacobs, private communication.
111. J. J. Keyayias, R. D. Bent, M. C. Green, M. Hugi, H. Nann and T. E. Ward, IUCF annual reports 1982 and 1983.
112. C. S. Mishra, G. S. Adams, G. S. Blanpied, B. M. Preedom, C. S. Whisnant, J. P. Egger, B. H. Wildenthal, H. Breuer, D. Benton, N. S. Chant, B. G. Ritchie, B. Hoistad, B. A. Brown, S. Gilad and R. Redwine, Bull. Am. Phys. Soc. 29, 1051 (1984).
113. R. Gilman, H. T. Fortune, M. B. Johnson, E. R. Siciliano, H. Toki, A. Wirzba and B. A. Brown, unpublished.

III.B.4.b. THE NUCLEAR MEAN FIELD FOR NEUTRONS AND PROTONS

Sam M. Austin and J.S. Winfield

A number of phenomena affect the difference in the mean field felt by protons and neutrons interacting with the same nucleus. If the nucleus has $N > Z$, then the symmetry potential makes the field for protons deeper than that for neutrons, reflecting the V_τ part of the two body potential (or alternatively, that the interaction between unlike nucleons is more attractive than that between like nucleons). But even for $N = Z$ nuclei, a number of phenomena can make the interactions different: core polarization effects, a change in the effective energy of the interacting proton because of the repulsion by the charged target nucleus, or the possibility of a charge symmetry breaking (CSB) component of the effective interaction. It is important to understand these effects both for their own interest, as in the case of any CSB potential, and because they enter into phenomenological evaluations of the mean symmetry potential. The symmetry potential affects many aspects of nuclear structure, for example, the splitting of the isovector and isoscalar components of giant resonances.

1. Charge Symmetry Breaking in the Nuclear Mean Field

Recently there has been a great deal of interest in the possiblity of change symmetry breaking (CSB) in the mean field because it has been adduced to explain the Coulomb energy anomaly[1] and because the presence of six-quark structures in the nucleus naturally leads to CSB.[2] We have tried to set limits on CSB in the nuclear mean field by comparing spherical and deformed optical model (OM) analyses of nucleon scattering on light N=Z nuclei.[3,4] The basic approach is to make a straight line fit to the volume integrals of the real OM potential for protons plotted as a function of energy, (see Fig. 1); results for neutrons on the same target nucleus are then compared to these fits. After corrections for the Coulomb repulsion of the protons through a Coulomb-induced energy shift and for the effects of core polarization (i.e. unequal density of neutrons and protons, the protons being pushed out by their mutual Coulomb repulsion), the remaining difference between the corrected proton and neutron volume integrals is assumed to arise from a CSB potential. The results after the Coulomb shift

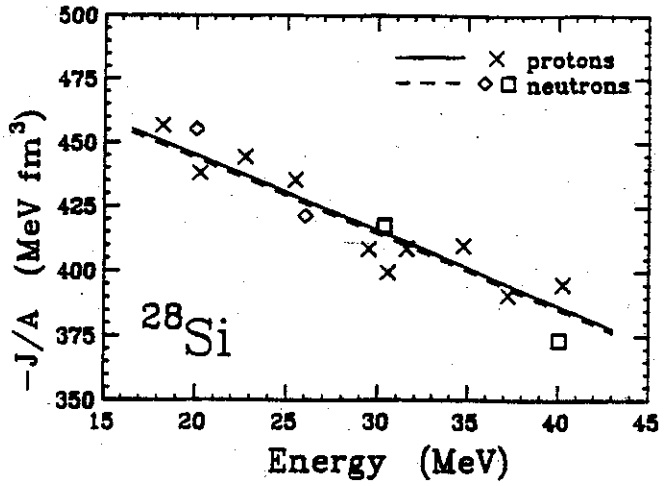

Fig. 1. Volume integrals per nucleon of the real potential describing proton and neutron scattering from ^{28}Si plotted against incident energy. The solid line is an unweighted least squares fit to the proton results. The dashed line is a fit with the same slope to the neutron results.

correction are shown in Fig. 2; after further correcting for core polarization effects one obtains for the volume integral of the CSB potential: 17±14 (^{40}Ca), -20±17 (^{32}S), -23±11 (^{28}Si), and 5±24 (^{12}C) MeV fm^3. For comparison, Negele's estimate[5] of the CSB potential needed to explain the Coulomb Energy anomaly[1] is -19 MeV fm^3.

We are currently trying to understand the somewhat marginal consistency of our results in the hope that more refined calculations will yield a definitive result. Future improvements to the procedure include a more accurate estimate of core polarization effects (see below) and analyses (possibly model-independent) without the constraint of a Woods-Saxon shape.

2. Corrections for Coulomb Effects

Commonly, the empirical OM potentials are corrected for the effect of the proton slowing in the Coulomb field of the target nucleus by assuming that the mean energy of the proton is reduced by the average Coulomb energy

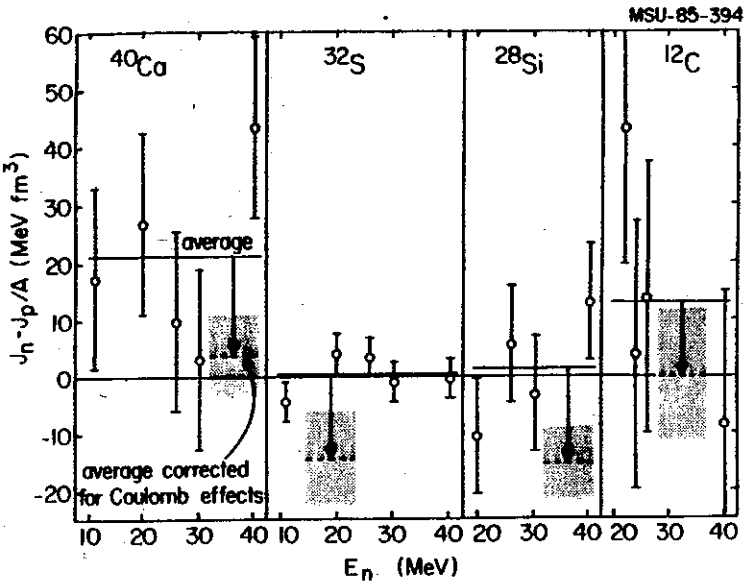

Fig. 2. Differences of volume integrals for neutron and proton scattering. The circles are the differences for the individual energies, the lines are the average differences for a given nucleus and the shaded regions give the values corrected by the coulomb shift.

E_c felt by the proton. If we take the real potential to have an energy dependence given approximately by $V_R(E) = V_R(E=0) - \alpha E$, the Coulomb correction $V_{cc} = \alpha E_c$. For $\alpha \approx 0.3$ this yields $V_{cc} = 0.4Z/A^{1/3}$. For N>Z nuclei, one then extracts the value of the OM symmetry potential by subtracting V_{cc} from the proton potential before comparing it with the neutron potential. Unfortunately, V_{cc} is not small compared to the effects of the symmetry potential and it seems unwise to rely entirely on such a simple theoretical model for the correction. For this reason, several attempts have been made to extract V_{cc} from comparisons of neutron and proton scattering on N=Z nuclei. Published results,[6] based on spherical optical model analyses for ^{40}Ca, ^{32}S and ^{28}Si, are generally consistent with $V_{cc} = 0.4Z/A^{1/3}$ although with rather large uncertainties. However, including the effects of coupled channels in the OM searches changes the situation, at least for ^{32}S and ^{28}Si, leading to results such as those of Fig. 2. The potentials for n and p

scattering are essentially the same, corresponding to $V_{cc} \approx 0$, and inconsistent with the $V_{cc} = 0.4Z/A^{1/3}$ of the simple model.

Since it seems clear that the coupled channels results should be more reliable and since the effects that led to $V_{cc} = 0.4Z/A^{1/3}$ are almost certainly present, other important effects must have been ignored. One of possible significance is the core polarization effect. In the CSB work described above, we corrected for this effect using the results of bound state Hartree Fock calculations. These calculations show that in N=Z nuclei the potential for neutrons is stronger in the outer part of the nucleus and for protons is stronger in the nuclear interior, but that the cancellation is imperfect, so the net potential is stronger for neutrons. The core polarization correction will be larger for scattering states, since absorption will prevent the projectiles from fully sampling the nuclear interior. To our knowledge no detailed estimates of this effect have been made, but it appears that it might be 25% of the usual value of V_{cc}. Another unanswered question concerns the apparent difference of the results for the spherical nucleus ^{40}Ca and for the deformed nuclei shown in Fig. 1. Were the core polarization correction larger for the deformed nuclei, this difference might be resolved.

A further complication is the usual neglect of the non-locality of the Coulomb interaction, i.e. the Coulomb interaction is assumed to be independent of energy. A crude estimate[3] of an upper limit for this effect indicates that it is probably small, but may not be negligible.

Because of the importance of accurate estimates of the symmetry potential for structure phenomena and of limits on CSB, we intend to study these effects further. Initially we will examine the effects of core polarization for neutron scattering on ^{40}Ca and ^{208}Pb via computer experiments based on Hartree Fock estimates for the difference on bound state potentials for neutrons and protons. This should sharpen our limits on charge symmetry breaking in the mean field and and give us a better

understanding of the variation of core polarization effects with mass. If core polarization has a different dependence on Z and A than the usual Coulomb correction, it will not be possible to take V_{cc} from measurements on light N=Z nuclei when analyzing scattering from heavy N ≠ Z nuclei to obtain the symmetry potential.

References:

1. J.A. Nolen, Jr. and J.P. Schiffer, Annu. Rev. Nucl. Sci. 19,471(1969).
2. V. Koch and G.A. Miller, Phys. Rev. C 31,602(1985). For further references see Ref. 4.
3. R.P. DeVito, S.M. Austin, W. Sterrenburg and U.E.P. Berg, Phys. Rev. Lett. 47,628(1981).
4. J.S. Winfield, S.M. Austin, R.P. DeVito, U.E.P. Berg, Z. Chen and W. Sterrenburg, Phys. Rev. C 33,1(1986); Sam M. Austin, Proc. Spec. Meeting on the Optical Model, Paris, Nov. 1985.
5. J.W. Negele, Nucl. Phys. A165,305(1971); J.W. Negele in "Proc. of the Int. Conf. on Nuclear Structure and Spectroscopy", edited by H.P. Blok and A.E.L. Dieperink (Scholars Press, Amsterdam, 1974).
6. J. Rapaport, Phys. Lett. 92B,233(1980); R.P. DeVito, S.M. Austin, U.E.P. Berg, R. De Leo and W.A. Sterrenburg, Phys. Rev. C 28,2530(1983).

III.B.4.c. WEAK NEUTRAL CURRENTS IN E1 TRANSITIONS

Wm. C. McHarris and J.O. Rasmussen[a]

With the mounting evidence for parity-violating effects in atoms caused by interference of neutral-weak and electromagnetic currents,[1] one is tempted to look for similar effects in nuclei. The major difficulty is that neutral weak ("neutral-β") transitions would have to compete with γ transitions, which are intrinsically faster by factors in the vicinity of 10^9. Parity-violating effects would be the most clear-cut signature; in addition, the first place to search would be where structure effects hinder γ-transitions but perhaps not the competing β-transitions. In addition to being interesting in themselves, such effects in nuclei might yield information on the coupling operational in neutral-weak currents.

The so-called anomalous E1 transitions in deformed heavy nuclei are good possibilities for scrutiny.[2] These transitions are often hindered by factors of 10^5 or more and in at least one case by as much as 10^7. In addition, the conversion coefficients for $s_{1/2}$ and $p_{1/2}$ electrons are anomalously large, at times by factors as high as several hundred. To a first approximation, the greater the degree of hindrance, the larger the anomalous conversion coefficient. In the past these have been explained, in a more or less ad hoc fashion, by considering the penetration of the electrons into the nucleus and expanding the electronic wave-functions within the nuclear radius.[3] In large nuclei, first-forbidden β transitions are increasingly enhanced, both because of the larger nuclear radii and because of the relativistic source-velocity terms, so that by the time the actinides are reached they are considerably faster than allowed transitions. A first-forbidden β transition would compete with an E1 γ transition, and for these particular "anomalous" E1's it is conceivable that much of the intrinsic difference in strength between weak and electromagnetic

interactions has been accounted for. Specifically, "neutral-β decay" would masquerade to first order as the emission of conversion electrons -- there would be a nucleon-electron interaction at both the incoming and outgoing vertices of the diagrams, resulting in a type of electron scattering. Is it possible that a portion of the excess electrons attributed to these anomalous E1 transitions originates, in fact, from neutral-β decay?

The amplitude for low-energy neutral-weak coupling between an electron and a proton or neutron can be written respectively as[4]

$$M(e,p) = -(G_F/2\sqrt{2})\bar{u}'_e\gamma^\mu(1-4\sin^2\theta_W-\gamma_5)u_e \times \bar{u}'_p\gamma_\mu(1-4\sin^2\theta_W-1.25\gamma^5)u_p$$

and

$$M(e,n) = (G_F/2\sqrt{2})\bar{u}'_e\gamma^\mu(1-4\sin^2\theta_W-\gamma_5)u_e \times \bar{u}'_n\gamma_\mu(1-1.25\gamma^5)u_n.$$

Thus, for the expected values of the Weinberg angle near 30°, neutrons, but not protons, contribute coherently to the amplitude, again enhancing the possible effect for very heavy nuclei.

We have been performing preliminary calculations and find it likely that neutral β-decay does contribute to the observed electron excess in some of these transitions. (This means that neutral-weak currents, in effect, were probably "observed" but not recognized as such some two decades ago.) Much remains to be done -- in particular, investigating the possible interference and parity-violating effects, such as recoil correlations.

a. University of California, Berkeley.

References:

1 P. S. Drell and E. D. Commins, Phys. Rev. Lett. 53 (1984) 1984; see also the review article by E. N. Forston and L. L. Lewis, Physics Reports 113 (1984) 289.
2 F. T. Porter, I. Ahmad, M. S. Freedman, J. Milsted, and A. M. Friedman, Phys. Rev C 10 (1974) 803.
3 S. G. Nilsson and J. O. Rasmussen, Nucl. Phys. 5 (1958) 617.
4 E. D. Commins and P. H. Bucksbaum, Weak Interactions of Leptons and Quarks, Cambridge Univ. Press (1983), Chaps. 4 and 9.

III.B.5. NUCLEAR ASTROPHYSICS

N. Anantaraman, S.M. Austin, T. Kajino[a], H. Toki[a] and J.S. Winfield

1. The Solar Neutrino Problem

The fact that the detection rate[1] for neutrinos in the Davis ^{37}Cl detector is a factor of 3-4 less than predicted by standard solar models is a problem of long standing. We participated in an experiment[2] on the important $^{3}He(\alpha,n)$ reaction and undertook a detailed review of the nuclear reaction rates involved to determine whether unreliable nuclear rates might be the source of the discrepancy.

Particular attention was paid to the $^{3}He(\alpha,\gamma)$ reaction because many new and somewhat contradictory data are available. The experimental results were normalized to new resonating group calculations and recommended S factors and reaction rates as a function of temperature were obtained (details and further references can be found in Ref. 3. We also recommend changing the rate of the $p+p \rightarrow D+e^{+}+\nu$ reaction, based mainly on the different axial vector coupling constant obtained from the results of measurements of angular correlations in neutron decay, rather than from the neutron half-life.

The new rates yield a predicted solar neutrino detection rate of 6.4 ± 2.3 SNU(Solar Neutrino Units) where the quoted uncertainty corresponds to 3σ. This value is in good agreement with another recent estimate of 5.8 ± 2.2 SNU,[4] but differs significantly from the measured value, 2.1 ± 0.3 SNU, indicating that the source of the solar neutrino problem is not in unreliable nuclear reaction rates; other possible explanations are that neutrinos oscillate into another form, for example, into muon neutrinos, on the way to the terrestrial detector or that the physics of the sun is not properly understood. It has, for example, been suggested that this might be a special time in the history of the sun when a mixing episode has greatly reduced its central temperature, switching off the production of the high energy ^{8}B neutrinos to which the ^{37}Cl detector is sensitive.

2. The Creation of the Light Elements

While most of the elements we see about us are synthesized in stars, those lighter than ^{12}C do not share this origin. Our laboratory has been involved for some time in measurements of cross sections and in theoretical developments related to this problem. Over the past decade an elegant picture has evolved[5] in which some of these elements are created in the the Galactic cosmic rays(^{6}Li, ^{9}Be, $^{10,11}B$) and the rest in the Universal Big-Bang expansion(^{2}H, $^{3,4}He$ and ^{7}Li). The credibility of this hypothesis lies in the fact that it provides a consistent explanation of all the abundances in an economical fashion, involving only mechanisms known from other evidence to exist in nature. There are, however, several weaknesses in the picture; in order to further evaluate its credibility they must be examined with care.

Two of these weaknesses lie in the cosmic-ray sector of the theory: possible contributions of low-energy cosmic rays to the production of ^{11}B (resolution of this concern requires further cosmic ray measurements) and the magnitude of the contributions of the $\alpha+\alpha\rightarrow$ (mass 6,7) reactions to the production of the isotopes of Li.

The situation regarding the $\alpha+\alpha$ reactions is as follows: the cross sections for mass 7 production have been measured up to 200 MeV,[6] and their exponential decrease over a significant part of this range makes it unlikely that the $\alpha+\alpha$ reaction contributes significantly to ^{7}Li production. However, the results are less clear for ^{6}Li; it is not yet certain that results are known over a large enough energy range to permit reliable extrapolation to the astrophysically important energies near 1 GeV/nucleon; taking the value of the ^{6}Li production to be that observed at the highest measured energy yields only marginal agreement with the observed abundances. Measurements of these cross sections, at least up to 300 MeV, will be carried using the K500 cyclotron, as its high energy performance increases, or using the the K800. These measurements are difficult, but use of the S320 (or preferably S800) spectrograph should allow clean results.

Another weak point has been that the Big-Bang predictions of the production of ^{7}Li have been rather inaccurate, especially in the region of

low Universal baryon density. Our studies of the $^3He(\alpha,\gamma)$ and $^3H(\alpha,\gamma)$ reactions[3] have better determined these important reaction rates, and allow us to predict the ^7Li production within ±16% at high densities and ±35% at low densities. These results, together with new measurements of the ^7Li abundance and the dependence of the predicted nucleosynthesis on the Universal baryon density ρ_B yield a new estimate of ρ_B (given as η, the number ratio of baryons to photons) as shown in Fig. 1. This value of ρ_B is

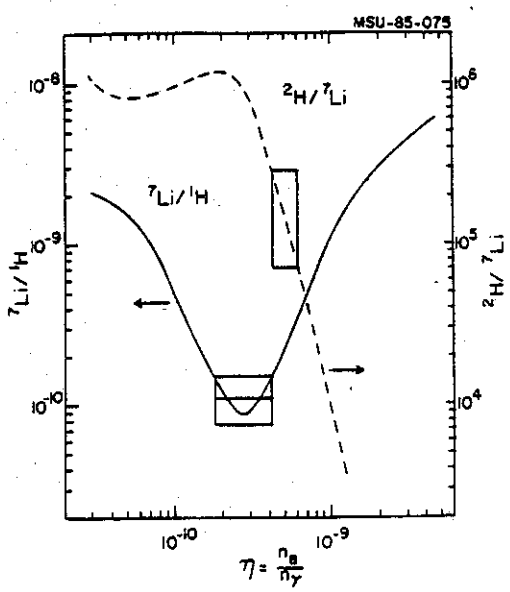

Fig. 1. Comparison of Big-Bang calculations from Ref. 2 with the observed abundance of ^7Li and the ratio of ^7Li to ^2H. The boxes delineate the uncertainties in the abundance determinations and in the resulting values of η.

consistent with values based on the other Big-Bang produced nuclides, strengthening the case for the standard scenario of light element production. These values of ρ_B are too small by an order of magnitude for the density of baryons to close the Universe. If it is indeed closed, as the Grand Unified Theories predict, then the bulk of matter must be non-baryonic in nature.

3. β^+ Strength in Astrophysics

Late in a star's life, following hydrogen and helium burning, the star passes rapidly through C-, O-, and Si-burning phases until its core is entirely converted into nuclei near iron. At this point, nuclear energy is exhausted and a gravitational collapse of the core ensues, presumably initiating a supernova explosion. During this process, electron capture

transitions in nuclei in the upper-sd and fp shells affect nucleosynthesis, neutrino cooling and neutronization (conversion of protons to neutrons by electron capture) in the stellar interior. The size of the iron core and nature of the supernova explosion are sensitive to these rates.[7]

Unfortunately, little information is available on electron capture (β^+) rates in the important nuclei. The collective Gamow-Teller strength is not energetically accessible to β decay in N>Z nuclei and charge exchange reactions such as (n,p), or (t,^{3}He) at low energies, present formidable experimental and reaction mechanism problems. Consequently, estimates of supernova behavior must rely on theoretical β^+ rates[8] which have not been tested against experiment.

As we have shown in Section B1(a), the (^{12}C, ^{12}N) reaction at energies above 50 MeV[9] may permit one to study β^+ strength. We intend as soon as possible to make preliminary measurements on ^{56}Fe(^{12}C, ^{12}N) as a prototype of these reactions and one which is itself important for the supernova problem. Initially we will use the S320 spectrograph and the new higher energy beams available with the ECR source on the K500 cyclotron. However, definitive measurements may have to await the energies of the K800 and the high resolution capability of the S800 spectrograph that will be available late in the grant period.

a. Tokyo Metropolitan University

References:

1. R. Davis, D.S. Harmer and K.C. Hoffman, p. 1037, Proc. Conf. on Interactions between Particle and Nuclear Physics, Steamboat Springs, Editor, R. Mischke (A.I.P. N.Y. 1984).
2. R.G.H. Robertson, P. Dyer, T.J. Bowles, R.E. Brown, N. Jarmie, C.J. Maggiore and Sam M. Austin, Phys. Rev. C27,11(1983).
3. T. Kajino, H. Toki and S.M. Austin, Submitted to Astrophysical Journal; Sam M. Austin, Proc. Int. Symp. on Few Body Meth., Guangxi, Aug. 1985, to be pub..
4. J.N. Bahcall, et al., Ap. J. Letters 292,79(1985).
5. Sam M. Austin, Prog. Part. Nucl. Phys. 7,1(1981).
6. L.W. Woo, et al., Phys. Rev. C32, 706(1985).
7. For an introductory review see H.A. Bethe and G. Brown, Sci. Am. 252, 60(#5,1985).
8. G.M. Fuller, W.A. Fowler and M.J. Newman, Ap. J. 252,715(1982).

9. J. Winfield, N. Anantaraman, Sam. M. Austin, L. Harwood, J. van der Plicht, H.-G. Wu and A.F. Zeller, Phys. Rev. C(to be published).

III.C.1.a. THE K=800 SUPERCONDUCTING MAGNETIC SPECTROGRAPH

J.A. Nolen, A.F. Zeller, and L.H. Harwood

One of the large pieces of experimental apparatus under construction for the phase II research program is the K=800 magnetic spectrograph (S800) shown in Figure 1. With the wide variety of beams available in phase II, from 800 MeV alpha beams to 10 GeV uranium beams (200 MeV/A and 40 MeV/A, respectively), the S800 will see a wide variety of applications. For Phase I we assembled a simple K=320 magnetic spectrograph (S320) with quite modest parameters ($p/\Delta p$=1000 and Ω=0.5 msr). The S320 has been extensively used with K500 beams for direct Q-value (mass) measurements, (e.g. ^{57}Cu), for charge-exchange reaction studies such as (^{6}Li,^{6}He) and (^{12}C,^{12}N), for heavy ion total cross section measurements via elastic scattering of ^{12}C beams, for measurements of the systematics of yields in heavy ion fragmentation reactions, and for heavy ion giant resonance studies. The results of much of this research with the S320 are given in the separate nuclear science sections earlier in this proposal.

With 40 times the solid angle, much higher energy resolution, and when used with a wide variety of higher energy and heavier beams, the S800 will permit much more than simple extensions of these studies. The usefulness of magnetic spectrographs with high energy heavy ion beams is already being demonstrated with the K=400 system SPEG at Ganil, which recently came into operation. Initial performance demonstrated that excellent energy resolution is achievable ($p/\Delta p$>10,000) with good angular resolution ($\delta\theta$~0.1°); elastic scattering studies demonstrate very rapid angular oscillations of the cross section.[1] With our high energy Phase II beams a high resolution spectrograph is essential even for the simplest reaction studies. For example with a 200 MeV/A ^{40}Ca beam elastic scattering studies require a resolution of $p/\Delta p$=20,000 to achieve an energy resolution of 800 keV. Furthermore, since the S800 has a solid angle of 20 msr, it can be used as a large solid angle, high resolution leg of a multiparticle coincidence setup. The S800 can be positioned at a scattering angle of -15° and large area gas counters positioned to detect particles on the opposite side of the beam (0-180°), for example. It will also be possible to use the S800 in a low-resolution, broad-momentum-range mode by placing detectors in the space between the two dipoles. At this location particle momentum can

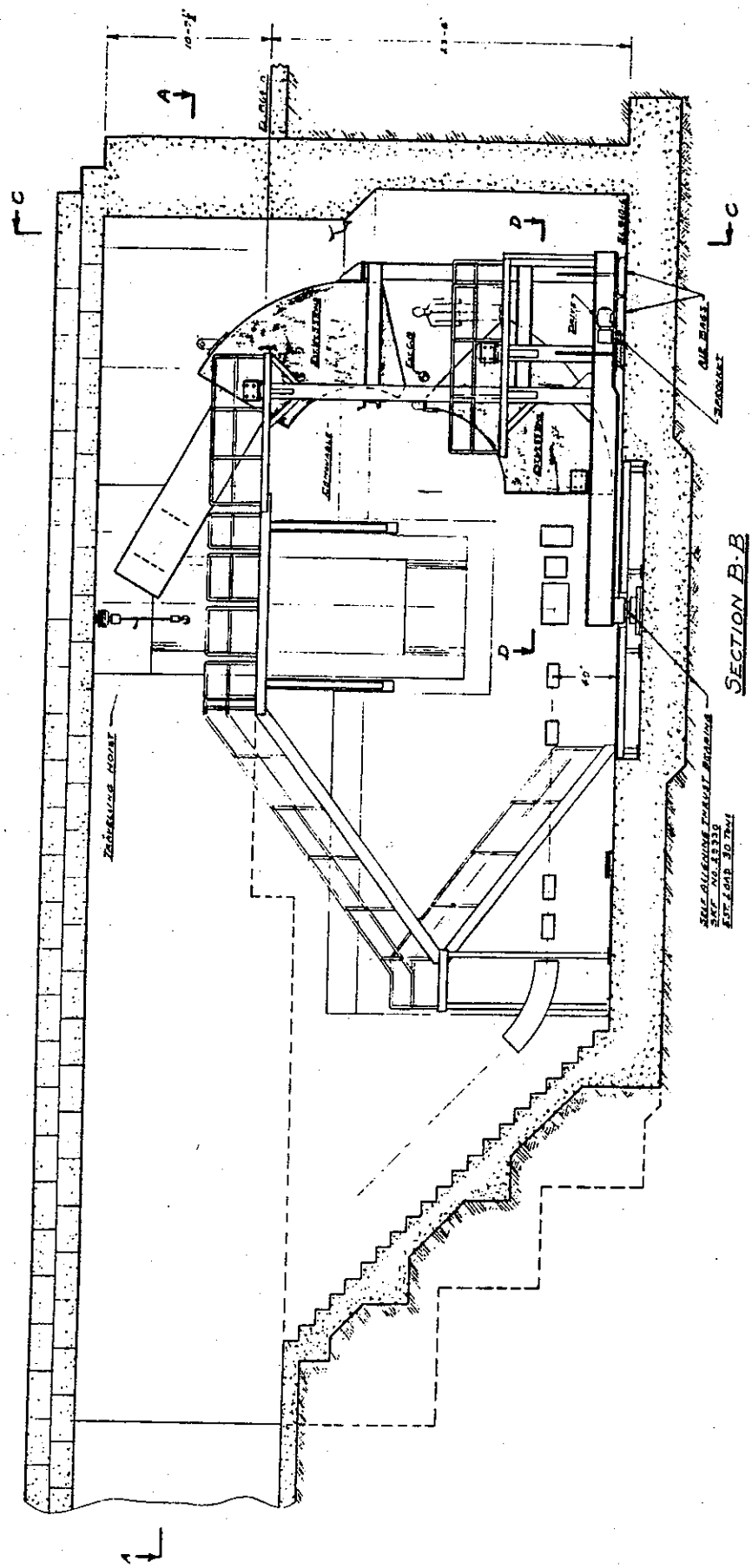

Fig. 1. Preliminary engineering drawing of the K=800 Superconducting Magnetic Spectrograph. The spectrograph is in a pit with both the analysis system and the spectrograph having momentum dispersion in the vertical plane. The scattering plane is horizontal.

be determined by ray tracing, i.e. measuring the position and angle of each trajectory.

Initial design studies presented previously,[2] convinced us that the S800 should utilize superconducting magnets. The main cost savings are due to three separate issues: 1. The solid angle can be greatly enhanced without increasing the overall dimensions of the layout by using a 2T pole-tip field quadrupole close to the target, 2. Solid angle can also be increased with minor increase in cost by using a larger than usual gap in the dipoles, 15 cm. (costs of conventional magnets scale much more rapidly with gap than do superconducting magnets.) and 3. For other parameters being equal, the superconducting dipoles are significantly less massive than conventional ones because the coils are more compact and the return iron can be operated at higher fields.

The parameters of the S800 are listed in Table I. The design may be

PARAMETERS OF THE MSU 1.2 GeV/c SPECTROGRAPH

ENERGY RESOLUTION:	$\Delta E/E=10^{-4}$ WITH 1MM RADIAL OBJECT SIZE FOR BEAM ANALYSIS SYSTEM
ENERGY RANGE:	$\Delta E/E=10\%$
SOLID ANGLE:	Ω = 10-20 MSR
RESOLVING POWER:	D/M= 12
RADIAL DISPERSION:	D=9 CM/%
RADIAL MAGNIFICATION:	M=0.78
AXIAL DISPERSION	R_{34}=0.74 MM/MR
ANGULAR RESOLUTION:	$\Delta\theta \leq$ 2MR(TOTAL OF BEAM PLUS SPECTROGRAPH CONTRIBUTIONS)
FOCAL PLANE SIZE:	50 CM (RADIAL)x15 CM(AXIAL)
FOCAL PLANE TILT:	15^0
MAGNETIC RIGIDITY:	$B\rho$ =4T-M
DIPOLE FIELDS:	B=1.5T(ρ=2.7M)
DIPOLE GAP:	D=15 CM
DIPOLE SIZE:	2 OF3.5 M LONGx100CM WIDE(75^0 BEND)
WEIGHT OF DIPOLES:	APPROX. 75 TONS EACH
QUAD SIZES:	# 1 20CM IDx40 CM LONG
	# 2 35CMx17CMx40CM
DETECTOR REQUIREMENTS:	TWO 2-DIMENSIONAL DET., 1M SEPARATION
	# 1 50CMx15CM
	# 2 62CMx16CM
	RESOLUTION: RADIAL 0.2 MM
	AXIAL 0.4 MM

Table I.

considered an evolution of the HRS at LAMPF, but the evolution is dramatic. The S800 has almost 10 times the solid angle of HRS (20 msr vs. the 2 msr normally used with high resolution at HRS) with the same resolution ($p/\Delta p$=20,000) and momentum range (5%). The S800 is much less massive than HRS and will cost about the same in 1985 dollars as HRS did in 1971 dollars.

At the present time, the S800 optical design is complete, both for the spectrograph itself and the beam analysis system.[3] It is partially constructed: the dipole steel is machined and in house, the dipole coil bobbins are complete, and the superconductor has been delivered. However, no manpower is currently going into this project due to the demands of construction of the K800 cyclotron, phase II beamline, 4π detector, and 92" chamber. Our manpower plan shows us resuming efforts on the S800 by early 1987 and completing it in 1989.

References

1. J. Gastebois, invited talk at the European Cyclotron Conference, Milan, Italy, October, 1985.
2. J. Nolen, Proceedings of the International Workshop on High Resolution, Large Acceptance Spectrometers. Argonne National Lab, ANL/PHY-81-2, September, 1981, paper III-B, J.A. Nolen, M.L. Mallory, M.J. Dubois, A.R. Gavalya, L.H. Harwood, E. Kashy, H.W. Laumer, A.F. Zeller, and H.G. Blosser, Proceedings of the 12th International Conference on High-Energy Accelerators, F.T. Cole and R. Donaldson eds. (Fermilab, Batavia, IL, 1983)p. 549., J. Nolen, Proceedings of the Tenth International Conference on Cyclotrons, IEEE publ., New York, 1984, P. 215.
3. A.F. Zeller, J. Nolen, L.H. Harwood, and E. Kashy, Proceedings of the International Workshop on High Resolution, Large Acceptance Spectrometers, Argonne National Lab, ANL/PHY-81-2, September, 1981, paper V-B, J. Nolen, ibid, paper IV-F, and A.F. Zeller, L.H. Harwood, and J.A. Nolen, MSU Cyclotron Lab Annual Report, 1981-1982, p. 88.

III.C.1.b. FOUR PI DETECTOR.

J. van der Plicht and G. Westfall

A multi detector array, capable of detecting particles ranging from pions to fission fragments over a 4π solid angle, is under construction at the NSCL. The detector consists of 32 modules, 20 hexagonal and 12 pentagonal conical shapes, together forming a truncated icosahedron (or soccerball) geometry. Each module consists of a Low Pressure Multiwire Counter (LP-MWPC) for heavy fragments, a Bragg Curve Counter (BCC) for intermediate fragments and a scintillator phoswich detector for light particles.

The detector modules will be mounted on hexagonal and pentagonal plates, which mounted on a framework, together form the vacuum vessel. The vessel layout is shown in Fig. 1. The vessel can rotate around the beam

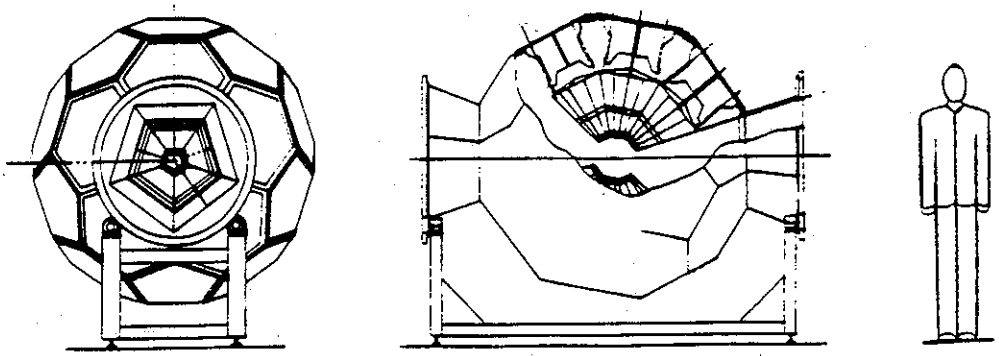

Figure 1.

axis for the purpose of taking modules in and out. Initially, the detector array will be placed on a beamline extended from the Enge spectrograph. This will allow us to use the detector with beams from the K500 cyclotron operating with the ECR source for detector commissioning and initial experiments.

The Multiwire Counter is a low pressure (typ. 2 torr) gas detector for heavy fragments. It is located at a distance of 15 cm from the target, and has a total thickness of 300 $\mu g/cm^2$. It consists of a central anode wire plane and 2 cathode foils, made position sensitive by a resistive NiCr strip (see Fig. 2.) The frames of this counter are only 0.125" thick, allowing a solid angle of 90% of 4π. The cables for signals and voltages are laid in

grooves in these frames. The gas lines are hidden in the corners of the BCC and scintillator module.

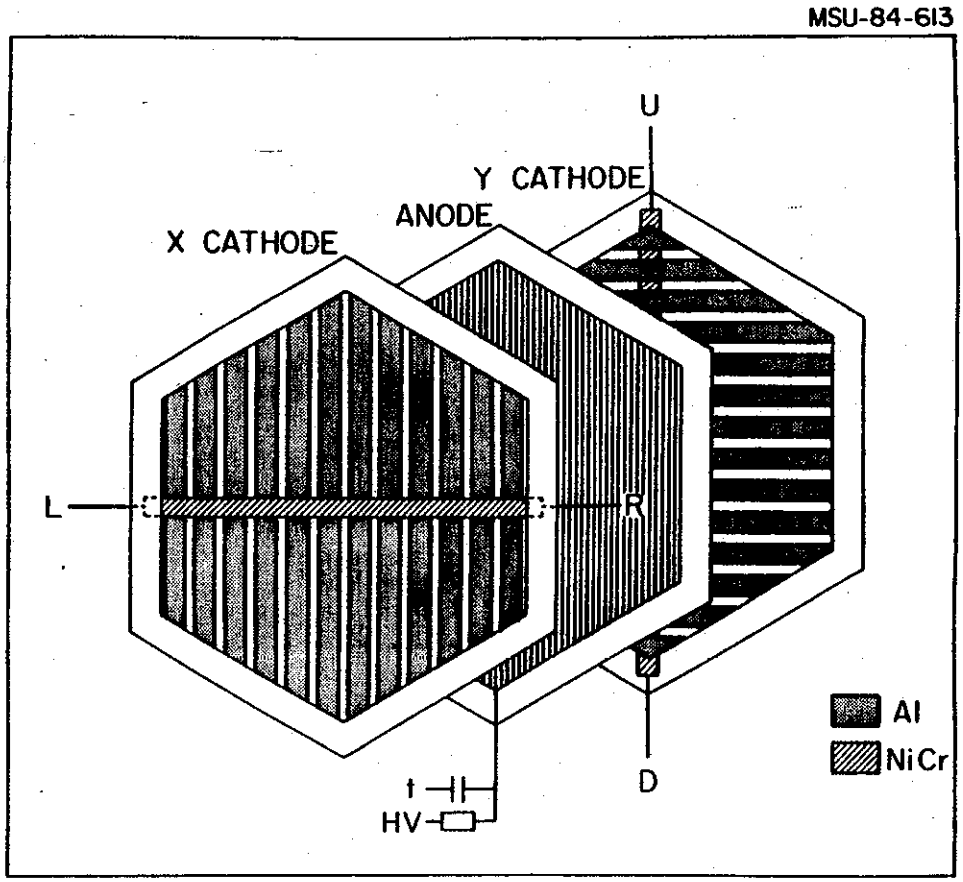

Figure 2.

The Bragg Curve Counter is a hexagonal pyramid with a length of 15 cm, attached to the plastic scintillator. The scintillator front is aluminized and will form the anode for the BCC. The detector is shown schematically in Fig.3. Since the electric field is parallel to the path of the particles, one measures the charge collected on the anode as a function of time, and thus obtains the complete energy loss distribution of the stopping ion - the "Bragg Curve". The charge Z of the ion is obtained from the maximum of the ionization; the integral of the ionization is a measure of the energy E. Charge identification up to Z=17 has been demonstrated with a prototype detector (ref.2).

The scintillator phoswich detector consists of a 3 mm thick ΔE, and a 30 cm long E scintillator. The phoswich detectors are subdivided in 6

triangular shapes for the hexagons, and 5 for the pentagons, corresponding

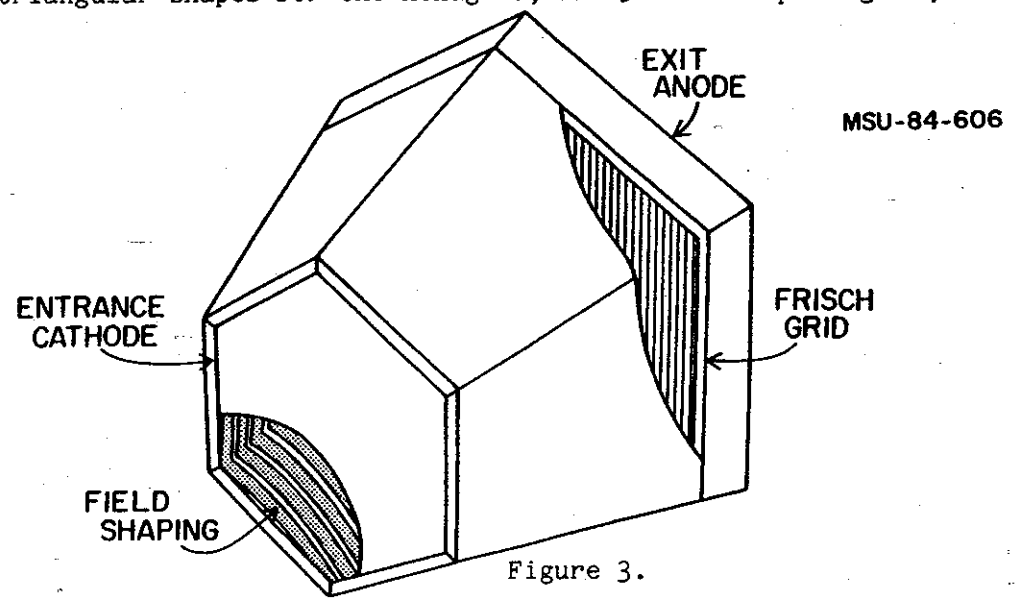

Figure 3.

to a grand total of 170 detectors. Each of these 170 elements will be read out by a 3" photomultiplier tube. The ΔE and E parts are both plastic scintillator, the only difference being the decay time constant which is 180 ns for the (slow) E part, and 3 ns for the (fast) ΔE part[1]. Thus one can obtain particle identification by applying a prompt, short gate for the ΔE signal, and a delayed, long gate for the E signal. The scintillator is capable of stopping protons with an energy of about 250 MeV.

A hexagonal prototype module has been built and used with success in various experiments. For a report on this prototype and experimental results, see Ref. 2.

This multi-detector Array also features a computer controlled gas handling system for the 60 gas detectors. The major part of the electronics consists of the fast, high density ECL line FERA ADC/TDC system.

References:

1. BC412 and BC444, Bicron, Inc., Newbury, OH 44065.
2. G.D. Westfall, J.E. Yurkon, J. van der Plicht, Z.M. Koenig, B.V. Jacak, R. Fox, G.M. Crawley, M.R. Maier and B.E. Hasselquist, Nucl. Instr. Meth. A238,347(1985).

III.C.1.c. CCD CAMERA DEVELOPMENT

S. Angius, G.M. Crawley, C. Djalali, M.R. Maier, V. Rotberg, D.K. Scott, R.S. Tickle[a], G.D. Westfall.

During the past few years, there has been an impressive growth in our understanding of high-energy heavy-ion collisions. As detailed in sections A3(e) and A3(f), it is now clear that single-particle or few-particle inclusive measurements are inadequate for many purposes and that meaningful comparisons of the experimental data with theoretical predictions are most easily made when 4π exclusive data are available. The ideal exclusive detector will have 4π solid angle, good angular and momentum resolution, high multitrack efficiency, and the capability of detecting and identifying a wide variety of emitted fragments. One such device, the MSU 4π array, has been described in section C1(b). A complementary method to study central collisions is to use a triggered streamer chamber.[1] Such a chamber, in which particular classes of events can be selected, provides many of the desirable features described above.

In the conventional use of the streamer chamber, events are recorded on film which must be manually scanned and the tracks digitized for reconstruction by computer. This is a slow and expensive process. Instead, we are developing a system which uses charge coupled devices (CCDs) as the recording medium. The CCD is a silicon image sensor consisting of a two-dimensional array of light-sensitive, electron-collecting potential wells called pixels (picture elements). This innovation promises to enormously enhance the attractiveness of the streamer chamber as a research tool. For example, CCD data which are recorded in digital form are well suited to almost fully automatic computer assisted analysis. Based on preliminary algorithms developed and tested at the NSCL, we estimate that the analysis rate for the CCD system will be 10 - 20 times faster than the manual scanning rate for events with multiplicities between 20 and 50.

Another advantage of CCDs is their large dynamic range which makes the outlook for Z identification far more promising than for film. In addition, CCDs are more sensitive than film to light and thus the streamer chamber can be run at lower electric fields, at which the chamber operates closer to the avalanche mode than the streamer mode. This ability to run at lower fields

also reduces the number of background flares, thus enhancing signal to noise and making the tracks easier to identify. Finally, since the picture is immediately digitized, image enhancing techniques can be used to improve further signal to noise.

The system was given a preliminary operational test in April 1985 when data were recorded from reactions induced by a beam of 100 MeV/A Nb on a Nb target at the LBL Bevalac streamer chamber facility. During this first test, the system operated extremely well and we feel that the results have conclusively proven the feasibility of recording streamer chamber events with CCDs.

During the April test run, about 60 near-central events were obtained and these are now being used to develop the analysis software. A representative unprocessed CCD picture is shown in Figure 1.

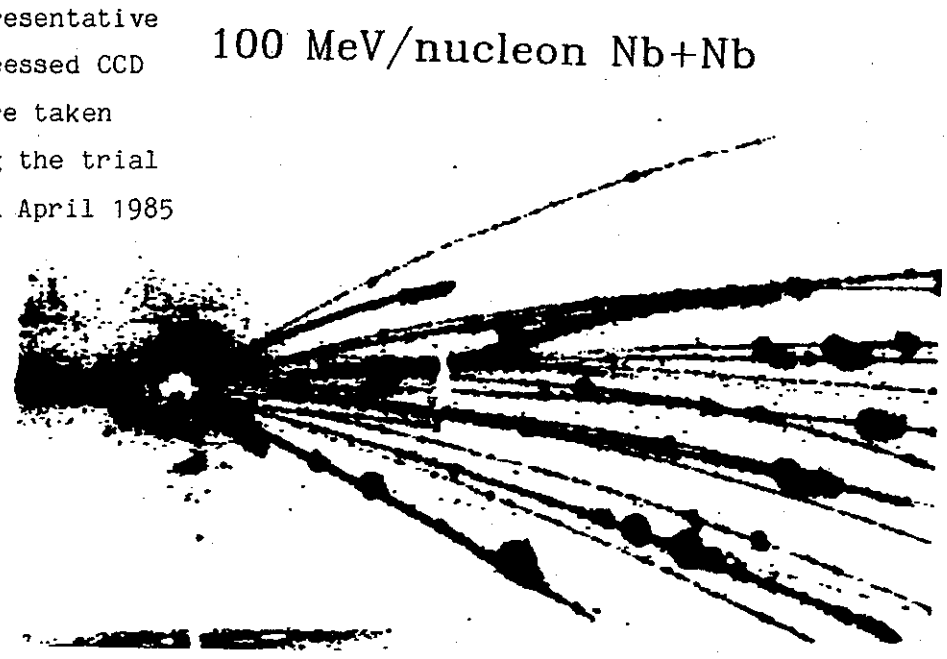

Fig. 1. A representative unprocessed CCD picture taken during the trial run in April 1985

An advantage of recording the data in digital form is the ability to use digital processing for image enhancement. Figure 2a shows a CCD picture in which the tracks are partially obscured by a intense flare, while Fig. 2b shows the same event after digital processing to make the tracks more visible. Without processing, this event would probably not be usable.

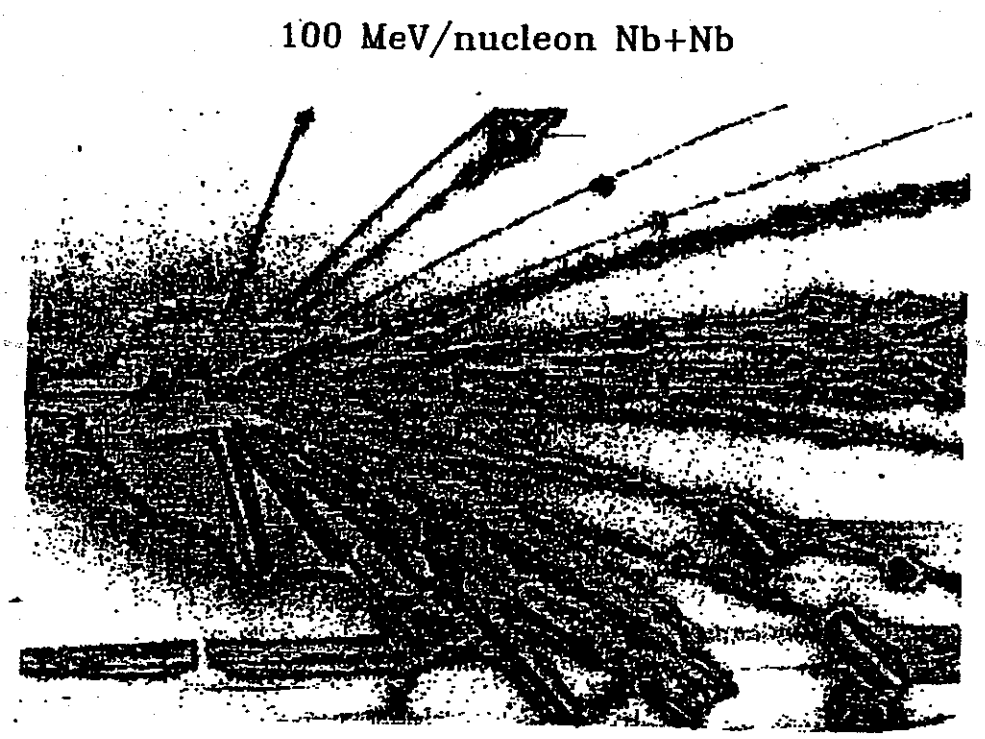

Fig. 2(a). A CCD picture in which the tracks are partially obscured by an intense flare. Without digital processing, this event would probably not be useable.

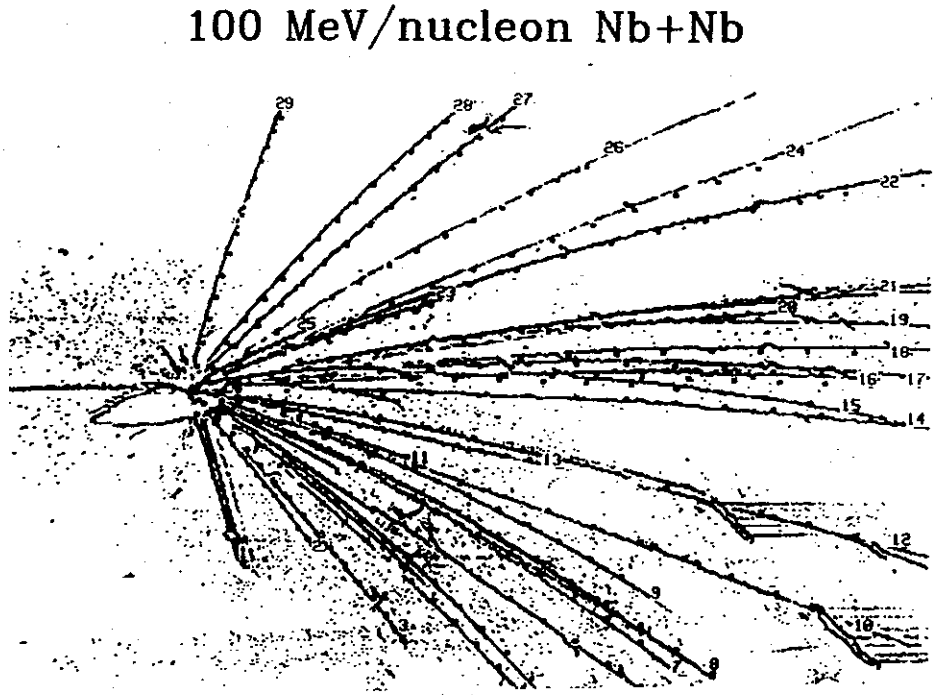

Fig. 2(b). Same event as shown in fig. 2(a) after digital processing to make the tracks more visible.

Some indication of the dynamic range of the CCDs is illustrated in Figure 3 where a vertical slice through one of the CCD pictures is shown.

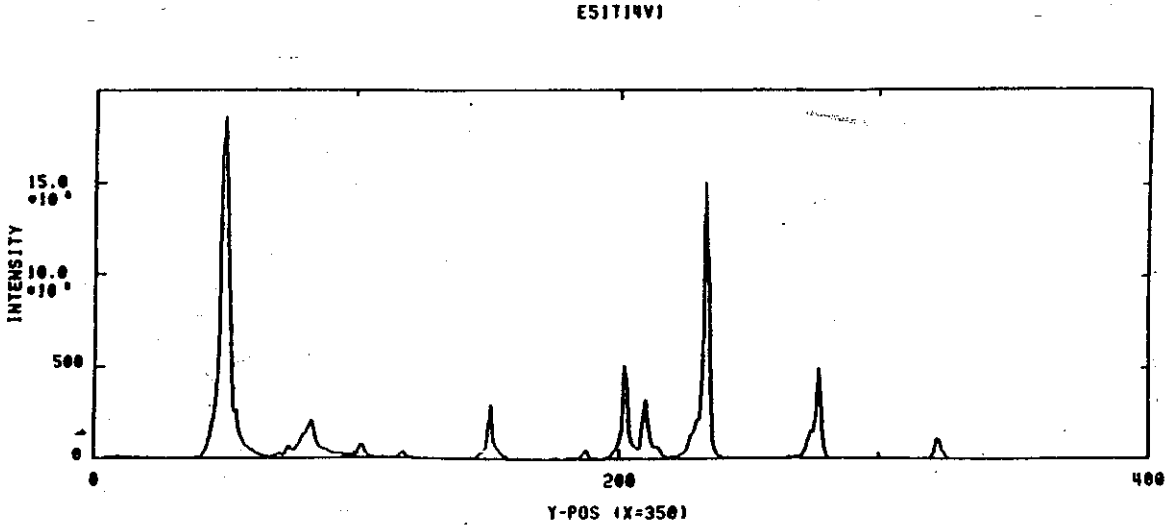

Fig. 3. A vertical slice through a CCd picture which gives some indication of the dynamic range. For reference, the dynamic range of film is around 20.

The use of the track recognition program is also illustrated in Figure 2b, where the program has found and labelled 30 tracks. We believe that the system will work even better with lower voltages and possibly with shorter pulses from the Marx generator which provides the electric field for the streamer chamber.

In summary, the CCD camera system and electronics have been assembled and tested on real events at LBL. The system works very well. The development of the analysis software has been started and already shows great promise.

Reference:

1. H. Ströbele, R. Brockmann, J.W. Harris, F. Riess, A. Sandoval, R. Stock, K.L. Wolf, H.G. Pugh, L.S. Schroeder, R.E. Renfordt, K. Tittel, and M. Maier, Phys. Rev. C27,1349(1983).

III.C.1.d. GAMMA-RAY HIT DETECTOR

D.J. Morrissey

The development of the γ-ray hit detector for installation as a Phase II device has now proceeded the mechanical design stage. The device, as envisioned during the Workshop on Phase II Apparatus in December, 1982, would measure only the number and spatial distribution of in-beam γ-rays and be built at the smallest possible cost. The initial research was geared to choosing the scintillator material and geometry of the system. Recent measurements of the populations of nuclear excited states by γ-ray emission and studies of the decay of exotic nulcei at the RPMS focal plane have pointed up the need for a large solid angle γ-ray detector with good energy resolution. Thus, the energy resolution and the timing characteristics of the scintillator became equally important in determining its usefulness as a γ-ray hit detector.

At the time of the Workshop, bismuth germanate (BGO) was a new scintillating material that warranted consideration. BGO was known to have relatively poor energy resolution, but its timing characteristics were not generally known. We have undertaken to study both of these characteristics. Commonly two different PMT's have been used, one selected for energy resolution (e.g., Hamamatsu R-1306) and one for timing (e.g., Hamamatsu R-329-2). The timing resolution of the highest quality 7.6cm x 7.6cm BGO crystal with an Amperex 2312B phototube was measured in two coincidence experiments triggered by either a NE-102 plastic scintillator using a ^{60}Co source or by a Si surface barrier telescope in-beam. No selection was made on γ-ray energy in the source measurement in order to be representative of continuum γ-ray spectra observed in-beam. The time resolution with the source, σ, was found to be 1.58 ± 0.03 ns, and in-beam was 1.40 ± 0.05 ns. These results indicate that the time resolution is dominated by the photoelectron statistics and is in fact the best that can be obtained. To see this we note that the best time resolution obtained with NaI(Tl) detectors[1] is 425 ns and the light output from a BGO scintillator is a factor of 10 lower than that of NaI(Tl), so we would expect approximately that $\sigma(\mathrm{BGO}) \approx \sqrt{10}\,\sigma(\mathrm{NaI}) = 1.34$, which is consistent with the value we have obtained.

In order to improve the energy resolution of BGO we cooled various detectors to low temperatures (as low as -50 °C), recognizing that the PMT noise and BGO light output are decreasing and increasing functions of temperature, respectively.[2] The temperature dependence of the energy resolution also was studied as a function of amplifier shaping time because the time constant of the light emission is also a strong function of temperature. These results are summarized in Figure 1. The dashed lines

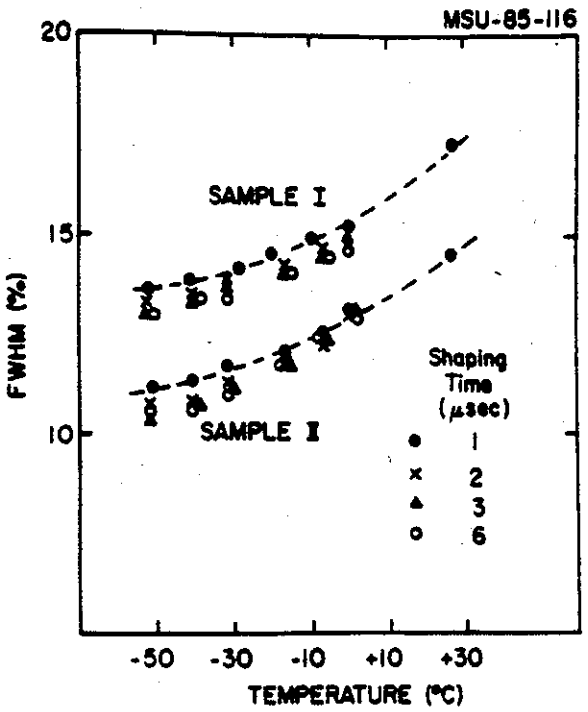

Fig. 1. The temperature dependence of the energy resolution of two BGO crystals including changes in the amplifier shaping time. [MSU-85-116]

connect data points obtained with a shaping time of 1 μs to guide the eye. At -52°C, energy resolutions of 13 to 13.5 % and 10.3 to 11.1 % (FWHM) were achieved for samples I and II, respectively. The relative improvement in the energy resolution due to cooling seems comparable to the results obtained with small crystals in Ref. 2. However, the absolute energy resolution of sample II at -52°C is much better than the result (14.1%) obtained at -78°C, which may be due to better crystal quality. Overall, the change in resolution with temperature is consistent with the decrease in PMT noise, and increased light output with temperature. However, we must conclude that the energy resolution of BGO can not be decreased to the point

where discrete line γ-ray studies could be done with BGO, and thus we are forced to choose NaI(Tl).

The conceptual mechanical design of the detector array is shown in Figure 2. The detector array will have 94 identical equal detector elements placed on eight rings with a high degree of symmetry.

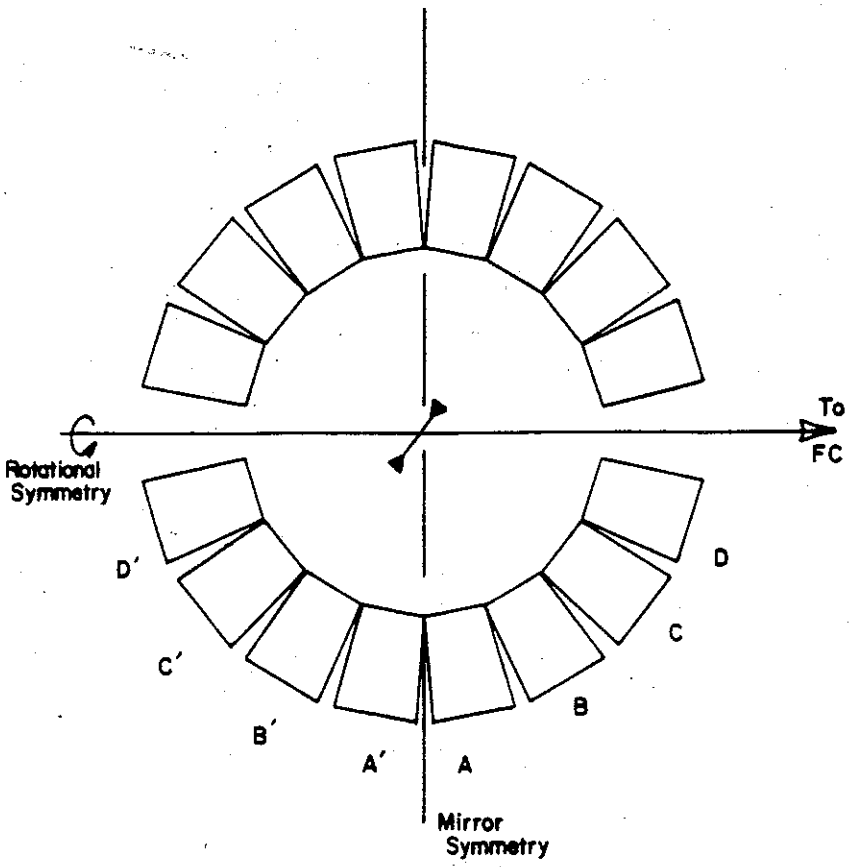

Fig. 2. A schematic drawing of the elements of the γ-ray hit detector array that emphasizes the symmetry of the arrangement.

These are important features that reduce the initial cost to construct the device and later on the data analysis time. Each crystal will have a truncated rectangular-pyramidal shape 7.5 cm deep, be placed at a radius of 17 cm and subtend 0.88% of 4π. The entire array will cover 88% of 4π, be separable into the 8 individual rings and have an inner thin- walled vacuum chamber. Use of the recently developed pulse-shape discrimination techniques for NaI(Tl) detectors would allow experimenters to use the γ-ray hit array to identify and tag the number of light charged particles in the array. This feature complements some of the abilities of the "4π plastic

scintillator array" in a device that may be easier to couple to other experimental apparatus.

References:

1. L.W. Richardson, G.. Wozniak, M.R. Maier, and L.G. Moretto, Nucl. Instrum. Meth. 173,485(1980).
2. H.V. Piltingsrud, J. Nucl. Medicine 20,1279(1979).

III.C.1.e. SPIN-SPECTROMETER

R.A. Blue, R. M. Ronningen, J.X. Saladin,[a] I.Y. Lee,[b] C. Baktash,[b] and R.A. Sorensen[c].

In our last operating proposal we described a gamma-ray total-energy, spin-spectrometer system, proposed to the NSF to be designed and constructed by the University of Pittsburgh under the direction of Prof. J.X. Saladin. After construction and testing it is to be brought to NSCL as a user facility.

The system consists of six high-purity germanium detectors, each with a large Compton-suppression shield made from bismuth-germanate(BGO), and 14 hexagonal BGO detectors configured about the target to act as a total gamma energy, multiplicity filter. The facility has now been funded by the NSF and the construction of the detector array is nearly complete. Two experiments using it were submitted to PAC V with one approved and the other approved with reserve-time status.

At present, four of the six suppression shields exist as do the 14 hexagonal detectors. The shield design differs somewhat from that presented in the last proposal. Figures 1 and 2 show the present design, from which three of the four shields were constructed. The design changes took place after consultations with the vendor, Harshaw, as to the most efficient use of the largest BGO boules available so that the amount of cutting would be kept to a minimum.

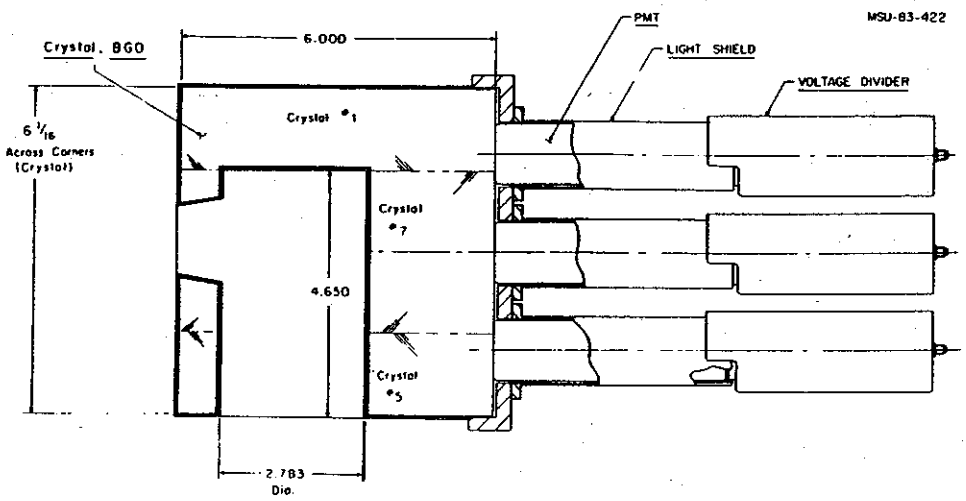

Fig.1

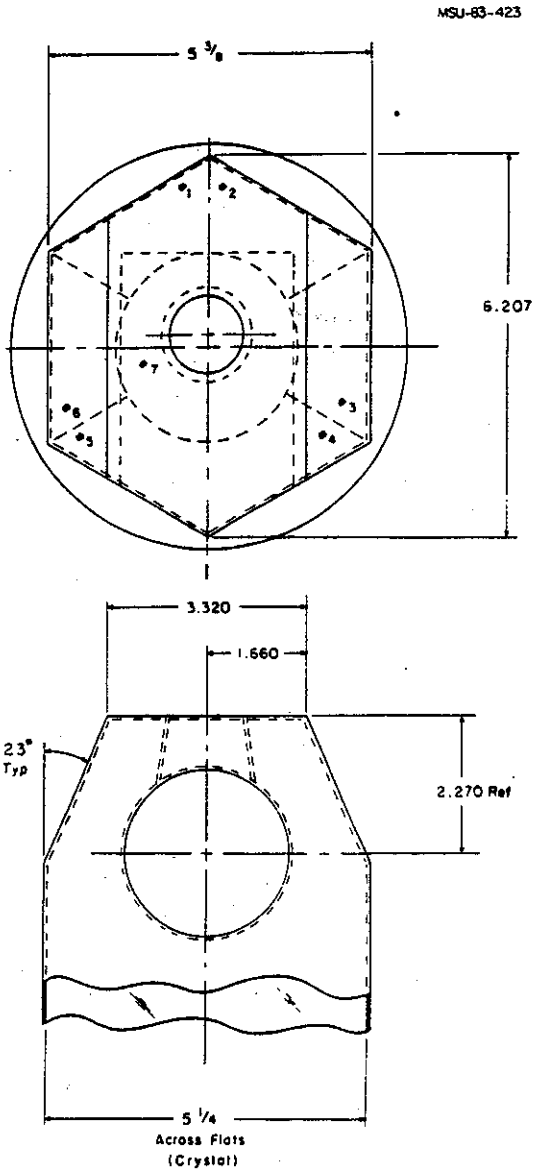

Fig. 2.

There have been significant improvements in the quality of BGO manufacturing recently so that the fourth shield is made from a single crystal. The new manufacturing process has reduced the cloudiness in the crystal core, which impedes light transmission. Tests show that this shield, coupled to a single five-inch phototube, outperforms the other shields, especially for low energy-gamma rays. Tests by Saladin at the University of Pittsburgh on the first two shields show suppression factors of 5-7. A better quantitative summary of the tests is shown in Table I. It should be remembered that the amount of Compton supression and the peak-to-total(P/T) ratio for a given system depends not only on the supression

system but also on the initial Compton event spectrum, hence the size and construction of the Ge detector.

Table I.

	P/T for bare Ge from 100 keV up	P/T for suppression system upwards from 50 keV	100 keV	300 keV
^{60}Co	23%	56%	57.6%	61.5%
^{137}Cs	33%	63%	64.6%	72.5%

We are also re-examining the electronics requirements in light of developments in that field since the system was first proposed. It now appears that there would be significant advantages in the use of ECL such as available through Lecroy's "ECLine". The signal processing speed and space- and cost-per-channel advantages compared to NIM-CAMAC setups are, of course, very important for large arrays of detectors. We are also investigating LeCroy's "FERA" ADC system for these same reasons but it is unclear whether for our modest-sized array there will be clear advantages. We will, however, monitor the implementation of FERA in the 4π-multiparticle array being constructed here at the NSCL.

a. University of Pittsburgh.
b. Oak Ridge National Laboratory.
c. Carnegie Mellon University.

III.C.1.f. LARGE SCATTERING CHAMBER

R. Blue and J.A. Nolen

A large general-purpose scattering chamber is under construction for use with the K800 cyclotron facility. Our design goal is to provide a chamber large enough to accommodate large arrays of detector telescopes and/or position-sensitive gas detectors as required for investigations of reactions at higher energies, which produce very penetrating light fragments and high particle multiplicities. The chamber is cylindrical, 92 inches in diameter by 120 inches long, with a horizontal axis. For access to the interior, the tank rolls back from a fixed end bell through which the beam enters. The internal equipment will be supported from beams cantilevered from the external frame to extend through the end bell into the chamber interior. These beams pass through bellows which provide the necessary mechanical isolation of the support structure from the walls of the vacuum vessel.

The mechanical design for the interior structure will emphasize adaptability so that a large variety of experimental configurations can be accommodated. Although the detailed mechanical design work remains to be done, the conceptual design calls for a modular construction with three main components: a central pivot post housing the target ladder drives which pivot in a horizontal plane about the central post. These arms will be demountable from the central post to allow the maximum space for fixed-position detector arrays, and the central post itself can be positioned anywhere along the length of the chamber or removed entirely. For example, the central post could be placed to position the target near the beam entrance providing essentially the full length of the chamber for time-of-flight measurements in the forward direction. The basic support beams for these demountable devices will be positioned near the tank floor, leaving as much room as possible for detectors below the scattering plane as well as above. Standard mechanical structural components, such as various detectors, can be fashioned from reusable parts to reduce the need for the custom machining of parts.

Another feature of the mechanical design is the large number of flanged ports on both end bells and along the tank body. These should provide for

signal feed-throughs, detector gas leads, cooling lines, optical ports, etc. and for experimental devices mounted from the chamber walls as well as from the internal structure. It is anticipated that arrays requiring one hundred or more coaxial signal feed-throughs will be common for experiments performed in this chamber. The types of feed-throughs now in use on scattering chambers will not serve these needs well, due to the low density of signal penetrations they can provide and the expense of the individual feed-throughs. We expect that some further development work will be required in this area before we arrive at a satisfactory solution to this problem.

The vacuum system design for the chamber is not yet finalized, although we are equipped to provide pumping which will be adequate for the less demanding experiments. We hope to achieve pumping speeds on the order of 40,000 liters per second through the use of cryopumps cooled by liquid helium. Our plan is to construct pumps based on the cryostat design that has been developed for the superconducting quadrupoles to be employed on the beamlines. Two such pumps will be mounted on 20-inch ports on the fixed end bell of the chamber. In the initial work with the chamber, we will use a 2000 liter per second turbo pump. Even after the cryopumps are installed the turbo pump may prove useful in the pump-down cyclo to minimize the need to expose the cryopumps to the higher gas loading of pump-downs. The need for the higher pumping speeds of the cryopumps is anticipated, due to the gas loads coming from organic materials typical of detector construction and signal cables as well as the leaks from gas-filled detectors.

The present state of the large chamber is that mechanical construction of the tank is nearly complete at a plant in Brooklyn, New York. Vacuum testing to our specifications remains to be completed before the tank will be shipped to the NSCL. Once the tank has been received, the external support structure should be completed quickly to make the tank available for further vacuum testing and development. As noted above, design and development work remains to be done for the internal structure and the cryopumps. Controls for remote mechanical motion devices and the vacuum system are encompassed by the overall controls design work for the laboratory and should be available as needed. We expect to have the chamber ready for an initial temporary installation near the beam exit of the K800 cyclotron early in 1987 if that should prove to be desirable for initial

experiments using beams from the K800. The planned final location for the chamber is in the vault at the northeast end of the high-bay area.

III.C.2.a. InSb AS A GAMMA-RAY DETECTOR

Wm. C. McHarris, Reg Ronningen, and Michael Maier

InSb is a material of extremes; Its potential advantages over Ge are formidable, but so are its drawbacks. Because its positive attributes are relatively straightforward, they require little explanation. Its pitfalls are less obvious and thus require more detail. Any very-high-resolution detector can be expected to be tricky to deal with, and InSb should prove to be no exception. A more detailed and quantitative discussion of its possibilities as a γ-ray detector can be found in Ref. 1.

In principle, InSb should make a superior γ-ray detector. Since the photoelectric effect scales as Z^5, the InSb effective Z of 50 results in an efficiency (per mole) of 9.3 times that of Ge, and a linear stopping power somewhat higher if the differences in densities are folded in. Also, single-event Compton scattering scales as Z, so if the resolutions of InSb and Ge were comparable, InSb would have a peak-to-Compton ratio six times better than Ge -- this on the basis of Z alone. (And, of course, assuming comparably sized detectors, which is not a reality at this time.)

The resolutions are not comparable, however, for the InSb band gap is much smaller, 0.165 vs 0.67 eV (at 290 K). The contribution to resolution (in eV) due to the statistics of charge collection is given by

$$\Delta E_F = 2.355\ (F\varepsilon E_\gamma)^{1/2},$$

where F is the Fano factor, ε is the average energy (in eV) needed to form an electron-hole pair, and E_γ is the γ-ray energy (in eV). Assuming ε to scale with the band gap and the Fano factor to be comparable to that for Ge, this yields a resolution for InSb better than that of Ge by a factor of at least two. Folding this in, we obtain a peak-to-Compton ratio improved by a factor of at least 12.

Unfortunately, difficulties immediately arise. The electron mobility is higher than the hole mobility by a factor of 100. (Actually, this is just one aspect of the properties of InSb that is not completely understood;

values of the electron/hole mobility ratio given in the literature vary from 100 down to about 20.) This leads to three separate, but related, problems.

First, the problem of compensation: The difference between the electron and hole mobilities means that Li^+ drifting of p-type InSb is impossible; indeed, p-type InSb itself is not readily produced. Instead, drifting n-type InSb with a small anion would be necessary, and F^-, the smallest anion, is many times as large as Li^+. And the small InSb band gap makes drifting at elevated temperatures unfeasible, so drifting becomes impossibly slow. The solution to this problem is to be able to fabricate detectors from "intrinsic quality" InSb. Zone-refining techniques have now developed to the point that such quality InSb is becoming commercially available, at least for very small infra-red detectors.

Second, the problem of complete charge collection: The relatively slow hole mobility is a potential source of trouble. Energy resolutions of a few percent require at least 90% charge collection, and resolutions approaching those of the best Ge detectors will require a much higher value, approaching 98% or better. The solution to this problem is not quite so straightforward as the solution to the first one, and it may turn out to be difficult to produce decent "large" InSb detectors. There are stoichiometric problems associated with growing extremely pure crystals of mixed semiconductors that are not encountered in growing extremely pure crystals of Si or Ge. However, it should be noted that the hole mobility in InSb, even though much slower than the electron mobility, is still considerably faster than the hole mobility in CdTe or HgI_2, so incomplete charge collection per se will probably not be quite so severe a problem with InSb as it is for those materials.

Third, the problem of geometry on charge collection and resolution. Detectors fabricated out of materials having widely different electron and hole mobilities show a decided geometrical dependence on the degree of (hole) trapping and thus a dependence on where in the detector the γ-ray interaction took place. Interactions taking place near the negative contact, in which the electrons traverse the entire width of the detector, show much more complete charge collection than do interactions taking place near the positive contact. Luckily, the very cause of the difficulty, i.e., the differences in mobility, also furnishes a solution to this third problem. There is a similar geometrical dependence on pulse rise-time, with

pulses having more complete charge collection being faster than those having less complete charge collection. Two types of electronic pulse-height correction have been developed to compensate for this. The first was developed to compensate for this problem in HgI_2 detectors.[2] The second was developed in our laboratory to compensate for varying incomplete charge collection in neutron-damaged Ge detectors;[3] it can also compensate for geometrical effects on rise-time in coaxial detectors. Both methods are equally applicable to solving this problem with InSb, requiring only slightly more complex electronics than are normally used for self-gated-singles coincidence experiments.

InSb cannot be drifted for compensation, but it shows promise for becoming available in quality good enough for "intrinsic" detectors, requiring no compensation. It has no destructive solid-state phase transitions (as contrasted with materials such as HgI_2), and zone-refining techniques have reached the point that very small "intrinsic" detectors are now commercially available for infra-red spectroscopy. The promise of InSb is great enough that working out techniques for dealing with it should definitely be worth the effort. We are currently negotiating for several of these detectors and plan to convert them into configurations suitable for γ-ray spectroscopy.

References:

1. Wm. C. McHarris, "InSb as a γ-Ray Detector", paper delivered at 6th Symposium on X- and Gamma-Ray Sources and Applications, 21-23 May 1985, Ann Arbor, Michigan; Nucl. Instr. and Meth., in press.
2. M. Finger, T. A. Prince, L. Padgett, B. Prickett, and W. Schnepple, IEEE Trans. Nucl. Sci. NS-31 (1984) 348.
3. N. Matsushita, Wm. C. McHarris, R. B. Firestone, J. Kasagi, and W. H. Kelly, Nucl. Instr. and Meth. 179,119(1981); N. Matsushita, J. Kasagi, and Wm. C. McHarris, Nucl. Instr. and Meth. 201,433(1982).

III.C.2.b. GAS COUNTERS

H. van der Plicht

Low-Pressure Multi-Wire proportional Counters (LPMWPC) for heavy ions came into use a few years ago following the pioneering work of Breskin, et al.[1] Such detectors feature good position resolution (0.5 mm), good timing resolution (175 ps) and a total thickness of about 300 µg/cm.[2] These detectors are used extensively in experiments for slow and heavy ions such as fission fragments and target residues[2]. However, heavy ions with energies of around 25 MeV/A, such as those produced by the K500 cyclotron do not lose enough energy in these type of detectors.

A recent improvement is the so called Multistep detector.[3] The Multistep detector is basically a LPMWPC with an added gas preamplification stage, as shown in Fig. 1. The central plane is the anode (wire plane), the outermost planes are the cathodes (thin foils) and the inner two planes are wire planes at ground potential. The wires of these inner two planes are connected to delay lines, making the counter position sensitive.

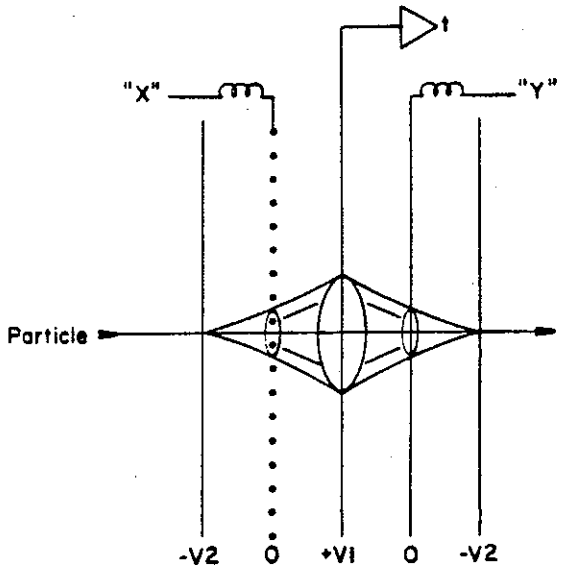

Figure 1.

Thus, the center part operates as a LPMWPC and the outer regions as an added-on PPAC (Parallel Plate Avalanche Counter). High gains can be obtained by the multistep process, typically 10 times larger than those of single step counters.

Futhermore, the signal-to-noise ratio can be much improved by using recently developed monolithic amplifier IC's (NEC - PC1651G), mounted directly on the detector frames.

One important application of multistep counters at NSCL is as a start-detector for the S320 spectrograph. Time-of-flight measurements are

necessary for particle identification, and are usually performed using the scintillator of the focal plane detection system and the cyclotron RF signal. However, for separation of Neon (and heavier) isotopes, the time resolution using the RF is not sufficient and the use of a start-detector is essential.

The Multistep technique can also be applied to one or more detector elements of the NSCL 4π array which is under construction.

References:

1. A. Breskin, R. Chechik and N. Zwang, IEEE Trans. Nucl. Sci. 27,133(1980).
2. J. van der Plicht, H.C. Britt, M.M. Fowler, A. Gavron, Z. Fraenkel, J.B. Wilhelmy, F. Plasil, T.C. Awes and G.R. Young, Phys. Rev. C28,2022(1983).
3. A. Breskin, R. Chechik, Z. Fraenkel, P. Jacobs, I. Tserruya and N. Zwang, Nucl. Instru. Meth. 221,363(1984).

III.C.2.c. NUCLEAR ELECTRONICS

M.R. Maier

Because of their increasing complexity experiments at the NSCL pose a challenge to electronics development. One solution is to pack as many electronic processing channels (discriminators, coincidences, etc.) into one NIM module as possible. With this approach one runs eventually into the problem that front panel space limits the number of channels that can be placed into one module; the board space inside the module is almost never a limitation. An extreme case for this kind of "cramming functions into one module" is the octal constant fraction discriminator. In the past year or so, we have built a number of modules along these lines: 20 four-fold logic units, 20 quadrupole gate generators for digital signals. Presently we are designing a quadrupole shaping amplifier in a size of one NIM module. These instruments are in wide use in the laboratory.

However, with the increasing number of channels, the difficulty of adjusting gains and thresholds increases dramatically and the number of cables begins to dominate the experimental setup. Therefore, we are now pursuing a different approach in the design of detector processing electronics that makes extensive use of computer control, e.g., via CAMAC. Fortunately, commercial modules compatible with this approach are available. In particular for the 4π detector, we plan to use the FERA ADC system and the associated connecting bus system "ECL-line" as introduced by LeCroy. This approach has the following advantages:

a) The fact that all modules can be controlled via CAMAC dramatically simplifies the set up of an experiment: parameters can be set and read from a computer, which makes control very easy and transparent.

b) The "ECL-line" uses very inexpensive multi-line cables, which reduces the cable labyrinth associated with the old-style electronics.

c) The FERA system allows a very fast readout of valid information (sparse readout). This will make possible trigger schemes which rely on the digitized ADC information, which again can be controlled and changed by a computer.

These features will allow experiments of complexity approaching those of high energy physics. Unfortunately it is not usually possible to simply

use the models commercially available for high energy physics. In most instances these are not sufficiently precise for the requirements of nuclear physics experiments. There is, for instance, no modern commercial peak-sensing CAMAC ADC which would allow spectroscopy with semiconductor detectors. In addition, commerical units rarely have the rate capabilities that are routinely required in nuclear physics experiments nor sufficiently good resolution. Fortunately there are well-known techniques for achieving the precision needed in "NIM style" processing electronics; we will incorporate these in the modules that will be developed at the NSCL.

Several special modules have also been built recently. These include:

(a) Divider-strings for photomultiplier tubes and charge integrating preamplifiers that can be used in vacuum. In order to mount these devices in vacuum, their power dissipation had to be minimized. For the charge-sensitive preamplifer, a low power version of the "standard" FET cascade circuit was used. Fifty of these units were built and used successfully in experiments at MSU, ORNL and GANIL.

(b) Eight particle identifiers with an analog multiplier I.C. These allow moderately fast identification of particles in experiments using silicon detector telescopes. They were used to suppress a large α-particle background by generating a fast veto signal from the output of the identifier. This design will be the basis for a more general particle identifer unit.

(c) A wave form analyzer to analyze the pulse shapes coming from the Bragg Curve Spectrometer in the 4π detector. This analyzer is based on the use of a 9 bit 20MHz flash ADC (TRW), and includes a memory for 256 samples. This unit will also be used to study pulse shapes of the scintillators NaI or CsI and BaF_2 to investigate the usefulness of pulse shape discrimination in these scintillators as a technique for particle identificaiton.

Special modules planned for the near future include: quad fast amplifiers, quad slow shapers with fast and slow outputs, and an octal Camac constant fraction discriminator. In addition, we plan to develop techniques for use of pulse shape discrimination to identify particles in inorganic scintillators. This will be crucial in the construction of very compact multidetector arrays for light particles and gamma rays.

Clearly, an important feature of the electronics development program is the close collaboration between the electronic design group and nuclear

scientists, leading to an appropriate and rapid response to the needs for particular experiments.

III.C.2.d. THE PRODUCTION OF RADIOISOTOPES WITH HEAVY-ION BEAMS

D.J. Morrissey, J.A. Nolen, Jr. and J.M. Tiedje[a]

Biological studies have used ^{13}N produced in (p,n) reactions at the Cyclotron Laboratory at Michigan State for a large number of years. The proton beams necessary for the production reactions are no longer available and a new technique had to be developed. The production of radioisotopes by projectile and target fragmentation has the advantage that a large target thickness can be used due to the long range of high-energy beams. As both projectile and target can be fragmented in a heavy-ion reaction, suitable choices can allow specific radionuclides to be produced as both projectile and target fragments. For example, a suitable projectile-target combination for ^{13}N production is ^{14}N plus water, since the target contains only oxygen isotopes, which lead to ^{13}N, and protons which cannot be fragmented.

In the first production runs, the target consisted of a Be foil (in the range of 0.25 to 2.03 mm thick) backed by a 1 cm^3 volume of water. The ^{14}N beam and its fragments penetrated the foil and stopped in the water. This version of the target system prepared sources in a batch process. The beam intensity was usually between 0 and 30 particle nanoamps, being limited by constraints on cyclotron operation. After irradiation the beam stop water was flushed through the accelerator shielding walls in a thin tube, approximately 20 m long, within 10 to 20 seconds after the end of bombardment. The source strengths produced by this batch transfer target were not reproducible. We subsequently developed a flow-through target system in which approximately 30 cm^3 of water was passed through a 4 cm^3 beam stop in a closed loop by a parastaltic pump in approximately 30 seconds. After the beam was tuned onto the target, the water was constantly irradiated by the beam and the researchers could remove aliquots from the system as needed. The sources produced by the flowing system were substantially stronger and reproducible, as discussed below.

The ^{13}N radioactivity was measured as a function of time by multiscaling the annihilation radiation observed in NaI(Tl) detectors. Multiscales of the outputs from up to 12 detectors were collected simultaneously by a new computer-controlled CAMAC system. Briefly, the outputs of the NaI(Tl) detectors were passed through discriminators into a

pair of CAMAC scalers. The scalers were cycled between data collection and readout by a CAMAC real time clock. The data collection and storage was performed by a VAX 11/750 computer. Least-squares decay curve analysis with a new code adapted to the CAMAC data showed the presence of ^{15}O, ^{13}N, ^{11}C, ^{18}F and a long-lived component, most likely ^{7}Be. In general, the bombardment of water targets produces both gaseous and aqueous radioactivities. During test runs the liquid water and gases were transferred into an evacuated flask. The activites of the aqueous and gas phases from a typical source are shown in Figure 1. The ^{13}N batch sources

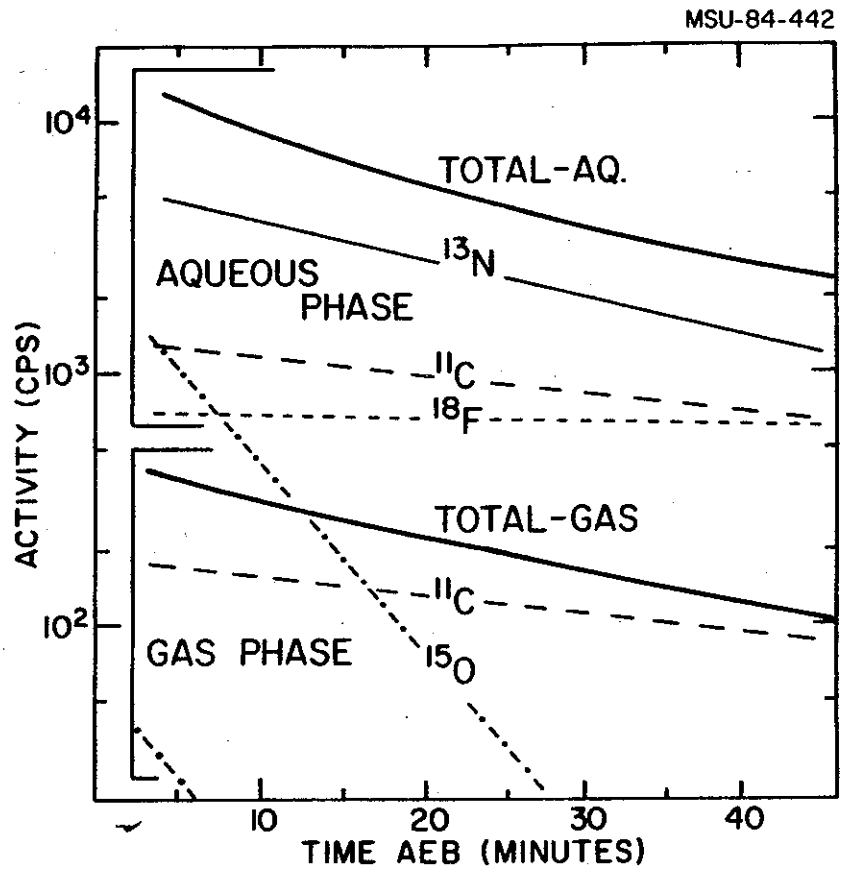

Fig. 1. Typical decay curves of the activities observed in the aqueous and gaseous phases, (see text). The thick lines indicate the total activity while the thin lines indicate the activity of the individual components in each phase. [MSU-83-442]

were typically 4 mCi/pμA. The source strengths produced by the circulating water target were approximately 20 mCi/pμA which is within a factor of two of geometrical reaction cross section predictions. The chemical composition of the ^{13}N in the aqueous phase was also studied with high-pressure liquid chromotography. This composition was consistent with distributions previously reported for proton radiations of water, depending on the beam power per unit volume of water. The target system that we have developed currently provides ^{13}N sources that are adequate for the biological studies. One remaining problem with this technique is that the ratio of ^{13}N to ^{14}N is rather low, or in other words the sources are not "carrier free." We expect that we could use the RPMS to separate all the reaction products by m/q and produce such carrier-free sources when required.

a. Michigan State University - DOE Plant Laboratory.

References:

1. D.J. Morrissey, J.A. Nolen and J.M. Tiedje, Nucl. Inst. Meth., B10/11 963(1985).

IV. STAFF RESEARCH: ACCELERATOR PHYSICS

(Antaya, Blosser, Gordon, Harwood, Johnson, Laumer, Mallory, Marti, Miller, Milton, Nolen, Vincent)

Availability of forefront experimental apparatus is a critical factor limiting or allowing progress in experimental nuclear science. Noting this, the program of the MSU Cyclotron Laboratory has from the beginning involved a large instrumentation development component. The largest sub-element of this instrumentation effort is in accelerator physics, addressing the goals of first, understanding the fundamental phenomena of particle accelerators and second, developing and testing accelerator systems which will perform more effectively in their end use in nuclear science experiments. Primarily the accelerator program has been concerned with the development of the isochronous cyclotron with occasional small efforts concerned with other types of accelerators, the latter usually by way of following up an idea or improvement originally conceived in the course of the isochronous cyclotron studies. As a consequence of this overall program, the Laboratory has come to be regarded throughout the world as a leading center of isochronous cyclotron development.

In the early years the primary objective of the accelerator program was development of the isochronous cyclotron as a precision device for study of nuclear phenomena. Techniques for achieving single-turn extraction were studied theoretically and numerically; in the late 1960's the MSU 50 MeV cyclotron began to operate in this mode, thereby giving the first experimental demonstration of the overall feasibility of such a system. Single-turn extraction largely eliminates loss of beam in the cyclotron and this has many benefits. The most important gain, however, in the nuclear physics application is due to the increased phase space density of the output beam, this density being the dominant factor determining overall system resolution when the cyclotron is coupled to a magnetic spectrograph.

Performance of such a cyclotron/spectrograph system was polished and perfected through the late 60's and these capabilities were utilized in a large number of nuclear physics experiments over the years. In parallel with these efforts, techniques were developed which provided an absolute energy calibration for the spectrograph in terms of accurately known nuclear masses; these techniques gave rise to a broad spectrum of significant spectroscopic studies hinging on accurate absolute energy measurements. An important sub-element of the single-turn extraction developments involved obtaining very short beam pulses through detailed manipulation of the central region dynamics in the cyclotron. This so-called "phase selection" system then provided the basis for another interesting 50 MeV cyclotron program based on time-of-flight analysis of reaction product energies and masses. In later years many of these 50 MeV cyclotron techniques were taken over at other cyclotrons, and a sizeable component of today's forefront nuclear research flows from accelerators which use one or another of these techniques.

In late 1973, the cyclotron development program began to study the possible benefits of adapting superconducting coils to cyclotrons. With a superconducting coil, main magnet power is removed from the family of constraints which define an optimized cyclotron design. This seemingly mundane change leads to a quite incredible major qualitative change in the basic cyclotron structure. Magnet weight perhaps illustrates this change most vividly. The 265-ton K800 superconducting cyclotron magnet at MSU, for example, has a magnetic bending power sizeably in excess of that of the 4,300-ton 184 inch synchrocyclotron magnet at Lawrence Berkeley Laboratory, and the 100-ton magnet of the MSU K500 superconducting cyclotron has more bending power than the 1700-ton magnets of the large room temperature cyclotrons at Ganil. Many other comparisons of magnet weights can be made; the results will depend on details of particular designs but a basic cyclotron scaling characteristic* dominates, and superconducting cyclotrons with fields around 5 tesla will invariably be 10 to 20 times lighter in weight than room temperature cyclotrons with fields around 1.5 tesla. Since

magnet steel is normally the single most expensive component of a cyclotron, this large reduction has a very favorable effect on costs.

---

*For a cyclotron of given maximum bending power, both the radius and the total magnetic flux vary inversely with the strength of the main bending field. The radius approximatly determines the length dimension of the magnetic path, while the flux determines the cross-sectional area -- the quantity of steel therefore varies approximately as $1/B^2$.

Major qualitative changes in any technical system usually involve a new set of difficulties and the superconducting cyclotron is no exception. Since the middle 70's the primary thrust of the Laboratory's cyclotron development efforts could be characterized as beating superconducting cyclotron problems into submission. With magnet power removed as a limiting constraint, the new limiting phenomena which come into play include: first, the fundamental current capacity of available conductors; second, the stress limits of the materials which must withstand the large mechanical forces produced by the high magnetic field (pole to pole force in the K800 is for example about 1600 tons); third, limits due to the maximum voltages which can be achieved in the electrical components of the cyclotron (the accelerating system and electrostatic deflectors); fourth, the "swiss watch" problem, namely the limits which come from the need to make normal cyclotron auxiliary systems such as water lines, probes, electrical leads, drive motors, etc. fit into a space which is very much smaller, etc. Solutions to all these problems were laid out in the K500 cyclotron design. When this cyclotron came into operation with internal beam in November 1981 and external beam in August 1982, the adequacies and deficiencies of various aspects of the initial design were brought to light.

The design solutions for the K500 were adequate in the sense that soon after the initial external beam was achieved, an experimental program began

that effectively addressed significant research goals. Through the intervening years, beams have been provided which are unique in the US and unmatched in the world except at Ganil. The K500 in its initial form also had a number of problem areas; a major activity of the accelerator physics program in the years of K500 operation has been, and is, concerned with remedying these problems. The other major ongoing activity of the accelerator physics group is upgrading the design of the K800 cyclotron to incorporate improvements which have been developed in response to problems of the K500 and to respond to problems which arise in the course of constructing the K800. (This last involves responding to information needed in decisions such as: Would shimming of observed magnetic field imperfections lead to a detectable beam improvement? Are bellows on cryostat penetrations really necessary? Would sliding sapphire bearings improve main probe reliability? Etc.)

In the months and years immediately ahead, the accelerator physics group will clearly be fully occupied with these activities related to upgrading the performance of the K500 and K800 cyclotrons. Further in the future, studies will shift to issues with longer range, broader significance. All present superconducting cyclotrons, for example, work at 5 Tesla reflecting the state of superconducting magnet technology in the middle 70's when the principal design features of this generation of cyclotrons were fixed. Solenoidal coils such as are used in these cyclotrons can now work at fields in the 8 to 10 Tesla range, using either Nb_3Sn at 4.5 degrees or NbTi at 2.5 degrees. Further large reductions in size and cost of cyclotrons would be achieved by stepping up to these higher fields, the system being particularly well-matched to the requirements of very heavy ions such as lead or uranium. Thus, a 10 Tesla booster for the K800 or an independent cyclotron at 10 Tesla, would be likely design options for producing Uranium beams in the 200 MeV per nucleon range. Other future topics which we will study as soon as time is available include the utilization of storage rings in the medium energy heavy ion regime and use of superconducting or cryogenic accelerating systems in cyclotrons.

The subsections which follow are organized on a topical basis covering the major present activities of the accelerator group and likely future directions. Most of these topical areas are relevant to both the K500 and K800 cyclotrons. Improvement of the deflector design to allow higher voltages is perhaps the most obvious topic applicable to both machines, although every topic tends to have some degree of overlap. Design studies of the extraction system for the K800, for example, have led to several ideas for improvements in the K500 extraction system, and even activities related to the final topic, "Medical Applications", have led to a number of ideas useful in solving problems in the K500 and K800 systems. The overall accelerator program is then highly interrelated and dynamic, with involved individuals usually working on a number of topics at any one time and with a lively and comfortable exchange of information between people working on various topics. The program also benefits greatly from flourishing and effective communications with other laboratories active in this area -- these latter contacts have on many occasions been the source of ideas which were of central importance in solving key problems.

A. Orbit Theory and Numerical Techniques

A continuing central goal of the MSU cyclotron program is the development of techniques for making the performance of cyclotrons predictable and calculable. Generally this utilizes theoretical analysis to provide a qualitative understanding of the fundamental features of a given phenomena, followed by numerical analysis to clarify precise details. In the early years the numerical analysis was accomplished using a vacuum tube computer with a 1024-word memory. Programs were written for this computer which tracked orbits in measured magnetic and electric fields, the equations of motion being exact and information on the fields coming from operating models. The intervening years have seen an exponential increase in available computing power, which allows work on much more sophisticated problems. However, computing power is still not quite to the point where

the complex three-dimensional geometry of a cyclotron pole tip can be economically included in a first principles calculation or at least not at the level of detail needed to accurately predict all the features of the field which one must consider to obtain well behaved cyclotron orbits. Following subsections describe some of the laboratories ongoing theoretical and numerical analysis accelerator activities.

1. Acceleration Through Linear and Non-linear Resonances

In recent years, Gordon and coworkers have examined effects arising from acceleration through or around certain linear resonances that occur in many cyclotrons. The first of these involves acceleration through the $\nu_r = 1$ resonance, which occurs in the central region of cyclotrons, and the resonant driving terms which arise in cyclotrons such as ours when there is an asymmetry in the voltages of the three dees.[1] This work has also examined the coherent oscillations that are produced by the rapid skirting of the $\nu_r = 1$ resonance rather than a traversal through this resonance.[2] Also, in collaboration with a group at the TRIUMF cyclotron, a successful theory for the emittance growth resulting from the rapid traversal of a half-integer resonance has been developed.[3]

In coming years this work will be extended by applying the same analytical technique to obtain corresponding results for certain nonlinear resonances, particularly those encountered in our K500 and K800 cyclotrons. These are the third-order and fourth-order coupling resonances, $\nu_r = 2\nu_z$, $\nu_r + 2\nu_z = 3$, and $2\nu_r + 2\nu_z = 3$, as well as the $4\nu_z = 3$ resonance, which has not been studied before. The relevant orbit computations required for this work can now be carried out more realistically with the use of the new Z[4] Orbit Code described in the following subsection.

2. Nonlinear Effects in Beam Extraction

The standard orbit codes used in the analysis and design of cyclotrons are based on an off-median-plane magnetic field representation that is correct only to first order in z. We have now completed and put into operation a new program, the Z^4 Orbit Code, which makes it possible to carry out a proper investigation of the non-linear effects important to the beam extraction process. A special input routine in this program processes the median plane field data to obtain all components of the main magnetic field correct to fourth order in z. Moreover, the program uses exact equations of motion.

The Z^4 Orbit Code has been employed to evaluate the growth in the radial and vertical emittance values in the extraction system of the K500 cyclotron,[4] and it is also being used in the final design of the K800 extraction system to evaluate the effects of various non-linearities. For such applications, the program is equipped with a special routine for calculating the exact fields produced by saturated focusing bars (i.e. iron elements in which the magnetic moments are fully aligned in the z direction). Since these focusing elements are typically located in the median plane, or very near it, the use of an exact computation for these elements plus the Z^4 computation for the remaining field components gives an overall computation which is highly accurate and also well-optimized with regard to computing efficiency.

3. Transfer Matrix Program for Energy-Phase Distributions

The K500 cyclotron will soon operate with injected beams from an ECR ion source. These beams will be bunched prior to inflection, so that the initial phase distribution will be much better defined than is the case for beams from the PIG sources. This definition can also be further improved in many circumstances by using the phase slit system described in a following subsection.

In these circumstances, it becomes desirable to develop a transfer matrix program for rapidly calculating the energy and phase distribution of the extracted beam. The theoretical basis for this program has already been described.[5] Such a program would quickly compute the effect of changes in machine parameters on the energy spread and time structure of the extracted beam. Important tuning parameters which might be studied include the energy and phase values at injection, the current settings for the trim coils, and the tuning of the rf frequency. The accuracy of the transfer matrix technique can be tested during its development by comparing the results with those obtained from our present orbit codes, which make use of numerical integrations.

The effect of a change in the trim coil currents on the rf phase of the beam is now determined by a semi-empirical formula which is known to have limited accuracy, or from computation of a full equilibrium orbit table, which is slow. The need for a faster, more accurate procedure has led to developing a Green's function technique which determines changes in equilibrium orbit properties produced by a given field perturbation. The procedure appears to be both fast and accurate and therefore meets the needs of fast response programs. The procedure may also become a standard part of our computer programs for determining trim coil currents and related parameters.

The transfer matrix program for phase-energy calculations is based on a theory of the longitudinal motion which isolates this motion from the radial and vertical oscillations of the beam. The effects of these oscillations can be determined through application of a general theory of accelerated orbits developed recently.[6] In the future this theory will be used to obtain analytical formulas for determining the effects of radial and vertical emittance values on the energy and phase of the extracted beam.

4. A Comprehensive High-Speed Code for Particle Dynamics in the NSCL Cyclotrons

The array of focusing resonances in the edge region of the K800 cyclotron, and the strong non-linear effects of the tightly spiraled field, place stringent requirements on the degree to which field imperfections must be compensated. Given these requirements, the customary separation of internal and extraction orbit design* is no longer workable and an iterative calculation must be made. In this calculation the internal beam is computed

*If the effect which magnetic extraction elements have on the internal beam can be made negligible by design details of the elements themselves or by adjustment of compensating elements, the design of internal and extraction orbits factors in the sense that each can be carried out independently without effect on the other.

in a standard isochronous field; a first extraction orbit is computed and magnetic focusing elements are adjusted to give good focusing along the extraction orbit; the internal beam behavior is then recomputed in a field which includes the revised fringing effects of the adjusted extraction elements; the extraction orbit is then recomputed using initial conditions from the revised internal beam; extraction elements are then again readjusted, and this cycle is repeated until a "self-consistent" solution is obtained, i.e. a solution in which both internal and extraction orbits behave satisfactorily in the field of a single array of identically adjusted magnetic elements. This process involves a massive amount of computing with large input arrays which need to be manipulated quickly in order to explore different magnet configurations, and massive amounts of output which need to be presented in a meaningful, easy-to-interpret form. Noting the requirements of this total problem, a new comprehensive computer program has been written, (in parallel with continuing to work on the K800 extraction problem with existing codes) with the objective of having a single very high

speed program which will handle all aspects of cyclotron extraction system design in an interactive mode in which the designer will be able to adjust extraction elements on-line, study graphical displays of the results, readjust elements, etc. This program is now in preliminary use -- primary elements have been checked for accuracy and the code is being used for first computations while refinements are being introduced to improve convenience.

Some of the basic computational capabilities which are included in the code and available to the user are:

1) The MSU field trimming code, which computes the main-coil and trim-coil currents which best produce a "desired" particle phase-vs-energy for a stipulated particle and final energy.
2) The equilibrium orbit code which locates closed orbits and computes first order focusing frequencies relative to those orbits.
3) A routine which locates "accelerated" equilibrium orbits.
4) An orbit tracking routine which tracks coasting or accelerated orbits including families of displaced orbits.
5) A routine which plots orbit tracking results in phase space, either relative to closed orbits or versus absolute coordinates.
6) A routine which plots radial and axial beam envelopes through the extraction system.
7) A routine which Fourier analyzes any part of the magnetic field as a function of radius.

Additionally, many developmental options have been included to enable parts of the calculations to be checked whenever questions exist about a particular result. Input and output is menu-driven on a graphics terminal from which hard copy is available. Users can look at current values of parameters, and see results in graphical form before deciding on hard copy; user efficiency is thereby enhanced.

The dominant feature in all steps of the procedure is calculation of the field; thus, speed in calculating the field is essential. The major

difference between the K800 extraction system and the K500 system is the close proximity of dipole bars to the internal orbits and the dangerously large phase slip at large radii. The beam passes so close to these bars that interpolation in a calculated/measured grid (the usual procedure) is unacceptable at times. Analytic equations exist for the field of a uniformly magnetized rectangular piece of iron; these were coded and a test showed that calculating the field of each bar for every integration step took about 30 seconds of VAX 11/780 time for one turn.

Two solutions are being used to overcome this accuracy/speed conflict: first, the analytic equations are used to build a grid for interpolation unless the field point is quite close to the bar where the analytical equations themselves will be used and second, an FPS-164 became available. (The FPS-164 is an attached processor with approximately 5-10 times the computing speed of the VAX 11/780.)

The new code is structured to facilitate upgrades and modifications by utilizing "kernel" subroutines wherever possible to eliminate re-coding at each use of an algorithm. In some cases, e.g. calculation of the magnetic field and its derivatives, this slows the overall execution of the code but ensures that the numbers calculated by one part of the code are consistent with those calculated with another part. In other cases, subroutines in the earlier codes were expanded into in-line code if they only occurred in a few places where speed was of the essence (the four-point interpolation coefficient routine is an example of this).

The code was written and tested on the VAX and then moved to the FPS. Time savings have been substantial. For example, fitting the trim coils to give a chosen phase curve took 10 to 15 min. on the VAX; the new code takes about one minute. Accuracy was investigated by comparing to the results of the earlier programs; with the VAX codes running in double precision, differences were less than 0.0001" in the integrated trajectories.

In summary, the new program provides a single, integrated code containing all the features needed for designing the extraction system of complex cyclotrons such as the K800. When used on the FPS, the program

allows a proposed configuration to be evaluated in about one hour versus one to two days for previous procedures.

5. Documentation of Computer Programs

Since laboratories around the world make use of MSU orbit codes and other programs, a continuing effort is directed toward maintaining and/or improving the documentation of these programs. A recent paper describes the theory underlying the routine for calculating isochronous fields, which is one of the elements of the Fielder program and other programs for determining trim coil settings.[7] Another paper presents details of the structure and function of the Equilibrium Orbit Code and its more sophisticated offspring, the Cyclops program.[8] A recent internal report describes the Z^4 Orbit Code and the focusing bar field equations used in beam extraction calculations; a publication based on this report will appear in the near future.

B. Magnetic Field Calculations and Measurements

One of the computational short-comings in the battery of codes at NSCL is a useful three-dimensional magnetic field code. Because of the large amounts of CPU time required by existing codes to calculate magnets of the complexity of the two cyclotrons, models are used which sacrifice accuracy in order to speed computing, e.g. using a uniform, vertical magnetization in calculations of the fields of the pole tips. Likewise, truly three-dimensional problems, such as the fringe fields of dipole or quadrupole magnets, have been modeled with two-dimensional codes. In addition to orbit calculations, a 3-D field code would have important application in calculating forces on three-dimensional parts of magnets, such as the K800 pole tips, where mounting bolts stretched in the first power-up of the magnet due to an incorrect estimate of radial forces, or end effects in the kidney-shaped coils of the S800 spectrometer, etc. With improved field

information, mechanical engineering of such devices can be done with much greater reliability.

The two most common three-dimensional codes in use are TOSCA[9] and GFUN3D,[10] each with its own problems; in the end, both suffer from the inability to adequately represent magnet intricacies important in the design problems of interest at NSCL.

Some recent developments improve the prospects of being able to develop a program which will overcome these difficulties. These include:

1) A corrected "stacking factor" in the POISSON program. (With this revision, comparisons of calculated and measured values of the azimuthal average of the magnetic field are in accurate agreement for the K800 magnet.)
2) A new code, GFUN3DIT, developed at BNL, which reformulates the solution of the integral form of the field equations to save large factors in running time, ie. running time is proportional to N^2 (N=number of pieces of iron in the problem) instead of N^3 as in GFUN3D; both GFUN3D AND GFUN3DIT have been acquired and are running on the NSCL VAX-780.
3) The FPS-164 attached processor with its 2 mega-variables of storage and pipe-lined, paralleled architecture providing computing power comparable to a large main-frame.

The procedure which we intend to try out in attacking the high-quality, three-dimensional field calculation problem involves the following steps:

1) Calculate the fields of the magnet in two-dimensions using POISSON and the stacking factor option. This will provide approximate values of the average field and magnetization at each point in the 2-D projection of the problem .
2) Set up the GFUN3DIT problem such that there is fine granularity in and near the median plane and a coarser grid elsewhere.

3) Use the magnetizations from POISSON to initialize the GFUN3DIT calculation.
4) Run GFUN3DIT to completion, to obtain the self-consistent magnetization distribution.
5) Calculate the magnetic field at the desired points in space. This step will include testing of a "re-granularizing" of the magnetization distribution (i.e. breaking the distribution up into smaller pieces) near field points to see whether this reduces errors coming from modeling of the iron shape.

Expected advantages of this procedure come from the initialization, based on the results of the 2-D calculation and the re-granularization of the magnetization distribution, the initialization hopefully increasing speed and the re-granularization hopefully increasing accuracy. Additional efficiency can probably also be attained by restructuring GFUN3DIT to better utilize the architecture of the FPS. The new code will initially be developed on the VAX, and a VAX version will therefore be available for use at other laboratories.

Irrespective of improvements in techniques for calculating magnetic fields, it is clear that measurements of fields will continue to be an important component of magnet design and construction for the foreseeable future. Improvements in either the speed or accuracy with which fields can be mapped are therefore important elements of an accelerator development program, making the process of magnet design more precise and more efficient. The need to map the magnetic field of the K800 cyclotron led to the development of a new measuring system which takes advantage of two key advances in technology, namely a much more sensitive, heavy water, NMR probe developed at CERN and a much faster and more accurate search coil integration system made possible by new, high frequency, voltage-to-frequency converters. The new measuring system then uses the D_2O NMR probe to read the absolute field at the center of the cyclotron and uses a search

coil to measure the difference in field between the center and the other point.

A map at a given azimuth is recorded by moving the search coil radially along a track from the center of the machine to the inner cryostat wall. The output of the search coil is input to a precision bipolar voltage-to-frequency (v/f) converter; the field change is directly proportional to the difference in the total "positive" pulses and the total "negative" pulses. The v/f scaler is read "on-the-fly" when strobed by signals from a radial position sensor. The coil starts on one side of the axis of the cyclotron, moves through the axis and at the end of its travel (-0.1 m to +1.0 m is the radius range of the coil) steps to the next angle. Measurements are made in both radial directions. Some details of the hardware are described below; for more information see Ref. 13.

The NMR system is a commercially available unit used without modification. Finding the resonance at the center point of the K800 magnet proved to be rather easy; in most cases the signal was large enough for the internal electronics to lock onto the resonance once a close manual setting had been obtained. The v/f convertor with a bipolar amplifier was obtained from Lawrence Berkeley Laboratory and was used without change. The unit has an inherent one in 10^4 accuracy, so a 1 Gauss error would be expected for the 1.0 Tesla range that the coil would see; this error is due to a differential non-linearily.

Field data is read "on the fly" as the coil moves, strobing the data acquisition system with a logic signal whenever one of the reflection-mode photosensors mounted on the coil cart senses an "edge" in a precision glass scale mounted on the coil track. This on-the-fly data-taking system makes it possible to map very rapidly compared to previous systems. For the K800 mapping, a 360 degree map in one degree steps with 440 data points per radial scan required 40 minutes. The Falcon CPU in the CAMAC data system also checks for errors as data is taken and, at the end of a map, the operator is notified if any angle needs to be remeasured.

Analysis of the K800 mapping data shows that the mapper worked well. Tests of differential accuracy indicate errors of less than 0.1 Gauss over 0.5 in. (Integral errors were found to be about three Gauss when the coil returned to its starting place after going from -0.1 m to +1.0 m and back, but this is offset by a linear correction.)

C. Radio Frequency Systems

Cyclotron radio frequency systems are traditionally difficult to understand from first principles. They are also typically the cause of a large part of the difficulty associated with ongoing cyclotron operation. The resonant cavities which provide the accelerating voltage are usually quite complicated in shape, the "dees" in modern dee-in-valley cyclotrons tending to be much more crescent shaped than "D" shaped. The crescent shape is further complicated by the need for mechanical members to add strength, by items such as trimming and coupling electrodes, by intrusions of pieces of iron which are needed to properly shape the magnetic field, and by various flanges associated with the vacuum system and construction joints. The main power amplifier which drives the resonator is similarly an extremely complicated cavity involving 100 or so different components, many of which have tuning adjustments and all of which operate in a borderline frequency range where lumped element circuit analysis begins to break down (the latter being particularly a problem when dealing with the need to suppress unwanted resonances associated with harmonics of the fundamental frequency).

In the past, the customary technique in designing a cyclotron rf system has been to construct prototypes -- usually full scale -- first of the resonator and then of the amplifier, and to make empirical changes in these prototypes until first, the desired resonant frequency, or range of frequencies, is achieved, and second, spurious resonances are suppressed such that the input power ends up dominantly in excitation of the desired fundamental frequency.

Numerical analysis of many aspects of rf system behavior is possible with today's computers; speed and effectiveness of the design process have thereby been considerably improved. The role of empirical adjustment is not yet entirely eliminated but is greatly reduced, and many more options can be explored at lower cost than was possible with the earlier prototyping process. Generally this leads to substantially more efficient designs, i.e. designs where required accelerating voltage can be achieved with less power consumption, and where operating difficulties can be diagnosed with greater reliability. The radio frequency system is typically responsible for about 75% of the power consumption of a modern cyclotron and power costs over 10 years tend to equal total construction costs; gains in rf system efficiency are therefore very important.

Another important area of ongoing rf system development is in the low-level side of the system, comprising the large number of circuits which actuate the tuning devices for the resonant cavity and the power amplifiers and which provide the feedback signals which stabilize the system. The three-phase rf systems typically used in three-sector superconducting cyclotrons place particularly extreme demands on the low-level tuning networks because the fundamental modes of the three dee system are degenerate with respect to phase, and the relative phases of the dees is therefore entirely determined by the feedback networks. In view of this sensitivity, and the strong effect of the dee-to-dee phase adjustment on external beam stability, upgrading reliability and stability of low-level circuits is an important on-going development activity at NSCL.

1. Resonator Design Techniques.

The most desirable method to model rf resonators, such as those on the K500 and K800 cyclotrons, would undoubtedly be a three-dimensional code whose input is generated by a CAD system. Unfortunately, no appropriate code exists. The dee stem sections of the K500 and K800 resonators are circularly symmetric and the program "Superfish",[15] an adaptation of the

magnetic field relaxation codes, can be used to solve this part of the problem. With considerable uncertainty, the spiral dee can in turn be represented as a set of transmission line segments extending outward from the dee stem to the tips of the dee; each of these line sections can be calculated with the relaxation code Poisson, and all the sections can then be coupled using the general circuit analysis program "Spice", which accepts transmission line segments as allowed circuit elements. Unfortunately, Spice was designed for low power, lumped element, circuit analysis and so does not compute overall circulating energy or power dissipation. Since power and circulating energy are key quantities in optimizing accelerator resonators, we are presently working to develop improved techniques for calculating these parameters.

An important step in this direction is the development of a new code "RESON", named after a collection of subroutines used by the late Jack Riedel. This code models the dee cavity and associated resonator more accurately and uses "Spice" to find resonant frequencies, voltages, and currents. Junction capacitances representing transmission line discontinuities are also automatically calculated and inserted. Transmission lines which are tapered (along the axis perpendicular to the wavefront) can also be defined by the user and inserted where desired. The computation includes resistive losses, circulating energies, equivalent shunt resistances, coupling parameters, etc. The RESON package will include:

1) On-line terminal driven input and output.

2) Short, but complete, on-screen input descriptions.

3) Report form outputs with a complete electrical description.

The segmented transmission line model which RESON uses for the spiral dee uses Poisson to compute the electrostatic stored energy in an

incremental length of the dee and liner conductor pair. With this process the actual cross section can be represented quite realistically. The dee to liner potential and the stored energy fix the characteristic impedance per unit length of a transmission line with the given cross section. Equivalent resistances for the dee and liner are computed using a quasi-static approximation in which the current density on the transmission line surface is proportional to the charge density from the Poisson solution. Analyzing N of these cross sections with Poisson and connecting them together appropriately with linearly tapering sections in RESON, gives a much more accurate model of the resonator system.

For the K800, results from RESON are being tested by comparing with the body of data from a previously constructed full scale, low power prototype of the resonator cavity. Data from this model include resonant frequency versus sliding short position for the fundamental mode and for several harmonic modes. Voltage distributions along the dee were also measured. If results from RESON agree with the prototype results in a reasonable way in this complex resonator situation, the RESON results can thereafter be used with considerable confidence in computing power dissipation in various sections of resonators. In the K800 such results will be important in setting initial cooling circuit water flows to match power concentrations. RESON should also provide a powerful new tool for use in design of possible future cyclotron rf systems.

2. Low-level Radio Frequency Component Development.

The low-level rf drive system for the K500 is an array of approximately 100 modules, of 30 or so different types. A corresponding array of modules is in fabrication for the K800. Each module performs a critical analog or digital task, and few modules are trivial design tasks. The required modules are also not available commercially (except for the frequency synthesizers). More detailed information about the individual

modules and the complete rf system can be found in the 1983-84 NSCL annual report.[17,18]

Given the magnitude of the design, development, and fabrication effort, it is pleasing that the first pass design of these electronics is mostly trouble free as used on the K500. The problems which have shown up in the K500 system will also hopefully be eliminated in the improved modules currently in fabrication or final development for the K800. Some of the problems and/or corrective actions include:

a) Higher signal levels will be available from the frequency and phase generation and distribution system.

b) Multipliers in the K500 phase detectors are hard to calibrate and keep calibrated -- these have been replaced in the K800 units by special frequency mixers and filters.

c) The K500 dee voltage regulators are a partial printed circuit (pc) board, partial wirewrap configuration. The K800 units are totally pc board with the components arranged in a more reasonable and stable manner.

d) All K800 servo controls use a new design based on high precision, pulse width modulation amplifiers. This change also facilitates coupling to control system computers.

e) A microprocessor based serial communications interface is being added to all modules. This allows every module to be fully coupled to the control system. Each module also retains manual capability via a front panel "computer/manual" switch.

f) Fast phase shifters in the K500 are partially electronic, partially mechanical devices which are a substantial maintenance problem. In

the K800 these are being replaced by a completely electronic version with a phase compensating delay module in the phase delay loop.

g) Hydraulic servo valves for the K800 will be newer, more responsive versions. (The K500 servo valves were military surplus units which are no longer available.) The new valves require new more stable controllers -- these are being fabricated.

The new electronics, developed for the K800, should remove most, if not all, of these difficulties and the availability and reliability of the accelerator to the nuclear physics program should thereby be significantly upgraded. As time permits the K500 will be retrofitted with the improved circuits, thereby making its operation more reliable and speeding energy changes. Future low-level rf design work will focus on problems either overlooked or not adequately resolved by the K800 design process, and on further efforts to decrease fluctuations in the overall system, since fluctuations, from the point of view of the experimental user, almost always act to degrade the usefulness of the final beam.

D. Central Region Studies and Phase Selection

The central region of a cyclotron requires special computing techniques due to the fact that electric forces are strong relative to the magnetic forces in this region of the cyclotron. Accurate central region calculations must therefore employ fully detailed electric field descriptions. In earlier years, needed field maps were obtained from voltage measurements in electrolytic tanks; this process, though laborious, gave satisfactory results for orbits in the median plane. The lowest order terms in the off-median-plane electric field, however, involve second derivatives of the voltage and the quality of electrolytic tank data was usually such that these derivatives were quite inaccurate.

More recently, the relatively confined geometry of the central region has made it possible to substitute three-dimensional relaxation calculations for the electrolytic tank. The relaxation approach is quicker, easier, and gives greater accuracy, particularly in the off median plane field component. Studies of the central region have taken a major step forward as a consequence of introducing this improved technique, and effort can now be concentrated on details of particle orbits rather than on the problems of constructing electrolytic tanks and measuring electric fields.

With the relaxation procedure, central region studies in a variable energy, multi-particle cyclotron evolve into a massive computing effort. Each change in the central orbit geometry requires a re-tailoring of the central electrode configuration for optimum performance; the fields and orbits must then be recomputed; etc. This entire process must be repeated for each of the ten or so different central geometries which an optimized, variable-energy, multi-particle cyclotron needs in order to adapt to different ion sources, different harmonic numbers, and different values for the turn number (the number of revolutions which the particle makes to reach final energy).

Fortunately, a full complement of K800 central region geometries is not immediately needed. Geometries appropriate for the expected initial interests of the program are being developed first -- other configurations will be added over the years as experimental emphasis evolves. The K800 will in fact initially use the center plug and central electrodes from the K500 -- therefore the central regions applicable to both cyclotrons have been the first to be studied. At present, four such central region configurations are fully developed, namely, central regions for first and second harmonic operation with the PIG source and for first and second harmonic operation with the ECR source, all with an orbit geometry corresponding to a turn number of 500 to 550 in the K500 and 1200 to 1300 in the K800, i.e. to dee voltages of approximately 100 kV for the case of fully stripped particles. At present, only one of these central regions has been utilized and tested in the K500, namely, the geometry for the PIG ion source

operating on first harmonic. The central region for the ECR ion source is, however, now being installed, along with the ECR injection line, and tests with this central region are expected to begin in February 1986. Initial use of a second-harmonic central region for the K500 is also expected in the near future in order to prepare for a second-harmonic run, which was accepted at the last meeting of the Program Advisory Committee.

Central region computer studies are now shifting to the development of lower turn number (higher voltage) operating points for the K800, since it is always advantageous to operate with the smallest turn number allowed by the available rf voltage. Voltages up to 200 kV are expected to be feasible in the K800, use of the highest available voltage being particularly important for very heavy, partially stripped ions. (The path length in the cyclotron is proportional to the number of turns and beam loss due to electron pickup or electron stripping therefore varies exponentially with the number of turns.) Overall, the completely developed central region geometry for the K800 will probably involve five or six turn number choices for the ECR source in the first harmonic mode, one or two choices for the ECR source in the second harmonic mode and in addition a few central regions for the PIG source since the PIG will probably remain the ion source of choice for the very lightest beams (deuterons and alphas).

Another central region development, in progress on the K500 as an accelerator physics thesis project, involves the installation of a phase selecting system in the central region. Modifications to the cyclotron to allow installation of appropriate hardware were completed in a recent shutdown and the first experimental run using the "phase slits" should occur in the next running cycle of the cyclotron. The immediate objective of the phase slit project is an experimental study of orbit dynamics in the K500. A key beam parameter, the degree of orbit centeredness, varies markedly with rf phase. This gives a broad smearing of orbit centers in the normal K500 geometry, with its 40 to 60 degree phase width, and this masks details of interesting orbit phenomena. With the phase slits, and a narrow ion source slit, the cyclotron should operate in a "single turn" mode, very much like

the earlier 50 MeV cyclotron, and orbit behavior can therefore be tracked in considerable detail in the thesis study.

Later, the phase selection system will provide beam capabilities of interest in several nuclear science experiments, even though the loss of intensity associated with the phase selection process will, in the heavy ion regime, tend to make the use of the system considerably less frequent than in a light ion cyclotron. (An example of an experiment needing tight phase selection is a proposal from Texas A & M to do neutron scattering experiments using the high energy deuteron beam from the K500 on a tritium target, with timing resolution sufficient to separate the two-body monochromatic neutrons from the three body continuum; the identified two-body neutrons are then the incident beam for secondary neutron scattering experiments.)

In the future, further central region studies will attempt to improve the optimization of the spiral inflector system used to inject the beam from the ECR ion source. These inflectors, in their customary configuration, induce severe distortions in the central region phase space distribution in the cyclotron. This is undoubtedly a dominant factor in the typically low (5-10%) transmission from ECR source to cyclotron external beam. It seems likely that presently available computing techniques will lead to significantly improved geometries. The potential for large gains in source-to-target transmission make a sizeable investment of effort on this problem appropriate.

E. Improved High Field Electrodes

Difficulties with achieving high electric fields are perhaps the most fundamental of the initial operating problems experienced in the K500 cyclotron. The design of the K500 assumed electric fields of 100 kV/cm in the rf system and 140 kV/cm in the extraction system, the clearances being such that both of these values correspond to peak electrode voltage of 100 kV. Interestingly, both the rf system and the deflectors achieved their

design voltage in the first few days of operation, in tests which appear to have been reliably calibrated. (The dee voltage was inferred from x-ray end points with detectors calibrated against known radioactive sources; the deflector voltage was measured with a resistive divider, which is not normally subject to error.)

Following the initial tests, the deflectors in particular degraded rapidly, the primary phenomena being growth of "dark current" (the more-or-less steady current which flows between cathode and anode) up to values such that the dark current would heat local regions of the anode to the melting point. After some months this problem was traced to an interesting solid state phenomena, namely growth of metal "whiskers" on the cathode surface, a typical whisker being perhaps 2mm long and 0.1 mm in diameter. Using a deflector test stand, built so that testing of deflectors could proceed without interfering with cyclotron operation, it was found that the growth of whiskers could be alleviated by making the vacuum somewhat poorer in the deflector region (presumably inhibiting whisker growth by either sputtering or by a chemical reaction with the background gas).

Problems with the design of the support insulators for the deflector cathode were also worked through in the test stand. A new insulator design was developed based on sapphire rods metallurgically bonded to molybdenum end-caps. The insulator-to-end-cap joint is a "planar" geometry, i.e. the traditional corona rings on the end-caps are omitted. This geometry reduces field enhancements at the insulator surface and also increases the effective length of the insulator. The new system is mechanically very rugged -- no insulators have failed mechanically in the K500 since the new design was introduced 18 months ago; previously mechanical failures of the insulators were common. The improved insulator geometry developed in this process is an important technical improvement applicable in any insulator situation where space is stringently limited.

In parallel with the test stand studies, computer studies of the electric field in the vicinity of the deflector electrodes indicated that the peak electric field near electrode corners was 50% higher than the

useful electric field in the main electrode gap. This led to development of improved electrode shapes in which the peak electric field is reduced to levels which are no more than 20% above the useful electric field. Electrodes incorporating this improved design are now in the process of being tested.

Another possible deflector improvement might come from using alternate materials for the deflector electrodes. Tests a number of years ago in the 50 MeV cyclotron led to the initial choice of materials for the K500 deflectors, namely stainless steel for the negative electrode and tungsten for the positive electrode. Sparking studies in the literature indicate that improvements might be achieved by changing to either titanium or anodized aluminum for the cathode material and by improved cooling of the anode. Tests of alternate materials are therefore included with the testing of revised electrode shapes in the test stand work plan.

The program of deflector testing, and the rate of improvements, has slowed relative to early stages of the program, since most structures now operate at or near the voltage maximum of the test stand and a change is needed in the test stand configuration or in the power supply to increase the working range of the testing facility. Results for a number of the changes discussed above are then not yet clearly established.

There is at this time a fairly clear indication that deflectors work less well in the cyclotron than in the test stand, although testing time in the cyclotron has been limited. (In recent months the routine operating regime of the cyclotron has been limited by rf system voltage rather than by deflector voltage.) Recent deflector "failures" in the cyclotron, (i.e. instances where deflector voltage has degraded to the point where the deflector must be changed) have all involved macroscopic dust-like particles on the anode surface. The presence of such particles in the cyclotron vacuum tank unfortunately appears to have increased significantly over the years as the tank has been opened and closed numerous times. A design modification to remedy the dust problem has been worked out. In this modification, the entrance and exit ends of the deflector, which were

originally fully open, will be partially closed by a cover with an entrance and exit hole just big enough for the beam. This will make a 20-fold change in the open area and greatly reduce the probability of a dust particle migrating into the deflector.

Another possibly important difference between the test stand enviroment and the cyclotron is that deflectors probably operate at higher temperature in the cyclotron due to heating from the beam and from background rf fields. A first step in establishing the significance of the operating temperature is to install a thermocouple temperature monitor on the cyclotron deflector (this is in process). Deflectors in the test stand will then be heated to an operating temperature matching that in the cyclotron and voltage effects observed. Cooling of the deflector anode is difficult in the tight geometry of the superconducting cyclotron (the most effective solution, water cooling, is extremely difficult). An improved anode cooling system which we are presently testing uses copper anodes plated with tungsten on the voltage holding side, the copper being a good conductor, the tungsten a good spark resisting material. With this arrangement, thermal conduction is very much larger relative to that of the tungsten sheets previously used and operating temperatures should be lowered.

Another deflector problem involves electrical breakdowns in the high voltage feed line. In the K500 this feed line operates at an electric field which is higher than the electric field in the deflector gap, and approximately equal in strength to the enhanced field at the deflector corners. In the test stand, a K500 high voltage feed limits at lower voltages than the main deflector electrodes. (The 95-100 kV test stand results use larger diameter feed through tubes.) An alternate solid-insulated high voltage rod has been procured, consisting of an aluminum oxide tube plated with a resistive layer on the inside and metallized on the outside. The inner conductor of this rod will be the high voltage electrode, and the outer will be the ground electrode. Since the dielectric strength of aluminum oxide is much higher than that of vacuum, this

structure should comfortably hold required voltages in the body of the tube and the breakdown characteristics will be determined by the details of the tube-end design. The goal of the testing program is to develop a set of corona rings for the tube ends which will hold the needed voltages and be compatible with the space available in the K500.

In summary, high electric field development studies will continue as a significant NSCL program activity for the foreseeable future.* This should contribute to steadily improved operating reliability for both the K500 and

---

* Specifically, the goal is high electric fields in the presence of high magnetic fields. Magnetic fields have a major effect on the breakdown process, so that developments not involving magnetic fields, such as for electrostatic accelerators, are of limited assistance in the cyclotron deflector problem.

---

the K800 cyclotrons. Reliable, high electric field structures will also greatly facilitate design of extraction systems of future cyclotrons. For example, the extraction system design for the K800 cyclotron has been modified in recent years to work at electric fields lower than those assumed for the K500 design (this is described in a following sub-section). The new design involves requirements on the magnetic elements which are undesirably tight due to the narrow separation between these elements and the internal beam. If higher electric fields were available, the separation between the internal beam and the extraction orbit would be increased and design of magnetic elements would be much easier.

The electric field in the extraction system is also the performance limiting factor for the lightest projectiles, ^{3}He and protons. This limit is so severe that most superconducting cyclotron projects do not plan to attempt to accelerate either of these projectiles, although the recently approved Orsay-Groningen project has this as a major goal. Particularly for these particles the development of techniques for increasing the electric

field will greatly facilitate the design of the extraction system and will expand the operating regime in which these particles can be utilized.

The rf system of the K500 cyclotron has also over the years experienced a loss of voltage holding capability, although with different characteristics from that experienced in the deflectors. An important element which has contributed to the rf system problems is the development of oxide surfaces in contact joints, increasing rf heating in the joint, and ultimately resulting in catastrophic failure. Thus far, each problem of this type has needed an individualized engineering solution since the characteristics of various joints in the K500 involve many different design constraints.

Recently, the limiting problem of this type involved joints in the large corona rings which protect the main dee stem insulators. A design change to make the corona ring contact more rugged involved extensive shop work just recently completed. The K500 is now fitted with a fully upgraded set of corona rings and is ready for testing of this revised design.

Earlier, design changes on the rf coupling line feedthru insulator and on the contact fingers of the outer conductor wall of the sliding short reliably eliminated problems which had been in turn the most frequent cause of cyclotron down-time. Hopefully the corona ring change will similarly eliminate the present limiting problem so that operation at higher rf voltages will be routinely possible.

A possible further factor in the rf voltage problem is the presence of contaminants in the vacuum system. Hydrocarbon contamination is cited in the literature as particularly bad for high voltage surfaces. Unfortunately, several accidents over the years have exposed the rf system to significant hydrocarbon contamination, and clean-up efforts probably fail to reach into all of the crevices where hydrocarbon contaminants might be present. The original all-metal vacuum system of the cyclotron has also been changed in several places to Viton seals due to vacuum leak problems in metal seals which were either exposed to corrosion or subject to

installation accidents. Restoring the vacuum system to its original, all-metal status would involve a lengthy shutdown. To clarify the gains which might result from such a cleanup, off-line tests are being set up in the deflector test stand to observe the effects of Viton and hydrocarbon contaminants. This data will guide a decision as to whether to undertake a major cleanup of the K500 vacuum system.

F. Extraction System Calculations

The initial extraction system for the K800 cyclotron has been selected and hardware is being constructed. The K500 extraction system exists as a fixed array of hardware. Further study of both of these systems are in progress to study possible system improvements, particularly improvements which would be reasonable to implement as upgrading projects on the respective accelerators.

The last focusing element on the K500 extraction trajectory is one element where additional studies are likely to lead to an improved design. This element is located in an aperture of the outer yoke of the cyclotron where the magnetic geometry is highly three-dimensional and where the field over most of the operating range of the cyclotron is fairly weak. In spite of the weak magnetic field, the original design of this focusing element utilized the saturation approximation, since no alternate viable computing technique was available. Operationally, the external beam direction at the edge of the K500 yoke, and the "effective source" position for the external beam, are observed to be significantly different from calculated values. The final focusing element is the most likely cause for these discrepancies. As three-dimensional computing techniques (described in a previous subsection) become available, further studies of this K500 element will be made.

The extraction system for the K800 cyclotron is basically like that of the K500, i.e., a combination of active electrostatic deflectors and inert magnetic focusing elements, but there are significant differences in

details. One particularly important difference is that the inner-most K800 focusing elements involve much more complicated arrays of iron to compensate the effects of these elements on the internal beam, and one of the iron elements in the K800 is arranged in a dipole configuration, in contrast with the quadrupole configuration of the other elements and of all the iron elements in the K500.

Basic characteristics of the K800 extraction system are described in internal Laboratory reports.[19,20] Focusing of the beam is comparable to that achieved in the K500 and electric fields are reduced by 10 to 15% relative to the strengths needed in the K500 system. With the basic K800 geometry now frozen for construction, further studies will address optimizing the operating characteristics of the system and possible future upgrades.

An immediate important K800 optimization study will analyze the accuracy with which the magnetic focusing elements must be positioned. Operating experience in the K500 indicates, for example, that the positioning of the focusing elements along the outer part of the extraction path is not critical (operators have tended not to reposition the elements as they shift from one beam to the next). This can be qualitatively understood in terms of the strong focusing aspects of the sequence of elements, which tend to make position errors self-correcting. The possibility of eliminating positioning drives on some or many of the elements would be a significant goal of such a study, and the new combined orbit code described previously will make it possible to carry out such studies with a much smaller investment of manpower. A first study of this type should be completed on a schedule which will precede a decision to release drive mechanisms for construction.

Another likely area for optimization of the K800 extraction system concerns the design of the intricate, inner-most magnetic element. This element, which has three-sector symmetry, affects the beam on the final internal orbits, on the extraction orbit as it leaves the first electrostatic deflector, and on the extraction orbit as it leaves the

magnetic dipole. Optimum beam tailoring at these three distinct regions leads to rather different requirements, and the actual design of the element is thus a complicated compromise which is probably not fully optimized at present. The small size of the element fortunately makes it relatively easy to construct alternate arrays.

The median plane injection system, which will be needed if the beam from the K500 cyclotron is injected into the K800, requires a focusing magnet just at the edge of the K800 yoke, i.e. in very much the same position as the final focusing magnet on the K500 extraction orbit. If or when we decide to couple the two cyclotrons, a detailed design must be developed for this magnet. By that time three-dimensional magnetic field computing techniques should be available; if they are not, the design will need to be based on measurements of the fields of mock-ups placed at the appropriate position in the K800 yoke.

G. Advanced Ion Sources

The ion source is a critical element in the performance of nearly every accelerator system. In recent years, heavy ion accelerators have received a major performance boost as a consequence of the development at Grenoble[21] of the so-called electron cyclotron resonance ion source (or ECR). These sources have now been installed on a number of cyclotrons and have typically doubled the available output energy (in the range where energy was limited by the ion charge state, i.e. for all except the very lightest particles). The ECR source also operates much more reliably, basically without attention, and has an essentially infinite lifetime, which are extremely important gains relative to the PIG source, previously the most effective source for highly charged heavy ions. Developments in ECR techniques appear to be well short of full optimization and further significant performance gains seem likely. An indicator of this is that 1984 highest, high-charge-state currents (as reported at an ECR source

conference[22] in January 1985) are now regularly exceeded by nearly an order of magnitude at many laboratories.

Unfortunately, the development of these sources is basically empirical, since efforts at developing a theory with significant predictive power have thus far not been successful. Empirical exploration is time-consuming and, for some parameters, expensive. Since ECR's involve many strongly coupled parameters, the number of configurations which needs to be explored is very, very large. Fortunately, there is excellent collaboration world-wide among the various laboratories involved in ECR development. Also, programs at the different laboratories are for the most part complimentary and this greatly broadens the total experimental effort on ECR optimization.

Some of the important parameters -- rf power, magnet strength, gas flow, etc. -- are easy to vary continuously and optimization of these quantities in a given configuration proceeds fairly rapidly. Other key parameters -- rf frequency, source size, multipole focusing, etc. -- require building or rebuilding major experimental elements in order to make changes. Intermediate between these two extremes, a number of important semi-flexible elements -- aperture sizes, rf coupling arrangements, gas feed location, etc. -- can be changed in a day, or a few days (most of these changes involving an opening and reclosing of the source in order to move to the new value of the parameter). The different laboratories where ECR development is in process tend to take different paths for the very difficult-to-change parameters, with individuals following up favorite hunches; in this way, a broadly based attack is created world-wide. Information on effective combinations of the readily adjustable parameters is freely exchanged, and on a number of occasions, joint experimental studies have been undertaken, with sharing of personnel and apparatus.

One line of recent effective improvement, which is quite expensive, involves increasing the rf frequency. In particular, a very significant improvement in charge states was achieved at Grenoble in an experiment in which a 16 GHz rf transmitter was substituted for the standard 10 GHz

transmitter. (This change involved an almost 10-fold increase in transmitter cost due to the combination of increased cost per watt in the higher frequency band and the increased power level needed for source optimization at the higher frequency.) The frequency change, in a source in which other elements were dominantly unchanged, gave an increase in usable charge states of about 20% (corresponding to a 44% increase in cyclotron beam energy). This is one of the most dramatic single improvements which has been accomplished in ECR source development. Another major experiment in this direction at Julich should soon come into operation -- this source has a superconducting magnet and an 18 GHz rf transmitter.

The MSU source at present uses one of the least expensive rf sources, which runs at quite a low frequency, 6.4 GHz. The Grenoble results indicate that an important gain could be expected from increasing the frequency, and a frequency of 10 GHz would be compatible with the magnetic field range of the present MSU source. To quantify the performance gain before committing to purchase of a power supply, we hope to carry out a joint frequency changing experiment with the group at Louvain-la-Nueve. One of our 6.4 GHz transmitters would be operated on their source or their 10 GHz transmitter would be operated on our source. Exploratory discussions are in process and hopefully this joint experiment will soon be implemented.

Another important, difficult-to-change source parameter is overall size. A rare, controlled experiment probing the importance of source size, involved a joint MSU-LBL effort in which the inner (confined plasma) diameter of the LBL source was increased by 25%, the original geometry of the Berkeley source fortuitously making it rather easy to make a one step increase of this amount (a few man months of fabrication effort). This radius change gave an important charge state improvement (about 12%). Noting this result, the design of the MSU room temperature source was laid out to make a further substantial increase (≈65% relative to LBL) in source size, while holding other parameters constant. At this time, a definitive evaluation cannot yet be made as to the gain resulting from this increase in size, since new ECR sources require extensive optimization of many details

(stage to stage spacing, the sizes of the stage to stage apertures, locations of gas and rf feed, etc.) in order to reach their peak performance. This is a time consuming process, and the MSU source is at present still in mid-stream in its optimization program.

Actual status of the MSU room temperature source, after five months of operation, is that the ion source is producing krypton beams with a slightly better high-charge-state performance than published results for the Berkeley source or the 10 GHz Grenoble source, but not dramatically better. This state-of-the-art performance of the source in a configuration which is only partially optimized is encouraging -- the essential next step is to press forward as rapidly as possible to full optimization.

Beyond the room-temperature ECR source, it is clear that at some point the Laboratory should undertake a superconducting source. Superconducting coils are clearly the design of choice at the field strengths needed for 16 GHz and higher frequencies. They are even more clearly the only viable option if a large increase in size, say 100% or 200%, is to be attempted, since a room temperature ECR of such size would involve power dissipations in the several megawatt range. Superconducting ECR sources have been attempted at several other laboratories, with rather disappointing results thus far, in that the projects have in several instances become bogged down in cryogenic problems, leading to years of delay. The one superconducting source which has actually operated, a large source at Louvain-la-Neuve, did produce an impressive enhancement of high-charge-state yields compared to a smaller source operated at the same laboratory. This supports the expectation of charge state gains from increased source size. The laboratories where superconducting ECR's have been attempted all lacked in-house superconducting magnet design experience. Therefore, all elected to try commercial procurement of superconducting elements of the sources and the commercial vendors failed to provide equipment meeting requirements. Even the source at Louvain-la-Neuve, which operated successfully for a number of years, has now been abandoned to avoid a difficult cryostat repair operation. Development of a superconducting ECR source seems an ideal

project for NSCL -- the Laboratory has very solid and extensive experience in both design and operation of ECR sources and in design and operation of large cryogenic systems. The Laboratory's future ECR plan is to continue the optimization of the room-temperature source to a point where reasonably thorough exploration of the parameter space associated with that source has been completed. The data from the room temperature source will be reviewed with particular care for evidence of the importance of the size parameter -- this will then be the basis for fixing the size of the second generation superconducting source.

The design of the coils for the superconducting source will include a large operating margin in field strength, this being relatively easy to do in the superconducting situation. With this capability, the source can later be upgraded to frequencies as high as 30 GHz, if gains in the frequency domain continue to be indicated. We are at present working to develop contacts which might give us access to surplus military transmitters, since the commercial cost of transmitters is quite high. (Varian, for example, offers a 1.7 kW 18 GHz transmitter for approximately $450,000.) Development of improved ECR sources will continue as a major element of the Laboratory's accelerator physics program for a number of years. Results should be broadly useful in most positive-ion based, heavy-ion, accelerator systems.

H. Beam Transport Systems

The K800 cyclotron beams (actually K=1200 max) will have momenta up to 1.6 GeV/c, ie. even higher than LAMPF beams. With the laboratory's existing liquid helium production capability, superconducting quadrupoles and dipoles are the design of choice for this transport system. At this momentum low-field, iron-dominated magnets, built with emphasis on cryogenic efficiency, are both cheaper to build initially and cheaper to operate in the long run than either conventional magnets or high field superconducting magnets*. The choice of 1.5 Tesla for bending magnets versus 5 Tesla for cyclotron

magnets comes from the different relationship between field level and flux in the two situations. In the bending magnet, the flux, for a given aperature, is length times field strength, and, if the field strength is raised, the length is reduced, and the product is constant; the volume of iron in the bending magnet is therefore more-or-less the same irrespective of field strength. In the cyclotron, as the field is increased, the radius decreases, and since flux is proportional to the square of the radius, the flux therefore decreases as well. This gives large reductions in the volume of iron required for a cyclotron of given energy as the field level is increased (see discussion in a previous subsection).

---

*At much higher momenta the length of low field bending magnets becomes too great, driving the choice of magnetic field to higher values.

The level of technological expertise required to construct an efficient and trouble-free superconducting beam transport system is obviously greater than that required for assembling a conventional system. A rather extensive R & D program is necessary to develop and test specific magnet designs which will be employed. On the other hand, successful demonstration of this technology at NSCL should benefit other nuclear physics projects in the future, and possibly also contemporary projects such as CEBAF and LAMPF II.

The superconducting beamline R & D program has benefited from discussions with many experts from other laboratories. The final choice for the "style" of the magnets and the cryogenic distribution system has been greatly influenced by ideas suggested by John Purcell, (now at General Atomics, formerly at ANL). These discussions led to the selection of a batch-transfer cryogenics system and a low heat loss, low operating current design for the magnets (currents are 12 amps for the quadrupoles and 100 amps for the dipoles).

The goal of the quadrupole magnet design is to have a one week cycle between batch-transfers of cryogens (helium and nitrogen) into its two 25-liter storage reservoirs. A low heat leak (0.15 liter/hr) cryostat design is matched to the operating current, so that the boil-off gas from the cryostat is just sufficient to operate the vapor-cooled leads. The batch-transfer cryogen filling uses a permanent transfer line similar to that used on the Tevatron rather than portable dewars; helium transfers should therefore be fast and simple. The transfer lines are allowed to warm up when not in use; this reduces the integrated total heat leak of the system by a large factor, since the steady-state transfer line losses which are eliminated are much larger than the refrigeration required for the weekly line cooldown.

Because of their efficiency and low operating current, the quadrupoles will remain connected to their (200 watt) power supplies during operation. This makes the process of focusing and fine tuning beams basically the same as it would be with a room temperature beam transport system. With 20 Volt power supplies, the quadrupoles can be changed from no field to full field in 100 seconds and can be fine-tuned at a rate of 1% per second. For the dipoles, the situation is somewhat less convenient, due to their larger stored energy (approximately 10 times higher). If the dipole current were the same as the quadrupole current, the inductance would be 10 times higher, and in the event of a quench, the voltage induced across the coil would be large and would probably damage the coil. To reduce this voltage higher currents must be used. Taking account of relevant factors, 100 amps is about the lowest full-field operating current at which the dipole coil is clearly safe. At this current, vapor-cooled leads give too much liquid boil-off ($\approx$0.3 l/hr) to be compatible with the weekly fill cycle; disconnectable, persistant mode leads will therefore be used in these dipoles. With such leads, the dipoles can operate in the persistent mode with greatly reduced heat load and therefore be compatible with the once-per-week helium distribution plan. Operationally, for a given beam, the dipoles will be set initially to within 1% of the required current, after

which the leads will be disconnected. Small conventional steering magnets at the entrance of each switching dipole will fine tune beams within this last 1%.

At this time (January 1986), a prototype quadrupole has been operated successfully in a small piece of test beamline located near the 800 Watt refrigerator. After eliminating an unexpected source of heat due to a thermo-acoustic oscillation in the helium feed and return lines, the cryostat performed as designed (<0.15 liter/hr for both liquid helium and liquid nitrogen). The superconducting quadrupole also works smoothly and magnetic field quality is excellant. The largest error harmonics measured with our mapping apparatus have amplitudes of less than 0.15%. (The largest error appears to be due to a pole positioning offset and should be eliminated by accurately doweling the pole tips to the yokes in production models.) The next step is to construct four additional quadrupoles packaged as doublets to debug the doublet design and to provide doublets for use in the Phase 1.5 program (described elsewhere). After this, a production phase will be concerned with completing the 60 total quadrupoles required for Phase II, with most manufacturing operations handled in commercial shops.

At this time, the prototype ±16° superconducting switching magnet is being assembled. When completed, it will be added to the end of our test beamline section for magnet mapping and other checkouts. The overall Phase II beam transport system requires six of these dipoles if the K50 cyclotron magnet is used as a switching dipole and eight or nine if the K50 is not used.

With the planned cryogenic efficiency of these superconducting beamline magnets, the entire phase II beam transport system will use less than 20% of the liquid He production capacity of the 800 watt refrigerator. With reasonable care as to the efficiency of the continuous feeds to the K500 and K800 magnets and cryopanels, and the possible superconducting ECR, the present refrigerator should have adequate capacity to handle all of these devices, plus the beamline, plus possible continuous use of the S800 spectrograph.

Batch-fed liquid helium cryopumps are a possible additional use of liquid helium in the beam transport system. Small appendage pumps appear to be the most cost-effective method to provide excellent vacuum in the distributed geometry of long beamlines. Larger versions of such pumps may also be the choice for rapid pump-down of large scattering chambers such as the 92" x 120" chamber. Small and large versions of such cryopumps are currently at the conceptual design stage. (An expert in this field, Robert Powers, is providing consulting help with these designs.) The additional helium usage required by these pumps is expected to be a few hundred liters per week. This should be compatible with the reserve capacity of the large refrigerator.

I. Cryogen Supply Systems

Large amounts of liquid nitrogen and liquid helium are needed to operate the laboratory's superconducting magnets and cryopanel-based vacuum pumps. These cryogens are distributed to points of use through a central cryo-distribution system.

Commercial procurement of liquid nitrogen is more cost effective than on-site reliquification. Cost is approximately $0.25 per gallon, delivered by tanker truck approximately every four days. The bulk delivery is stored in two 3600 gallon tanks and distributed to points of usage. (The storage tanks are former liquid fuel storage tanks from an Atlas missile silo.)

Liquid helium is produced in-house by two refrigerator-liquifiers, one, a 25 liter/hour CTI-1400 purchased in 1975, which we continue to operate mostly to satisfy the needs of the K-500 cyclotron, and the other, an 800 watt refrigerator or a 200 liter/hr liquefier, built by Cryogenic Consultants, Inc. (CCI). The latter unit is intended to handle the long range helium needs of the laboratory. The CCI unit is a one-of-a-kind refrigerator and is comparatively power efficient. It has however, been subject to a number of startup problems since first coming into operation in

September 1982 and a component (15%) of its cost is still being withheld pending resolution of these problems.

The CCI unit uses two Sullair, oil-flooded screw compressors. These were not well-matched as delivered, and even with subsequent changes, have yielded a mass flow of only 50 to 55 gram/second, which is well short of the 62 g/s compressor specification. The high-pressure gas system also had a faulty oil removal system as originally delivered. This problem became apparent when the 1400 refrigerator was connected to use gas from the large compressor system. (Gas for the 1400 was originally supplied by three reciprocating compressors which provided a total mass flow of 13 g/s; more frequent maintenance needs of these compressors motivated the connection to the Sullair screw compressors.) Almost immediate plugging of the 1400 coldbox following this shift alerted us to an entrained oil problem in the gas supplied by the large compressors. To remedy this problem, a major modification of the oil removal hardware was implemented in December, 1984. This change reduced oil contamination in the high pressure helium supply stream to below 0.05 parts per million (ppm). Unfortunately, effects due to contamination of the refrigerator cold boxes with oil were not easily reversed, and it was necessary to clean the high pressure coils of the refrigerator heat exchangers with solvent. This procedure was reasonably successful in restoring refrigerator performance.

To replace the failing CTI-1400 compressors, and provide some redundancy, we purchased and brought on-line (7/30/85) a third screw compressor with a capacity of 30 g/s; it can be operated independently or in parallel with the original Sullair compressors. With this addition, and with other changes including a set of modifications to the expanders of the refrigerator, a more complete performance test of the CCI refrigerator was carried out. Table 1 summarizes results of performance tests at various times. In the most recent tests, the refrigerator operated close to specifications for refrigeration capacity, but not at the design temperature due to another major defect which was uncovered, namely that when the refrigerator is operated at maximum refrigeration capacity, the cold gas

Table 1: Performance tests of CCI refrigerator.

Date	Liquifaction (g/s)	Heater Power (watt)	Trial Length (hrs)	Comments
12/ 8/82	4.3 -0.2	0	1.78	
12/10/82	1.3 -0.1	200	1.85	
12/10/82	0.0 -0.3	250	0.95	
12/21/82	0.3 -0.2	380	1.35	1
12/21/82	0.6 -0.4	450	0.67	1
12/21/82	4.2 -0.2	0	1.53	1
1/11/83	4.4 -0.1	0	1.83	2
1/14/83	1.1 -0.1	300	4.32	
3/23/83	4.6 -0.3	0	0.85	
3/31/83	4.2 -0.2	0	1.30	
4/21/83	4.6 -0.2	0	1.43	
6/ 8/83	4.1 -0.2	0	1.27	
7/26/83	4.7 -0.4	0	0.58	
7/26/83	5.4 -0.2	0	1.17	3
7/27/83	1.8 -0.1	400	2.07	3
8/16/83	6.2 -0.1	0	1.13	3
8/16/83	0.3 -0.1	510	1.72	3
8/17/83	4.12-0.03	0	2.68	
8/8/85	4.3	0	2.9	4
12/14/85	7.4	0	2.45	5
12/16/85	3.0	420	3.0	6
Acceptance Specs.	2.79	400		

1. A temporary 1 ft tube extension was fitted to the delivery line of the transfer line during this run.
2. The transfer line was lengthened by 1ft to get dewar gas return inlet out of the bayonet sheath.
3. The three CTI-1400 compressors adding a nominal total of 13 g/s were operated in parallel with the Sullair compressors.
4. Total flow to coldbox 60 g/s.
5. Total flow to coldbox 74 g/s, corresponds to rate of rise of 325 ℓ/hr in the dewar.
6. Total flow to coldbox 83 g/s

return pressure is near 12 psig. At this pressure, helium boils at 4.9 degrees rather than at 4.4 degrees as required in our specification. (4.9 degrees is also well above the design safe operating regime of the K500 and K800 cyclotron coils.)

Discussions are in process concerning best remedies for this liquification temperature problem. A device such as a cold compressor may have to be added to the system if the maximum operating capacity of the refrigerator is to be achieved at the design temerature. (The design temperature can be achieved at present at reduced capacity, and the refrigerator has been in use since April 84, operating the K-800 coil for magnetic field measurements and other purposes.)

A present puzzling helium system problem involves blockages which gradually build up in liquid lines. The problem began at a well-defined point in time (August 1985) but no useful correlation has been made between this date and other events which might affect the system. Small orifices such as metering valves are subject to gradual plugging, and over a period of a few hours, flow through a valve can diminish to the point where operation of the associated device is impaired. Stopping the flow of the liquid helium completely for a short period (seconds to minutes) usually clears the plug. A further puzzling characteristic is that the refrigerators seem to be immune to plugging by this contaminant. To cope with this problem, we have constructed a dual-filter assembly (an array of two micron filters) for the liquid helium stream. This minimizes operating inconvenience due to the blockages and residues from the plugged filter can be fed to analyzing equipment for study. Positive identification of the specific contaminent is clearly a central key in fully eliminating the problem.

The liquid blockage problem emphasizes a continuing need for quick identification of trace impurities in the helium system. A system which continuously checks for shifts in base line conditions is more valuable and in many ways easier than a system which gives absolute levels of particular contaminants, the latter being hard to correlate with troubles since the

system always operates with a background of many small contaminents each of which is a potential trouble source. Presently, the helium stream is monitored for water content using a Panametrics hygrometer and for oil contamination with a PPM Inc. Aerosol detector. In the near future, a gas discharge analysis system will be added, modeled on a Fermi Lab installation, and using a commercial optical monochrometer for spectral analysis. Selected emission lines are monitored to detect N_2 or H_2 contamination, for example. Monitoring variations of differential pressures in gas and liquid helium piping is also a useful diagnostic tool. Manifolds which facilitate these measurements have been installed in the last three years. As the final control system comes on-line, these diagnostics will be expanded and will include computer logging and remote readout capability.

Various helium system difficulties have clearly indicated an important need for additional redundancy and flexibility in what is as much a utility for the NSCL as magnet cooling water is in other laboratories. Purchase of the additional compressor was one significant step in this direction. A valving station is also presently in process which will allow the main refrigerator's spare gas expander engine to be substituted for either of the engines in use, without disturbing system operation. This should greatly facilitate engine maintenance and provide increased flexibility in operation.

Several other system upgrades are highly desirable: (1) A second large charcoal vessel in the helium gas purifying system would facilitate changes of the charcoal and eliminate changeover downtime -- a second vessel would also allow more complete vapor pump out of the charcoal before putting a new bed in service. (2) A third Balston coalescer unit (these devices remove compressor oil from the helium stream) would provide additional protection against oil carryover; (3) a larger nitrogen-cooled charcoal trap to augment the present contaminant adsorber unit (which can take a flow of only a few g/s) would speed deriming operations during warm-up of refrigerators and for general decontamination as needed. (4) Equipment to address the problem of high return gas pressure by either identifying and

remedying the responsible component in the cold box or by adding a cold compressor to the system.

A planned project which will have some impact on refrigerator operating costs will be carried out as it fits into construction plans. The nitrogen shields of the K-500 operate somewhat inefficiently and some liquid and much cold gas comes out of the coil exhaust. This overflow and cold gas will be piped to the liquid nitrogen cooled heat exchanger of the CCI refrigerator, where its cooling capacity will be used to precool the incoming warm helium stream.

J. Accelerator Applications

In November 1981, publicity concerning the start-up of the K500 cyclotron came to the attention of a medical group in Detroit that had been working to obtain a cyclotron for neutron therapy. Comments in the newspaper article as to smaller size and reduced cost of the superconducting cyclotron led the group to ask the Laboratory if a superconducting cyclotron might be a more attractive neutron therapy system than a conventional cyclotron. Responding to this request, a modest study was set in motion which led to some quite appealing conclusions -- the superconducting cyclotron could indeed achieve a major reduction in the size and complexity of a neutron therapy system. The primary advance would come from mounting the cyclotron directly on a rotating gantry so that neutrons produced in an internal target could be directed at a patient from any desired direction. This eliminates the beam extraction system, the beam transport system, and the beam swinger system, all of which are complicated and expensive components of a conventional room temperature neutron therapy system. The cyclotron is also exceedingly simple compared to the variable energy multiparticle research cyclotrons, which the Laboratory is customarily designing, because the neutron cyclotron involves only one projectile and one energy. The rf system thus operates at a single frequency and no field shaping corrections are needed in the magnet. One novel requirement, which

involves some intricacy, is the need for the helium vessel to continue to function as it rotates on the gantry through a full 360 degrees -- a design having this capability has been worked out and experimentally tested in a mock-up vessel.

A few months of initial design studies established the basic characteristics and workability of a possible neutron therapy system. An extended period of negotiations followed between MSU, Harper-Grace Hospitals of Detroit, and the National Science Foundation. From the beginning it was recognized that if the project was successful, it would probably be an element of a future commercial enterprise. The three organizations involved were just beginning to develop policies aimed at encouraging spin-off of research based technical developments into commercial enterprises. Negotiations as to an appropriate organizational format for handling such a project were then significantly prolonged by the desire of the several institutions to arrive at an arrangement which would be an appropriate model for future spin-off situations and which would be consistent with institutional policies which were then in the midst of being developed. These negotiations culminated in September 1984 with the signing of an agreement between MSU and Harper-Grace Hospitals to proceed with construction of such a cyclotron, with the National Science Foundation concurring in the arrangement and allowing use of NSCL facilities in the project on a non-interfering basis relative to the main NSF program. The MSU/Harper agreement provides for 100% funding of the project by the hospital, including full overhead, etc., in accord with normal MSU procedures for research projects. Specifications on expected performance and anticipated total cost were based on the prior MSU study, and the achievement of these goals was recognized as being on a best effort basis. If there are unexpended funds at the end of the project, they will be shared between the hospital and NSCL, with no restriction on the use of such funds by the Laboratory. The project is under the direction of H. Blosser who will work on the project on a 5% of full-time basis, assisted in special situations by other Laboratory personnel up to a total level estimated to be

3,000 man hours. Primary manpower for the project is furnished by the hospital in the form of a technical team of approximately five full-time persons who work at NSCL under Blosser's direction. Rights to commercialize the venture pass to the Hospital (following a pattern which is normal at MSU for fully funded research enterprises) but with the University retaining royalty rights on future commercial sales.

Implementing the above agreement, Harper-Grace Hospital organized a small corporation, MedCyc, and contracted with this corporation to provide the technical group. Harper also passed through to this corporation, in exchange for stock, the manufacturing rights which it obtained under its agreement with MSU. The corporation also involves participation of a Michigan venture capital group with expertise in management of start-up companies and participation by a number of Laboratory staff members as shareholders. The project has been moving forward under this format since September 1984.

Detailed design of the neutron therapy cyclotron considered three beam options, namely 50 MeV protons, 75 MeV ^{3}He, and 50 MeV deuterons. Deuterons were ultimately selected primarily because the rf frequency is in the commercial fm transmitter band (for the desirable, high-energy-gain, third harmonic mode). Pre-engineered transmitter packages for this band are readily available from several commercial vendors and maintenance for such transmitters is broadly available throughout the country. The magnet required for the deuterons is somewhat more massive, namely 25 tons compared to 15 tons for the proton or ^{3}He magnets, but remains compatible with a reasonable 360° rotating support system. Deuterons, moreover, have significant targeting advantages, giving a much higher neutron yield than either of the other projectiles. Higher forward peaking of the neutron yield from the deuteron reaction reduces activation of machine components and a reduced low-energy-tail in the deuteron induced neutron spectrum is thought to help avoid skin overdose during treatment.

Construction of this cyclotron is now in midstream, with all major parts on order from various vendors and with winding of the main

superconducting coil about to begin. The cyclotron magnet is expected to be ready for first operating tests in the spring of 86 and ready for rf and beam testing a few months thereafter. Following these tests, the cyclotron will be transported to the hospital in Detroit and the MSU project will end, as the hospital technical group takes over responsibility for installing the cyclotron in Detroit and starting up the machine there.

Recently the Laboratory has become involved in another medical application study in response to inquiries from the Harvard Cyclotron Laboratory and from Fermilab as to whether superconducting cyclotrons might constitute a competitive accelerator solution for providing proton beams for radiotherapy. In this latter application, a beam energy of 250 MeV is desired with a current of 20 nanoamps. A small study, involving several man-months of total effort, concluded that a superconducting synchrocyclotron might well be the most attractive accelerator for this application. The beam current requirement and the beam quality requirements are compatible with routine synchrocyclotron performance and superconducting techniques make the accelerator smaller and less costly.

A likely superconducting synchrocyclotron design would utilize a 5.5 tesla central field and an rf system modulated over the range 65 to 85 MHz. Extraction of beams from synchrocyclotrons is normally accomplished by "regenerative" extraction, an entirely magnetic technique. It appears that this technique can continue to be utilized in the high magnetic field regime but quantitative calculations remain to be done to firmly establish this.

More recently we have learned that a group at the SIN Laboratory in Switzerland is interested in developing a cyclotron for proton radiotherapy and NSCL/SIN discussions are in process regarding a possible joint project in which MSU would undertake design studies of the magnet and SIN would undertake design studies of the rf system. Such a project could ultimately evolve into a pattern paralleling the neutron facility, depending on whether some medical organization is able to obtain the necessary funds.

The laboratory is also participating in an ongoing adhoc national study aimed at comparing the advantages of various types of accelerators in

the proton radiotherapy application. Several meetings were held on this topic in 1985, with initial meetings at Fermilab, sponsored by Fermilab, and since then sponsored by an adhoc panel, the Proton Therapy Cooperative Group (PTCOG). The Laboratory's participation in this study provides an element of balance, since other accelerator laboratory participants are dominantly from synchrotron backgrounds and the NSCL group is the only one involved in study of the synchrocyclotron option.

Overall, the applications program has brought a great deal of favorable public comment and public appreciation of the Laboratory's program. Appreciation of possible benefits of nuclear physics spin-offs has been greatly enhanced in the mid-Michigan and Detroit areas. The applications program is also enthusiastically supported by a number of members of the Michigan congressional delegation. We believe this enhances political support for the overall national nuclear science program. In summary, we feel the applications program is important and useful, provided it is kept at a level which does not significantly impede or delay the mainline programs of the Laboratory.

References:

1. M.M. Gordon, IEEE Trans. Nucl. Sci. NS-30,2439(1983).
2. M.M. Gordon and Felix Marti, IEEE Trans. Nucl. Sci. NS-32,2285(1985).
3. R. Baartman, G.H. Mackenzie and M.M. Gordon, Tenth International Conf. on Cyclotrons (IEEE Publ., New York, 1984) p. 40.
4. M.M. Gordon and V. Taivassalo, IEEE Trans. Nucl. Sci. NS-32, 2447(1985).
5. M.M. Gordon, Tenth International Conf. on Cyclotrons, (IEEE Publ., New York, 1984) p. 279.
6. M.M. Gordon, Particle Accelerators 13,119(1983).
7. M.M. Gordon, Particle Accelerators 13,67(1983).
8. M.M. Gordon, Particle Accelerators 16,39(1984).
9. A.G. Armstrong, C.J. Collie, J. Simkin, and C.W. Trowbridge, Proceedings of COMPUMAG conference, Grenoble, 1978.
10. J. Simkin and C.W. Trowbridge, Three dimensional computer program (TOSCA) for nonlinear electromagnetic fields, Rutherford Laboratory Report No. RL-79-097.
11. L. Harwood and D. Johnson, Proceedings of the 10th Int. Conf. on Cyc. and their Appl., April 30-May 3 (IEEE Publ., New York, 1984, ed. F. Marti) 99.
12. J.E. Pasciak, BNL report AMD 873R1.

13. L. Harwood and J.A. Nolen,Jr., Proceedings of the 10th Int. Conf. on Cyc. and their Appl., April 30-May 3 (IEEE Publ., New York, 1984, ed. F. Marti) 101.
14. L.H. Harwood, et al., IEEE Trans. Nuc. Sci. NS-32, 3734 (1985).
15. K. Halbach and R.F. Holsinger, Particle Accel. 7, 213 (1976).
16. POISSON User's Guide, R.F. Holsinger, unpublished.
17. J. Vincent, et al., "K500 RF System Development", NSCL Annual Report 1983-84, pg. 203.
18. J. Vincent, et al., "Current Status of the K800 RF", NSCL Annual Report 1983-84, pg. 234.
19. D. Johnson, V. Taivassalo, M. Gordon, & H. Blosser, Internal Report MSUCP-44(1985).
20. D. Johnson, L. Harwood, M. Gordon, & H. Blosser, Internal Report MSUCP-46(1986).
21. R. Geller, IEEE Trans. Nuc. Sci. NS-26 2120(1979).
22. Sixth International Ion Source Workshop, C. Lyneis, editor, Lawrence Berkeley Laboratory PUB-5143(1985).

V. IMPLICATIONS OF THE TRANSITION TO PHASE II

During the period covered by this proposal, the NSCL will undergo a transition from construction of the Phase II facility to its operation as a national user facility. Some of the issues raised by that transition are discussed in this section. One of these involves laboratory manpower. Individuals presently involved in construction of the facility will transfer their efforts to facility operation, some to be involved in the day-to-day running of the cyclotrons and their ancillary equipment and some in the continuing development and improvement of laboratory facilities. Still others will provide services to facility users that have not been possible because of the demands of the Phase II construction project.

Another issue is the significant investment in ancillary equipment: detector and target laboratories, computing facilities, data acquisition and analysis systems, detection systems, etc., that will be necessary to make efficient use of this new and powerful facility for nuclear science. These needs are discussed in Section VI.

Finally, this transition will make it possible for the laboratory to expand its program of research and development in accelerator and instrumentation physics. This program will build on the unique expertise and long term interests of the MSU group to fill a national need for research and the training of students in this area.

A. Manpower Implications

We assume that the manpower requirements for operating and using the facility are approximately those required for its construction. This rule of thumb is reinforced by our desire to keep in place the unique technical skills of the design and construction team, by our ongoing plans for the further development of the laboratory and by our plan to expand the program in accelerator and instrumentation physics. We have compared our present staff with an estimate of our needs, based in significant part on our experience in operating the K500 based Phase I program and on the staffing at other comparable facilities. All such estimates are subject to a considerable uncertainty, but they support maintaining our overall staff at about the present level.

The skills required for operation are, of course, not precisely the same as for construction, but an inspection of the affected part of the manpower pool indicates that the present staff, taking into account the effects of attrition and retirements, will be effective during the operation phase. For example, as design tasks on the K800 wind down, some of the mechanical designers will supervise installation of the parts they have designed, and, afterward, will be involved in retrofitting and upgrading tasks associated with the K800. Others will continue design work associated with the remaining Phase II facilities and other research equipment. Further in the future, the group will be involved with the ongoing development of research equipment that has been a hallmark of the NSCL. The machine shop may well be too large for the steady state, but will be fully occupied with construction until completion of the Phase II project; by that time retirements will remedy the situation.

The schedule of the transition to operations is based on the cost-and-manpower-to-complete studies we have made for the construction project and is enumerated in Table V.1. The detailed use of the manpower freed up by completion of construction tasks is hard to forecast and will

Table V.1. Manpower involved in the operating and Phase II construction activities, including that supported by MSU.

ACTIVITY	85-86	86-87	87-88	88-89
Operation	86.5	100.0	114.5	131.0
Phase II Constr.	58.0	45.5	30.5	12.5
Total	144.5	145.5	145.0	143.5

depend on the ease of bringing the Phase II facility into efficient operation. Operation of the K500 facility has been somewhat more difficult than was foreseen and a substantial amount of retrofitting and development has been required to achieve reasonable reliability of operation. The K500 has been extremely valuable as a prototype for the K800 and many items that caused difficulty on the K500 have been redesigned. As a result, the K800 design is more conservative than that of the K500 and the cyclotron should operate reliably at an earlier date. Nevertheless, it is prudent to assume that significant manpower will have to be devoted to improvements after operation of the facility begins and to accelerator physics calculations aimed at a better definition of operating parameters. We assume that

almost all the manpower transferred to the operation grant during the first year will be devoted to that task as will most of the staff presently involved in maintaining and improving the K500.

We now turn to an examination of manpower needs during initial operation of the K800 cyclotron. The present group of operators consists of six shift operators and a supervisor; after accounting for vacation, illness, etc. this provides single coverage on most shifts. Given the load of auxiliary duties: ion source maintenance, record keeping, coordinating repair of minor breakdowns, etc., this has proven to be the minimum crew necessary to operate the K500. Since the present operator group will have responsibility for day to day operation of the K800, a task at least comparable to operating the K500, it will not, initially, be possible to operate the K500 and the K800 simultaneously. During this period we will also assign a group of technicians, about eight in total, to be available for repairs to the K800 on a two shift basis. Except when actively involved in repairs, these individuals will devote their time to the ongoing construction activity. A similar system was employed on the K500 and proved invaluable in expediting development of the cyclotron.

During the period immediately preceding the operation of the K800, we will begin to augment the operator group. A group of about ten operators is necessary to provide two operator per shift coverage. Our experience on the K500 indicates that this is highly desirable, and greatly increases the efficiency of operation, particularly when it is necessary to deal with operational difficulties. The overall cost of running the facility makes this additional investment in operator manpower highly cost effective.

Although simultaneous operation of the two cyclotrons will not be possible initially, it seems that it would be effective in terms of the overall productivity of the laboratory, to run the K500 to provide beams for experiments when the K800 is down for repairs and improvements, especially for those experiments that require apparatus not initially available to the K800. The layout of the Phase II experimental areas is such that the K500 has access to all experimental areas and to some areas with simultaneous K800 operation.

While these plans are not final, they represent the directions in which we presently think that operations will evolve. Our ideas will become

firmer as we gain experience in operating the K800 and the associated Phase II equipment.

Once the operation of the K800 has become more-or-less routine, it should be possible to dedicate additional manpower to other laboratory functions which we cannot presently support at a desirable level. Critical areas include: computer group support for the experimental program; design, mechanical and electronic shop support for ongoing experiments; specialists for the major pieces of experimental apparatus; design, mechanical and electronic shop support for MSU staff research; a cryogenic technician; detector development technicians; and a target laboratory technician.

A summary of these changes and the resulting division of effort among Facility Operations, User Services, and MSU Staff Research in Nuclear Science, and Accelerator Physics/Nuclear Instrumentation is given in Table V.2.

Table V.2. Manpower and budget by function.

	86-87		87-88		88-89	
FUNCTION	FTE	K$	FTE	K$	FTE	K$
Facility Operations	31.7	2901	34.2	3118	36.3	3284
User Services and Support	11.8	1129	14.8	1232	17.2	1080
Staff Research	44.4	2415	47.3	2491	51.4	2688
Accel./Instrum. Physics	10.1	499	11.2	575	12.6	665
Major Special Item		0		0		500
NSF supported total	98.0	6944	107.5	7416	117.5	8217
MSU contribution	2.0	154	7.0	339	13.5	590
TOTAL	100.0	7098	114.5	7755	131.0	8807

B. Accelerator and Instrumentation Research

The NSCL has a long history of research and development of instrumentation for nuclear science. This has, as outlined in earlier sections, involved not only a precision sector focused light ion cyclotron and superconducting heavy ion cyclotrons, but also much other instrumentation that has greatly extended the capability for measurements of nuclear phenomena. Present activities in these areas are described in Sections III.C and IV. Because of the demonstrated interest and expertise of the NSCL in accelerator and instrumentation physics, and the national need for research and training of personnel in this area, we propose to strengthen that area of research at the NSCL. Another motivation for this

proposal is the longstanding Ph.D. program in accelerator physics at MSU and the absence of such programs at most other institutions. The tenured faculty involved in the accelerator/instrumentation physics program are Professors Blosser, Gordon and Nolen. In addition, two Continuing Appointment faculty, work in this area: Assistant Prof. L. Harwood in accelerator physics and Associate Prof. M. Maier in electronics instrumentation, and there are presently three Ph.D. students in accelerator physics. As in all searches for tenure stream faculty in experimental nuclear science at MSU, the present recruiting process is explicitly open to those with expertise in accelerator/instrumentation physics.

Because this is a new emphasis for the laboratory, a detailed budget for the first year is presented in Table V.3. These funds are included in the Summary Budgets in Section VII. We anticipate that this activity will grow as Phase II construction winds down; the projected changes are outlined in Table V.2. Eventually it may be better to fund this group separately, to provide a better focus and visibility. However, at present its activity is so closely tied to the construction and operation programs of the NSCL that inclusion in the overall operating proposal seems appropriate.

Table V.3. Budget for Accelerator/Instrumentation Physics 1986-87.

CATEGORY	MANPOWER FTE	COST (K$)
PI's and Faculty	0.2	14.5
Other Senior Personnel	2.9	103.1
Post Doctoral Assoc.	1.0	24.0
Other Professional	1.0	23.0
Graduate Students (4)	2.0	41.4
Undergraduate Students	2.5	18.2
Secretarial-Clerical	0.1	2.1
Other	0.3	6.4
Total Salary & Wages		232.7
Fringes		38.1
Total with Fringes		270.8
Travel		3.8
Publication & Page Charges		2.5
Consultant Services		5.0
Computer Maintenance		19.3
Materials and Supplies		52.5
Indirect Costs		145.1
	Total	499.0

VI. CAPITAL EQUIPMENT

An important implication of the transition to Phase II operation is that a significant investment in ancillary equipment (detector and target laboratories, data acquisition and analysis systems, and detection systems are examples) will be necessary to make efficient use of this new and powerful facility for nuclear science. In this section we enumerate these equipment needs.

The proposed equipment includes both items to be purchased during the first year of the grant and items which will be needed later in the three year period. Examples of the latter are the advanced data acquisition system discussed below, which will be implemented over a three year period, and the continuing purchases of nuclear electronics.

Table VI.1 lists the equipment and its procurement cost proposed for the first year's operation. The table is divided into three segments, reflecting the tasks of the laboratory. The first two categories in Table VI.1 are for operation of the facility, upgrade of laboratory equipment, and user support in general. The last category deals specifically with equipment for use in the research programs of the MSU nuclear science group.

Table VI.2 details expenditures for the second and third years of the grant period. Items which we can anticipate are specified. However, we also include a substantial amount of unspecified equipment: the myriad relatively small items that experience indicates are necessary to operate the facility and support the MSU research programs in nuclear science and instrumentation. This will include many items needed for improvements of the K800 and other Phase II facilities that we are unable to specify in advance because we have no experience in K800 operation.

In the following paragraphs we discuss the various items in the tables, often referring to other sections where a more detailed discussion or background information is presented. We omit comment on items where the tables seem self explanatory. In most cases costs have been estimated by reference to a specific piece of equipment, but the values have been rounded to reflect the uncertainties in items to be purchased a year or more in the future.

A. Facility Operation and Development

In the accelerator operation section, the largest item addresses the problems with impurities in the cryogenic liquid helium system (see Sec II.A and IV.I), and the need for a closer monitoring of this central utility for the operation of a laboratory employing superconducting technology on a large scale. The leak detector will replace a detector whose maintenance cost and unreliability make its continuing use untenable.

The items for radiation monitoring address an added monitoring requirement for beams of higher energy and of higher mass. Until now, the residual radioactivity produced in the laboratory consisted of beta and gamma emission. Since the heavier beams can produce the actinides, we must now anticipate the production of alpha particle emitters. Stringent limits apply to these nuclides and we must be equipped to properly monitor this type of radioactivity.

The requests for the beam lines and target rooms are to meet some of the urgent needs. The pumping stations and the NMR units will reduce the time lost in having to switch these devices continually from one beam line or magnet to another, and thus improve the overall efficiency of operation.

B. User Services and Support

An important item for the convenience of users and overall Laboratory efficiency is a state-of-the-art electronics pool adequate to allow setup of one large experiment while another is running. Moreover, this pool needs continual upgrading to replace outdated and unreliable modules and to purchase new and improved equipment as it becomes available. In general, it will be cost effective to upgrade the pool to higher density electronics and much of our effort will be in this direction. A modest amount is also included here for in-house development of unique electronics modules for the facility pool by M. Maier's group. An equal amount is requested for electronics during the second and third years of the grant period: similar annual amounts will probably be necessary for the life of the facility. The color hardcopy units will provide on-line plots of multiparameter data, both for diagnosis of problems during setup and to document data analysis; our

Tektronix hard copy unit is mainly useful for quick access to one dimensional spectra.

The detector and target laboratories are an essential part of the NSCL's support of the user community. The ability to design, construct, and test new detection systems often leads the way towards more fundamental experiments. The detector facility has already produced many new detection systems for laboratory apparatus, including both complicated gas detectors and scintillator detectors. The equipment proposed, especially the electron gun evaporator, will allow an important upgrade of that laboratory to meet the anticipated needs of the user community. For example, the nichrome evaporator will provide the resistive coating used for position measurement in the thin window gas detectors many experiments require.

The overall system for data acquisition and analysis is extremely important for efficient acquisition of data and for its timely analysis. The following paragraphs summarize our present thinking on the most important needs for computer related equipment in the next three years.

The laser disc systems becoming available are an attractive and cost effective alternative to the more traditional tape drives. As a storage medium, the laser disk will in the future be less costly as well as more compact; the disks can hold the information equivalent of 20 high density magnetic tapes. Furthermore, the disc shelf life is probably greater than that of tape and maintenance of disk drives is expected to be less costly than that of tape drives. Interfacing would be via the industry standard SCSI and could be directly linked to the VME bus or networked into the VAX system. An obvious difficulty is that there is, as yet, no industry standard for the medium (i.e., the disk itself) and efforts will have to be made to provide compatibility with the user community. We will have to maintain our high density tape drives to service users who do not support laser disk readers. In spite of these difficulties, it appears that laser disks will become the dominant data storage medium and that we should move to acquire this technology.

The high speed networks will allow rapid transfer of data from acquisition stations to the various computers. The funds requested for the first year are for a four node system connecting both of the current data acquisition stations to two VAX 750's. The network will be expanded in the following years to include connections to the multi-processor data analysis

facility discussed below, to the laser disc drives which can then be used with any machine, and to the remaining data acquisition stations. This ability to transfer data to two CPU's simultaneously will be useful when an ongoing experiment requires a large amount of on-line processing of incoming data, as well as for later data analysis.

Extending control system stations to the data U's will provide access to the control system (and hence to most of the experimental parameters) from each data acquisition area. This will become an urgent need as the three acquisition areas are called upon to serve the much larger number of experimental devices and the use of a single control panel for a single device becomes more and more inconvenient. Users will be able to monitor and tune beam lines leading to their targets using the output of their detection systems as a guide. This extension will also insure that key settings are automatically recorded with other end-of-run data.

The two portable multidimensional data acquisition systems will allow users to set up and check detectors in locations away from the vaults and without the use of the data acquisition computers, a real gain as the number and complexity of detection systems increase. These systems are based partly on equipment (LSI 11-23's) freed up by installation of the new fast data acquisition systems.

The advanced data analysis system is a multi-processor computing engine. As has been discussed in Section II.A.3, the major motivation for this device is the bottleneck in data analysis which will accompany the growth in the size of experiments anticipated when the Phase II facility comes into operation. The goal is to provide inexpensive high speed computing which may be applied to this and to other problems with a high degree of inherent parallelism. Since the proposed approach may not be familiar, we outline it in some detail here. The system we propose to develop is modeled after the FermiLab Advanced Computing Program (or ACP)[1,2].

The FermiLab ACP is a multiprocessor computing engine mainly intended to analyze event data from nuclear and high energy physics. Problems of this sort can be handled in a parallel-processing format since each event is independent of all other events. For such problems, the cost/performance ratio appears to be about $3000 per VAX 780 CPU equivalent. The ACP will

use an array of 120 VME bus based processors connected to a host computer via a high speed network. Initially, the host computer is used to develop and debug programs intended for the ACP processor array. In production mode, programs are loaded into the ACP processors, and the host simply serves as a source of event data to be sent to the array and as a sink of analyzed data returned from processors in the array. The FermiLab system is a good starting point for the NSCL system, and indeed, we intend to take the conservative approach of bringing our system into operation using the software developed at FermiLab. However, several modifications would greatly improve the power of the system for our applications and we will implement them as availability of time for software development permits. We now briefly discuss these planned modifications.

a. The FermiLab ACP is a heterogenous array in that there are multiple processor types. We propose to use only the 68020 processor board developed for the ACP project. This will reduce development and support costs by restricting software development and purchases to those required to support a single processor.

b. The FermiLab ACP system interconnects computing nodes to a host via a high speed parallel network which is very strongly of Master/Slave character with a host/development processor μVAX-II serving as the host. This limits the modes of interprocessor communication which can be conveniently supported to Master to Slave and Slave to Master; Slave to Slave communication is accomplished by a high overhead Slave to Master to Slave transaction pair. We propose to substitute a true peer/peer network between nodes and their host(s). Initially, this network will likely be ETHERNET, although the high speed data network will be used as it becomes available. The assumption inherent in this choice is that the problems being solved are compute bound problems with computing parallelism such that network transactions are rare.

c. In the FermiLab system, each node is a single processor, while in our system, a node will be defined as a set of processors sharing a common backplane and served by a network processor. Processors within a node may cooperate or operate independently.

d. In the FermiLab ACP system, processors share a VME bus enclosure, but typically they do not own shared memory. This was done to lower

VME contention (to zero). We propose to add shared memory to each cluster of processors. It will be used for high speed intercommunication between nodes sharing a VME bus to allow tighter coupling of subsets of nodes (pipeline and tree processing support) which would otherwise incur excessive communications overhead; to provide a central repository of results in the cases where results typically represent sums of computations (examples are spectra in nuclear event data analysis and Monte Carlo simulations); and to provide a centralizeable data store for mesh problems such as those involving nonlinear differential equation solvers, where values computed on a mesh of points are influenced by some limited set of neighboring points.

e. FermiLab software currently assumes that the entire array of processors is to be assigned to a single problem. Our proposal allows subsets of the array to be shared among multiple concurrent users. It will still be possible to use the whole array for a job with critical throughput requirements.

f. Currently, FermiLab software requires that software in control of the processor array busy waits (loops actively), polling for events of interest in the processor array. This will be modified to allow more 'normal' event flag or AST notification of significant events.

The ACP system is expected to be operational at FermiLab by summer, 1986, and shortly thereafter performance data will be available from which more detailed plans can be made. In particular, it will be possible to evaluate whether the μVAX II is an adequate host or whether greater I/O capability must be provided. Our current intent is to phase in the NSCL multiprocessor system in three stages:

a. In the first year (1986-87), we will build a kernel system consisting of a μVAX-II host processor, disk, two nodes consisting of 10 processors per node, network hardware and development software. Estimated cost of phase 1 is $120,000. On the completion of this phase, the system will already be available for use on a test basis. We estimate that 1/2 man year of software development will be required.

b. In the following year we would add 5 more nodes of 10 processors each for a total of about 50 processors. Estimated cost of this phase is

about $115,000. After the completion of this phase, the system will be put into a useful production mode with only periodic downtime during which software would be upgraded and additional processors (phase 3 below) would be installed.

c. Later in the second year another 5 nodes of 10 processors each would be added, completing a system of 12 nodes with 120 processors. Estimated cost is $115,000. As noted above this upgrade can take place during relatively short maintenance periods on the already functioning system.

C. MSU Staff Research

Funds are requested for four items of research equipment:

1. Neutron Detection Array: We propose to build a granular neutron detection array designed to measure the neutron decays of particle unstable nuclei with masses $5 \leq A \leq 15$ with better resolution and an order of magnitude better efficiency than obtained in the measurements discussed in Section III.A.4(d). The reconstruction of the excitation energy of a particle unstable nucleus requires the high resolution measurement of coincidences between neutrons and isotopically resolved fragments with masses $4 \leq A \leq 16$. The physics motivations for this device are discussed in greater detail in section III.A.4(d).

The device consists of 30 liquid scintillator neutron detectors. When built in house the price for one detector is $2000, including the cost of the liquid scintillator and container, a plastic scintillator for rejecting charged particles, and two photomultipliers with bases. In addition, $7800 is needed for 3 Lecroy charge integrating ADC's and $2500 for neutron and charged particle detector mounts, yielding a total equipment cost of approximately $70,000. To complete the experiment, it will also be necessary to purchase 6 triple telescopes ($3000 each) for detection of the accompanying complex fragments. Funds for these detectors are not included in this request.

2. High Energy Gamma Ray Modules For The 4π Array: Measuring high energy gamma rays in coincidence with charged particles in the 4π array is probably the best way to investigate the high energy gamma ray production

mechanism (Section III.A.4(d). If the observed high energy gamma rays turn out to be bremsstrahlung, then gamma rays may provide a convenient trigger for violent central collision events. These experiments will be limited in statistics by the low event rate of high energy gammas, making it important to cover a large solid angle with gamma ray detectors. We therefore propose to build two gamma ray detectors which would replace two of the 32 modules of the 4π array.

3. Large Lead Glass Array: The high energy gamma spectrum observed in reactions with 40 MeV/A ^{14}N beams extends beyond 100 MeV (as described in Section III.A.1(a)) and with heavy beams at 100 MeV/A will probably extend to $E_\gamma > 300$ MeV. In this range the Cerenkov counter range technique developed at MSU does not work because of the dominance of radiative energy loss for the $e^+ - e^-$ pair. Lead glass detectors by comparison work well for $E_\gamma > 200$ MeV, but poorly for $E_\gamma < 100$ MeV. Thus a lead glass array would allow us to extend our gamma ray measurements to very high energies. Another obvious use of the array would be as a single telescope to do π° measurements, and a third use would be to veto π° gamma pairs in gamma ray continuum measurements. This will become important for measurements of high energy gamma ray production at beam energies above 100 MeV/A where pion production will introduce a background.

We propose to build an array of 25 two element telescopes, each consisting of a 2 radiation length front element followed by a 15 radiation length back element. Each element would have a rectangular cross section 15 cm x 5 cm.

4. Multiplicity Filter: The multiplicity filter will be used in conjunction with the unstable resonance detection system. The device would consist of 30 fast/slow plastic scintillators of a very rugged and simple design, arranged in a close packed array. This type of counter lends itself to large numbers of counters ($\approx$ 30) because of the low cost, simplicity of electronics and high count rate capabilities. Initial use of this array would be for two experiments at the NSCL and one at LBL. Because of the small size of the elements, the array would provide the high granularity needed for high multiplicity events, especially at very forward angles.

REFERENCES

1. "The FermiLab Advanced Computer Program Multimicroprocessor Project" T. Nash et al. Proceedings of the 1985 Conference on Computing in High Energy Physics, Amsterdam, Netherlands, June 25-28, 1985.

2. "Software for Event Oriented Processing on Multiprocessor Systems" M. Fischler et al. Proceedings of the Symposium on Recent Developments in Computing Processor and Software Research for High Energy Physics, Guanajuato, Mexico, May 8-11, 1984.

TABLE VI.1

EQUIPMENT BUDGET FOR FIRST YEAR OF GRANT PERIOD* TOTAL 836K

Facility Operation and Development

1. Accelerator.....Subtotal 70K

Beam diagnostic equipment: particle identifier (3K), phase width detector (12K), phase probes (6K), centering readout (2K).

Cryogenic systems: automatic logging of parameters (4K), pressure transducers (2K), alternate charcoal vessel for oil absorption unit (10K), nitrogen cooled contaminant adsorber units (11K).

Temperature recording system (multi channel) for rf development (6K), leak detector (14K)

2. Radiation monitoring upgrade.....Subtotal 39K

Modicon upgrade (3K), portable monitors (7K), two hand and foot α monitors (26K), shielding materials (3K)

3. Beam lines and target areas.....Subtotal 68K

Optical alignment equipment (15K), 2 pumping stations (movable, with turbos) (20K), foil stipper mechanism (4K), target ladder drive for activation beam station (4K), vacuum interlock/valve controls (10K), digital scope for beam profile scanner (5K), expansion of NMR system by 6 probes (10K).

User Services and Support

1. Nuclear Electronics Pool.....Subtotal 122K

New electronics modules to keep electronics pool up to date, new cables, high voltage supplies, etc. (110K), color hard-copy units (3) for data acquisition and analysis (12K).

2. Detector laboratory, target laboratory.....Subtotal 78K

100 Mhz oscilloscope (2K), 4096 channel MCA (5K), dedicated precision pulser (3K), bias supply (1K), bit out register (2K), turbo pump and roughing pumps (8K), diamond wheel saw and drill press (6K), calibration sources (4K), prototype detectors and S320 start detector (8K), electron gun evaporator for target making and nichrome film evaporation with thickness monitor (32K), airtight glove box for handling and preparation of reactive targets (7K).

3. Data acquisition and analysis computer equipment.....Subtotal 245K

Laser disk drives for data acquisition/analysis VAX 750's: two in the first year, one in the second (42K). High speed data networks, four in first year (32K). Extend control system to data U's, one per year for 3 years (includes graphics tube & board, terminal and I/O cards, and

Arcnet (14K)). Two portable data acquisition systems, one in first year (9K).
Advanced Computer system for very high speed data analysis, to be implemented over a 3 year period. This first year cost consists of: a) VAX host with disk, memory, network, interface, and operating system (64K); b) two parallel nodes, each containing 10 processing elements, with floating point and 2 Megabytes of memory, and network interface (56K). Software, including LN01 graphics, Dec Calc, 68K fortran, Rsx-11s operating system, DecNet-11s network software, Ethernet interfaces, 68000 cross compiler, μVax/Cmi C compiler (28K).

Staff Research.....Subtotal 214K

1. Neutron detection array (70K)

   This device includes 30 liquid scintillators, constant fraction discriminators and charge sensitive ADC's. For costs, see the text.

2. Two high energy photon detector modules for 4π array (40K).

   The cost of 20K per module is based on the cost of the following items: frame and vacuum enclosure,4K; Bicron B0480 Cerenkov detectors, 6K; 20 photomultiplier tubes, bases and shields, 0.5K each.

3. Large lead glass array (80K).

   The cost for the array of 25 lead glass gamma ray telescopes is: support structure and mounting hardware, $2500; unit cost of the telescopes, 1.5K for lead glass and 1.6K for phototubes, bases and shields.

4. Charged particle multiplicity filter (24K).

   The device consists of 30 plastic scintillator telescopes at a unit cost of 0.7K (21K), and a mounting hodoscope (3K).

*Costs for later years are given in Table VI.2.

TABLE VI.2

EQUIPMENT BUDGETS FOR SECOND AND THIRD YEARS OF GRANT PERIOD*

Budget for 1987-88.....TOTAL 770K

Nuclear electronics pool(110K); Laser disk drive (21K); Control system in one Data U (14K); High speed networks, 3 nodes (24K); Complete Advanced Computer system, 50 processors at 4.6K per processor(230K); Portable data acquisition system (9K);
Unspecified equipment (362K).

Budget for 1988-89.....TOTAL 490 K

Nuclear Electronics Pool (110K); Control system in one Data U (14K); High speed networks, 2 nodes (16K); Unspecified Equipment (350K);

* All specified equipment is for User services and support. We anticipate that unspecified equipment will include approximately $150K for support of the nuclear science and nuclear technology programs and the remainder for facility operations.

D. Major Special Item:

Our experience with the NSCL VAX 780 system leads us to propose an upgrade of this system during the third year of the grant period. By that time the 780 will have been in service for 7 years (it was delivered to the NSCL in 1982), and will be nearing the end of its useful life as the central processor in the NSCL computer system. It appears that a VAX 8600 series computer would meet most of our anticipated needs and to be specific, the discussion below will be in terms of that machine. Of course, other computers may be available in three years (for example the VAX 8800 mentioned below) and we would make the most cost effective choice from among the hardware available at that time.

Below we discuss the limitations of the current 780 and why we expect its current performance problems to be exacerbated over the next few years as the laboratory computing load increases. Then we demonstrate that an upgrade to a VAX-8600 (or its superior) would ease the problems we currently experience while leaving room for a future expansion of laboratory computing load.

Analysis of the behavior of the VAX-780 at NSCL has led to the conclusion[1] that the capacity of this machine is being outstripped by the demands imposed on it by the local and outside user community. At present the 780 serves as a sort of catch-all processor, assuming tasks not already delegated to other processors. As such the job mix consists of a heavy load of both interactive and batch jobs. Interactive usage includes program development and execution, word processing, graphics, SMP runs and data base manipulations; it demands a fast response from the processor to the user while producing a heavy terminal I/O overhead on the 780. Batch usage includes theoretical nuclear physics computations, accelerator physics, and Monte Carlo simulations, operations which require large numbers of both CPU cycles and memory words.

At present, interactive response on the 780 is extremely slow, and batch turnaround time is too long. As the NSCL has become more computer dependent, the complexity of the batch jobs run on the 780 has increased, as has the interactive load due to more users and to higher demands on the CPU from each user. These include, among others, FPS-164 program development work and increased use of the operations listed above. This problem will be

aggravated over the next three years when the 780 is pressed into service as a network routing node for external networks both on and off campus; these include BITNET (inter university network), Physnet (physics network), and the campus-wide extension of Ethernet onto the broadband.

Due to its present load, the 780 spends a substantial fraction of its time performing overhead I/O. This I/O includes paging and swapping due to insufficient physical memory (too many programs running concurrently for the physical memory available), and a high volume of terminal interrupt service activity (too many terminals for the processor interrupt response time). These problems can be solved only by an increase in CPU speed and central memory. Clearly, it is not possible to increase the CPU speed of the 780, and, while it is possible to increase the physical memory capacity of the 780, it is not cost effective to do so since that would involve a massive revision of the CPU, memory controller, as well as installation of a new backplane. At first sight it might seem that distributing the load between the 780 and the recently acquired FPS-164 might improve the 780 responsiveness. However, the FPS-164 is a single user batch only processor, and there are significant differences between the operating environments of the two machines. Currently, the FPS-164 is almost completely utilized by accelerator design physicists and experimentalists performing Monte Carlo simulations. The FPS-164 will continue to be useful and superior to an 8600 for many large compute-bound programs. However, it cannot serve the flexible multiuser demands placed on the 780.

A particular example of this situation is that of the NSCL theory group; the computing facility is their main research tool. Part of the work requires the needs of a dedicated computer which provides maximum speed and/or core memory. At present this need is partly met by the BATCH queue on the VAX-780 which runs as a "background" to the interactive users. In addition the FPS-164 is available for jobs which require more CPU time (and two megawords or less of core memory), and time is available on CRAY's at the Supercomputing Centers. However, on a day-to-day basis the computer needs of the theory group are provided by the interactive use of the VAX-780. This includes writing and debugging programs, running these with a variety of inputs in order to test the procedures and to judge the sensitivity of the results to various parameters, plotting the results in order to quickly visualize the functional dependences and the comparison to

experimental data, and combining the results into final figures, tables and texts. For any given project all of these activities are usually being carried out more or less simultaneously. Often projects start out in the interactive mode and develop into a computation-intensive mode. The shell-model program OXBASH described in Sec. III.B.4 is an example of a code which is used extensively in both modes. OXBASH has been used to obtain the results presented in more than 20 recently published papers, and most of the theoretical nuclear structure projects underway or proposed rely on the continual development of this and other computer codes. Already the VAX-780 is being used to its capacity in the interactive mode, and an upgrade in this facility is important for the continued growth in productivity of the nuclear theory group.

It is important to note that the 780 is based on mid 1970's medium scale integration technology and, as such, component counts are high, as is power dissipation. Machines of this class are not only difficult to maintain (high component count means many things can go wrong), but also more vulnerable to failure (high power dissipation means more heat and excessive heat leads to component failure). This is expected to reduce the reliability of the 780 greatly as it continues to age.

We also note that the 1984 report of the NSAC Instrumentation Subcommittee recommends a continued upgrading and timely replacement of data acquisition and analysis computer systems, and notes that "this replacement should take place about every 7 to 8 years to remain competitive."

In view of these observations, the NSCL proposes to upgrade the VAX-780 to the recently announced DEC VAX-8600 processor system. This processor offers performance in excess of 5 780's while allowing straightforward physical memory expansion to up to 64 Mbytes and retaining software compatibility with the 780. The increased memory capacity and processor speed will greatly improve performance for both batch and interactive jobs. The increased memory will reduce disk paging and swapping, while the increased CPU speed will improve terminal I/O responsiveness. VAX-8600's are known to support over 100 concurrent interactive users[2]. Batch jobs will turn around faster due both to the increased processor speed and to the larger memory (many batch jobs in our job mix are both memory and CPU intensive). Interactive jobs will run with improved responsiveness because of the increased processor speed (faster interrupt servicing), and the

larger physical memory capacity (less paging/swapping among batch jobs, other interactive jobs and the processor's own working set). Further, more simultaneous interactive jobs can be supported; the VAX-780 has over 200 users, but only about 10% of that group can have access simultaneously, well below the usual demand.

The upgrade to a VAX-8600 would involve trading in the current 780, it's memory and the RP07 disk drive for a VAX-8600 series computer with 16 Mbytes or more of physical memory and an RA81 disk drive. The disk drive trade in, while not essential to the 8600 upgrade, replaces a device which has become expensive to maintain for a device that is more cost effective to run. Total cost of the upgrade is $500,000 (see Table VI.3).

Table VI.3. Cost estimate for VAX 8650 Computer

8650 CPU, 4 Mbyte, C.I. Controller	475K
1.2 Gbyte Disk System	50K
Floating Point Accelerator	28K
Intelligent Controller	34.5K
Disk and Tape Channels	16.2
12 Mbytes Memory(third party)	16K
Total	619.7K
Less 17% GSA Discount on DEC equip	517.1K
Less 780 Trade-in	≈500K

As we have noted previously, this discussion has been in the context of a VAX 8600 as an example of a device that would meet most of the needs defined above. By 1988-89 when a decision on hardware would actually be made, other hardware might be more cost effective. One possibility is a cluster of μVAX's. Another is the recently announced DEC VAX-8800[3], a machine with advertised performance equivalent to 10 or more VAX-780's--at present, this product is too new for a detailed evaluation.

References:

1. "Guide to VAX/VMS Performance Management" Digital Equipment Corp. Sept. 1984 for performance issues which led us to believe 780 is memory and CPU bound.

2. Demonstration of VAX-8600 at the 1986 Anaheim Decus Symposium.

3. See "Computerworld" magazine January 27, 1986 article page 1: DEC to Offer Powerhouse Top-end VAX for 8800 product announcement.

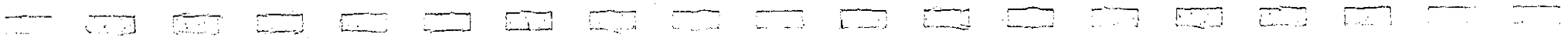

VII. BUDGETS

In the previous sections we outlined the transition to operation of the Phase II facilities and discussed some of the implications of that transition. We also proposed a significant expansion of our activities in accelerator and instrumentation physics. Finally the capital equipment requirements for the grant period were presented. Here we discuss other relevant issues that affect the proposed budget, following the categories of the budgets given at the end of this section.

DISCUSSION OF BUDGET ITEMS

A. Senior Personnel

1. Project Directors and Principal Investigators

Sam Austin and Henry Blosser are Co-Directors of the Laboratory, Austin having responsibility for guiding the nuclear research program and day to day laboratory operation, and Blosser, responsibility for construction of the Phase II facility. The PI's are tenure stream professors in the Departments of Physics and Chemistry, plus two individuals (R. Au and P. Miller) responsible for facility operations. The requested funds are for 20% of the twelve month salaries of the faculty members (D.K. Scott's salary is paid from University funds), and for the fraction of the salaries of Au and Miller attributable to operation.

1-4. Faculty Associates

Included here are tenure stream faculty members in the Departments of Physics and Chemistry and the four individuals presently holding Continuing Appointment Professorships in the NSCL. We are presently recruiting to fill two additional open tenure stream positions.

5. Others

This category includes members of the NSCL Continuing Appointment system who are appointed as Engineer, Staff Engineer, Senior Engineer, or as Physicist, Staff Physicist, Senior Physicist. These ranks are roughly analogous to the usual academic ranks.

A list of senior personnel is included in Section VIII and a list of the salaries of Principal Investigators is sent separately.

B. Other personnel

1. Research Associates and Visiting Faculty

The present proposal requests 10 postdoctoral research associates, an addition of one to the present number. The added individual will work in accelerator/instrumentation physics, the number of research associates in nuclear science remaining the same.

2. Other Professionals

This category includes primarily members of the MSU Administrative Professional category, and includes: cyclotron operators, mechanical designers and detailers, research professionals, research technicians, purchasing agents, administrative assistants, electricians, etc..

3. Graduate Students

Presently there are 31 graduate students in nuclear science and accelerator/instrumentation physics at the NSCL. We request funds to increase this number by two over the life of the next grant, one additional student in accelerator/instrumentation physics and one in nuclear science.

4. Undergraduate Students

We employ a number of undergraduate students on an hourly basis in both the construction and operation aspects of the NSCL. This is an excellent

way to introduce promising undergraduates to laboratory research and at the same time provides a source of flexible and well motivated manpower that is particularly useful in routine data analysis tasks and in meeting peaks in the manpower demanded by projects such as moving shielding walls, pulling cables, etc.

5. Secretarial Clerical

This category includes the 4 secretaries, 3 individuals from the purchasing accounting group, a computer librarian, and drafting for publication. Of these, 4.5 FTE will work on operations in the first grant year, increasing to 8.5 by the third year. As discussed below those involved in purchasing and accounting are supported by MSU funds.

6. Other

Included here are electronics technicians, machinists, welders, cryogenics and vacuum technicians, a stockroom assistant and messenger.

D. Permanent Equipment

A breakdown of the equipment request into the categories of facility operations and development, user support, MSU staff research and major special items is given in in Section VI and Tables VI.1-3.

E. Travel

Domestic travel costs fall into three main categories: (1) travel of NSCL personnel to meetings and conferences, to vendors for inspection of orders, to training sessions, etc. (2) travel of NSCL scientists to perform experiments at other laboratories. (3) Travel of non-laboratory personnel on business related to the laboratory, including consultants, seminar speakers, candidates for positions, and PAC and Executive Committee members. Total travel costs increase from year to year through the grant period because of the larger number of personnel supported by the operating grant

(rather than the construction grant), but less than proportionally to this number.

We propose to continue to use facilities at other laboratories on a regular basis. Such research is relatively inexpensive, the principal cost being travel, and has a number of advantages. First, by experiencing the off-site user role at other laboratories, the MSU group is able to more sensitively provide for the needs of such users at the NSCL facility. Research at other accelerators also complements and extends research done at MSU. For example, the work on spin flip done by lab members at Orsay is closely related to work proposed for the NSCL, as is work at the the IUCF involving charge exchange reactions. Studies at the Bevalac are a natural extension to higher energies of the work at the NSCL, and measurements of nuclear temperatures from proton induced reactions at Triumf will complement the large related program underway here. In other circumstances, unique experimental facilities, such as the spin spectrometer at Oak Ridge, make possible experiments that cannot be done elsewhere. Perhaps most important, the cross fertilization of ideas and technique from working at other laboratories will clearly, over the long run, strengthen the facilities and program at the NSCL.

Table VII.1 shows how we expect travel costs to be divided for the first year of the grant.

G. Other Direct Costs

1. Materials and Supplies

The major groupings include equipment maintenance supplies, office supplies and services and expendable technical supplies. The equipment maintenance component is expected to grow through this period as more and more of the equipment developed and constructed during Phase II becomes operational and requires maintenance. Office supplies and services include items such as copy machines, telephones, postage, delivery services, etc. Technical supplies include items such as computer paper and ribbons, drafting supplies, graphic services, user magnetic tapes, silicon detectors, etc. These costs have been estimated based on present expenditures by assuming that they remain constant on a per person basis. As the manpower presently

involved in construction activities moves into operation, the materials and supplies budget is increased proportionately. Table VII.2 is an itemization of costs for the first year.

2. Publication Costs

We estimate that publication costs will initially decrease somewhat, with reduced page charges in APS journals partly compensated by increased reprint costs, and then increase with increasing activity in the operations grant.

3. Consultant Services

These services fall into two major categories as detailed in Table VII.3.

The members of the Program Advisory Committee are paid an honorarium of $500 per meeting of the PAC. Presently the PAC meets twice per year, but with uncertainties associated with commissioning a new accelerator and the anticipated interest in the new beams, we plan to shift to a more frequent meeting schedule, meeting every four months.

The other category of consulting provides for laboratory initiated reviews of major experimental devices and for assistance of outstanding experts in addressing problems of accelerator and equipment maintenance and development.

6. Other

a. Electricity: The cost of electricity is the largest single item in this category and will grow rapidly as the K800 cyclotron moves into full scale testing and operation. The largest change will occur between the current year (1985-86) and the first year of the next grant (1986-87), as the K800 cyclotron rf system comes into operation. This system is the largest single electrical load in the laboratory.

Electrical power usage was estimated by examining the power consumption of four groups of equipment. The first two are the rf systems and trim coils of the K500 and K800 cyclotrons. K500 power usage will probably remain

about the same over the next three years, with reduced operating time being compensated by higher energy operation. K800 needs, however, will grow significantly due to the operation of the rf transmitter triad, which at peak operation will draw 1.5 megawatts from the line, and the conventional magnet trim coils which at peak operation will draw 150 kilowatts. The K800 power consumption estimate was made by projecting the changes in duty factor for the rf system, as system testing and the transition to scheduled operation take place over the next several years, and assuming an average power when operating of 1.0 megawatt.

The third major consumer of electrical power is the compressor system required for the helium refrigerators. It is most efficient to keep the superconducting coils constantly cold, and cryogenic capability must therefore be provided essentially 100% of the time, including most maintenance periods. Two compressors will be used to assure continuous operation and still permit a reasonable allowance for scheduled compressor maintenance and unplanned breakdowns. A single large compressor capable of providing the entire projected steady state cryogenic need is predicted to operate 80% of the time and a smaller, less efficient compressor to operate 50% of the time.

The fourth element of electrical power consumption is for pumping for water cooling circuits, electronics for cyclotron and experimental facility control, data acquisition instruments and computers, normal temperature beamline magnets, etc. These miscellaneous needs were assumed to grow at 10% per year for two years reflecting additional operating hours of the beamline systems at higher energies and and then level off as superconducting elements take over most beamline functions. Projected electrical consumption is shown in Table VII.4. This Table also displays expected 1985-86 usage to provide a reference for following years.

In 1978 Michigan State University agreed to provide 2631 MWH per year of electrical power for a fixed fee of $35K per year for a period of 15 years. At the rates expected to hold during the period of this proposal this means that approximately $96.6K worth of power is available for $35K, asubsidy of $61.6K. In addition it should be noted that the academic area power consumption is excluded from all the above figures since it is included as an element of the University overhead expense.

b. Cryogens: During the period of this proposal we will continue to buy helium gas and liquid nitrogen. We project that the quantities needed will increase sightly from the present value, with the gradual increased demand mostly matched by improved utilization procedures. The anticipated costs are $40,000 for helium gas and $110,000 for liquid nitrogen.

c. Computer maintenance: Another large cost item is maintenance of the laboratory computer facility. In the past the Laboratory has contracted with the equipment manufacturers for nearly all maintenance work. Recently these costs have increased sharply due to the addition of additional equipment: the Intergraph automated drafting facility and the FPS-164 high speed processor. This stimulated a search for a more cost effective maintenance method. Our goal is to hold maintenance procurement expenditures approximately constant while improving the current level of availability and accommodating the modest facility expansion described in this proposal.

During the period covered by this proposal we will selectively increase our self maintenance efforts. This follows the pattern which worked very effectively for our previous computer the Σ7; in its later years this facility was operated on a complete in-house maintenance basis. Shifting to self-maintenance will involve training for Laboratory technicians, acquiring a spare parts inventory and purchasing non-inventoried replacement parts as required. Contract maintenance will be continued for items of equipment when the manufacturer's knowledge or resources are essential. This will generally be true for new equipment until it reaches a maturity threshold, and for unique items.

Details of the first year budget are given in Table VII.5.

MSU SUPPORT

MSU support of the operating program consists of providing 80% of the twelve month salaries of the tenure stream faculty involved in the NSCL program and additional support as itemized in Table VII.6.

The University supports a number of members of the MSU technical staff; at present, most of these individuals are involved in the Phase II construction program, but during the latter years of the grant period will

transfer their efforts to the operating program as is noted in Table VII.6. We anticipate that the full amount will be available during the first year of the succeeding operating period. At that point MSU funds will support about 18 members of the technical and administrative staff, the latter including the group that handles the normal university functions of purchasing and accounting that the laboratory has assumed to increase the efficiency of its programs.

For the period November 1, 1986 to October 31, 1987

(SEE INSTRUCTIONS ON REVERSE BEFORE COMPLETING)

SUMMARY PROPOSAL BUDGET

OMB No. 3145-0058
Exp. Date 12/31/88

FOR NSF USE ONLY

ORGANIZATION: National Superconducting Cyclotron Laboratory
Michigan State University, East Lansing, MI 48824

PROPOSAL NO. | DURATION (MONTHS) Proposed | Granted

PRINCIPAL INVESTIGATOR/PROJECT DIRECTOR: H.G. Blosser and S.M. Austin

AWARD NO.

A. SENIOR PERSONNEL: PI/PD, Co-PI's, Faculty and Other Senior Associates (List each separately with title; A.6. show number in brackets)	NSF FUNDED PERSON-MOS. CAL.	ACAD.	SUMR.	FUNDS REQUESTED BY PROPOSER	FUNDS GRANTED BY NSF (IF DIFFERENT)
1. (see sections VIII A and VIII B, plus two to be named)	54			$ 290,500	$
2.					
3.					
4.					
5. 24.5 OTHERS (LIST INDIVIDUALLY ON BUDGET EXPLANATION PAGE)	294			858,600	
6. (29) TOTAL SENIOR PERSONNEL (1-5)	348			1,149,100	
B. OTHER PERSONNEL (SHOW NUMBERS IN BRACKETS) (FTE's shown)					
1. (10) POST DOCTORAL ASSOCIATES	120			240,000	
2. (20) OTHER PROFESSIONALS (TECHNICIAN, PROGRAMMER, ETC.)	240			459,700	
3. 15.5 GRADUATE STUDENTS (at 0.5 FTE per student)				318,400	
4. (10) UNDERGRADUATE STUDENTS FTE				72,900	
5. 4.5) SECRETARIAL-CLERICAL				71,500	
6. (9) OTHER				214,600	
TOTAL SALARIES AND WAGES (A+B)				2,526,300	
C. FRINGE BENEFITS (IF CHARGED AS DIRECT COSTS) (22% except students)				469,700	
TOTAL SALARIES, WAGES AND FRINGE BENEFITS (A+B+C)				2,996,000	
D. PERMANENT EQUIPMENT (LIST ITEM AND DOLLAR AMOUNT FOR EACH ITEM EXCEEDING $1,000:) (see table VI.1)					
TOTAL PERMANENT EQUIPMENT				836,000	
E. TRAVEL 1. DOMESTIC (INCL. CANADA AND U.S. POSSESSIONS) (see table VII.1)				128,300	
2. FOREIGN				0	
F. PARTICIPANT SUPPORT COSTS					
1. STIPENDS $					
2. TRAVEL					
3. SUBSISTENCE					
4. OTHER					
TOTAL PARTICIPANT COSTS					
G. OTHER DIRECT COSTS					
1. MATERIALS AND SUPPLIES (see table VII.2)				413,500	
2. PUBLICATION COSTS/PAGE CHARGES				17,000	
3. CONSULTANT SERVICES (see table VII.3)				31,000	
4. COMPUTER (ADPE) SERVICES (see table VII.5)				275,000	
5. SUBCONTRACTS				0	
6. OTHER (electricity and cryogens) (see table VII.4)				471,000	
TOTAL OTHER DIRECT COSTS				1,207,500	
H. TOTAL DIRECT COSTS (A THROUGH G)				5,167,800	
I. INDIRECT COSTS (SPECIFY) 41% except equipment					
TOTAL INDIRECT COSTS				1,776,000	
J. TOTAL DIRECT AND INDIRECT COSTS (H + I)				6,943,800	
K. RESIDUAL FUNDS (IF FOR FURTHER SUPPORT OF CURRENT PROJECTS GPM 252 AND 253)				0	
L. AMOUNT OF THIS REQUEST (J) OR (J MINUS K) (in 1985-86 dollars)				$ 6,943,800	$

PI/PD TYPED NAME & SIGNATURE*: H.G. Blosser, S.M. Austin — DATE: 3/14/86

INST. REP. TYPED NAME & SIGNATURE*: H. WARD G. GRUER — DATE: 3/14/86

Director Contract and Grant Administration

FOR NSF USE ONLY
INDIRECT COST RATE VERIFICATION
Date Checked | Date of Rate Sheet | Initials - DGC Program

NSF Form 1030 (4-83) *Supersedes All Previous Editions*

*SIGNATURES REQUIRED ONLY FOR REVISED BUDGET (GPM 233)

For the period of November 1, 1987 to October 31, 1988

(SEE INSTRUCTIONS ON REVERSE BEFORE COMPLETING)

SUMMARY PROPOSAL BUDGET

OMB No. 3145-0058
Exp. Date 12/31/88

ORGANIZATION National Superconducting Cyclotron Laboratory Michigan State University, East Lansing, MI 48824				FOR NSF USE ONLY PROPOSAL NO.	DURATION (MONTHS) Proposed	Granted
PRINCIPAL INVESTIGATOR/PROJECT DIRECTOR H. G. Blosser and S. M. Austin				AWARD NO.		
A. SENIOR PERSONNEL: PI/PD, Co-PI's, Faculty and Other Senior Associates (List each separately with title; A.6. show number in brackets)	NSF FUNDED PERSON-MOS. CAL.	ACAD.	SUMR.	FUNDS REQUESTED BY PROPOSER	FUNDS GRANTED BY NSF (IF DIFFERENT)	
1. (see sections VIII A and VIII B, plus two to be named)	54			$ 290,500	$	
2.						
3.						
4.						
5. (27.5) OTHERS (LIST INDIVIDUALLY ON BUDGET EXPLANATION PAGE)	330			963,700		
6. (32) TOTAL SENIOR PERSONNEL (1-5)	384			1,254,200		
B. OTHER PERSONNEL (SHOW NUMBERS IN BRACKETS) (FTE's shown)						
1. 10 POST DOCTORAL ASSOCIATES	120			240,000		
2. 22 OTHER PROFESSIONALS (TECHNICIAN, PROGRAMMER, ETC.)	264			505,700		
3. 16 GRADUATE STUDENTS (at 0.5 FTE per student)				328,700		
4. 10 UNDERGRADUATE STUDENTS FTE				72,900		
5. 4.9 SECRETARIAL-CLERICAL				71,500		
6. 13 OTHER				310,000		
TOTAL SALARIES AND WAGES (A+B)				2,783,000		
C. FRINGE BENEFITS (IF CHARGED AS DIRECT COSTS) (22% except students)				523,900		
TOTAL SALARIES, WAGES AND FRINGE BENEFITS (A+B+C)				3,307,000		
D. PERMANENT EQUIPMENT (LIST ITEM AND DOLLAR AMOUNT FOR EACH ITEM EXCEEDING $1,000:) (see table VI.2)						
TOTAL PERMANENT EQUIPMENT				770,000		
E. TRAVEL 1. DOMESTIC (INCL. CANADA AND U.S. POSSESSIONS)				137,400		
2. FOREIGN				0		
F. PARTICIPANT SUPPORT COSTS 1. STIPENDS $ 2. TRAVEL 3. SUBSISTENCE 4. OTHER						
TOTAL PARTICIPANT COSTS						
G. OTHER DIRECT COSTS						
1. MATERIALS AND SUPPLIES				460,400		
2. PUBLICATION COSTS/PAGE CHARGES				18,000		
3. CONSULTANT SERVICES				31,000		
4. COMPUTER (ADPE) SERVICES				225,000		
5. SUBCONTRACTS				0		
6. OTHER (electricity & cryogens)				535,000		
TOTAL OTHER DIRECT COSTS				1,269,400		
H. TOTAL DIRECT COSTS (A THROUGH G)				5,483,800		
I. INDIRECT COSTS (SPECIFY) 41% except equipment						
TOTAL INDIRECT COSTS				1,932,600		
J. TOTAL DIRECT AND INDIRECT COSTS (H + I)				7,416,400		
K. RESIDUAL FUNDS (IF FOR FURTHER SUPPORT OF CURRENT PROJECTS GPM 252 AND 253)				0		
L. AMOUNT OF THIS REQUEST (J) OR (J MINUS K) (in 1985-86 dollars)				$7,416,400	$	

PI/PD TYPED NAME & SIGNATURE* H.G. Blosser, S.M. Austin S M Austin	DATE 3/14/86	FOR NSF USE ONLY INDIRECT COST RATE VERIFICATION	
INST. REP. TYPED NAME & SIGNATURE* H. Blosser Howard G. Grider	DATE 3/14/86	Date Checked / Date of Rate Sheet / Initials - DGC / Program	

NSF Form 1030 (4-83) *Supersedes All Previous Editions*

*SIGNATURES REQUIRED ONLY FOR REVISED BUDGET (GPM 233)

HOWARD G. GRIDER
Director Contract and Grant Administration

For the period November 1, 1988 to October 31, 1989

(SEE INSTRUCTIONS ON REVERSE BEFORE COMPLETING)

SUMMARY PROPOSAL BUDGET

OMB No. 3145-0058
Exp. Date 12/31/88

FOR NSF USE ONLY

ORGANIZATION: National Superconducting Cyclotron Laboratory
Michigan State University, East Lansing, MI 48840

PROPOSAL NO.

DURATION (MONTHS): Proposed | Granted

PRINCIPAL INVESTIGATOR/PROJECT DIRECTOR: H. G. Blosser and S. M. Austin

AWARD NO.

A. SENIOR PERSONNEL: PI/PD, Co-PI's, Faculty and Other Senior Associates (List each separately with title; A.6. show number in brackets)	NSF FUNDED PERSON-MOS. CAL.	ACAD.	SUMR.	FUNDS REQUESTED BY PROPOSER	FUNDS GRANTED BY NSF (IF DIFFERENT)
1. (see sections VIII A and VIII B, plus two to be named)	54			$ 290,500	$
2.					
3.					
4.					
5. 30.5 OTHERS (LIST INDIVIDUALLY ON BUDGET EXPLANATION PAGE)	366			1,068,900	
6. (35) TOTAL SENIOR PERSONNEL (1-5)	420			1,359,400	
B. OTHER PERSONNEL (SHOW NUMBERS IN BRACKETS) (FTE's shown)					
1. (10) POST DOCTORAL ASSOCIATES	120			240,000	
2. (23) OTHER PROFESSIONALS (TECHNICIAN, PROGRAMMER, ETC.)	276			528,700	
3. 16.5 GRADUATE STUDENTS (at 0.5 FTE per student)				338,900	
4. (10) UNDERGRADUATE STUDENTS FTE				72,900	
5. (6) SECRETARIAL-CLERICAL				95,300	
6. (17) OTHER				405,400	
TOTAL SALARIES AND WAGES (A+B)				3,040,700	
C. FRINGE BENEFITS (IF CHARGED AS DIRECT COSTS) (22% except students)				578,300	
TOTAL SALARIES, WAGES AND FRINGE BENEFITS (A+B+C)				3,619,000	
D. PERMANENT EQUIPMENT (LIST ITEM AND DOLLAR AMOUNT FOR EACH ITEM EXCEEDING $1,000:) (see table VI.2) including special item 500,000					
TOTAL PERMANENT EQUIPMENT				990,000	
E. TRAVEL 1. DOMESTIC (INCL. CANADA AND U.S. POSSESSIONS)				146,500	
2. FOREIGN					
F. PARTICIPANT SUPPORT COSTS					
1. STIPENDS $					
2. TRAVEL					
3. SUBSISTENCE					
4. OTHER					
TOTAL PARTICIPANT COSTS					
G. OTHER DIRECT COSTS					
1. MATERIALS AND SUPPLIES				507,400	
2. PUBLICATION COSTS/PAGE CHARGES				19,000	
3. CONSULTANT SERVICES				31,000	
4. COMPUTER (ADPE) SERVICES				250,000	
5. SUBCONTRACTS				0	
6. OTHER (electricity & Cryogens)				553,000	
TOTAL OTHER DIRECT COSTS				1,360,400	
H. TOTAL DIRECT COSTS (A THROUGH G)				6,115,900	
I. INDIRECT COSTS (SPECIFY)					
TOTAL INDIRECT COSTS 41% except equipment				2,101,600	
J. TOTAL DIRECT AND INDIRECT COSTS (H + I)				8,217,500	
K. RESIDUAL FUNDS (IF FOR FURTHER SUPPORT OF CURRENT PROJECTS GPM 252 AND 253)				0	
L. AMOUNT OF THIS REQUEST (J) OR (J MINUS K) (in 1985-86 dollars)				$8,217,500	$

PI/PD TYPED NAME & SIGNATURE*: H.G. Blosser, S.M. Austin — DATE: 3/14/86

INSTITUTIONAL REP. TYPED NAME & SIGNATURE*: H. G. Blosser, Director Contract and Grant Administration — DATE: 3/14/86

FOR NSF USE ONLY
INDIRECT COST RATE VERIFICATION
Date Checked | Date of Rate Sheet | Initials - OGC Program

NSF Form 1030 (4-83) Supersedes All Previous Editions

H. G. BLOSSER II—16
Director Contract and Grant Administration

*SIGNATURES REQUIRED ONLY FOR REVISED BUDGET (GPM 233)

For the period November 1, 1986 to October 31, 1989

(SEE INSTRUCTIONS ON REVERSE BEFORE COMPLETING)

SUMMARY PROPOSAL BUDGET

OMB No. 3145-0058
Exp. Date 12/31/88

FOR NSF USE ONLY

PROPOSAL NO. | DURATION (MONTHS) Proposed | Granted

AWARD NO.

ORGANIZATION: National Superconducting Cyclotron Laboratory
Michigan State University, East Lansing, MI 48824

PRINCIPAL INVESTIGATOR/PROJECT DIRECTOR: H.G. Blosser and S.M. Austin

A. SENIOR PERSONNEL: PI/PD, Co-PI's, Faculty and Other Senior Associates (List each separately with title; A.6. show number in brackets)	NSF FUNDED PERSON-MOS. CAL.	ACAD	SUMR	FUNDS REQUESTED BY PROPOSER	FUNDS GRANTED BY NSF (IF DIFFERENT)
1. (see sections VIII A and VIII B, plus two to be named)	162			$ 871,500	$
2.					
3.					
4.					
5. ( ) OTHERS (LIST INDIVIDUALLY ON BUDGET EXPLANATION PAGE)	990			2,891,300	
6. ( ) TOTAL SENIOR PERSONNEL (1-5)	1152			3,762,800	
B. OTHER PERSONNEL (SHOW NUMBERS IN BRACKETS)					
1. ( ) POST DOCTORAL ASSOCIATES	360			720,000	
2. ( ) OTHER PROFESSIONALS (TECHNICIAN, PROGRAMMER, ETC.)	780			1,494,200	
3. ( ) GRADUATE STUDENTS				986,000	
4. ( ) UNDERGRADUATE STUDENTS				218,700	
5. ( ) SECRETARIAL-CLERICAL				238,300	
6. ( ) OTHER				930,100	
TOTAL SALARIES AND WAGES (A+B)				8,351,100	
C. FRINGE BENEFITS (IF CHARGED AS DIRECT COSTS) (22% except students)				1,571,900	
TOTAL SALARIES, WAGES AND FRINGE BENEFITS (A+B+C)				9,922,000	
D. PERMANENT EQUIPMENT (LIST ITEM AND DOLLAR AMOUNT FOR EACH ITEM EXCEEDING $1,000:) (see tables VI.1 and VI.2)					
TOTAL PERMANENT EQUIPMENT				2,596,000	
E. TRAVEL 1. DOMESTIC (INCL. CANADA AND U.S. POSSESSIONS)				412,200	
2. FOREIGN				0	
F. PARTICIPANT SUPPORT COSTS					
1. STIPENDS $					
2. TRAVEL					
3. SUBSISTENCE					
4. OTHER					
TOTAL PARTICIPANT COSTS					
G. OTHER DIRECT COSTS					
1. MATERIALS AND SUPPLIES				1,381,300	
2. PUBLICATION COSTS/PAGE CHARGES				54,000	
3. CONSULTANT SERVICES				93,000	
4. COMPUTER (ADPE) SERVICES				750,000	
5. SUBCONTRACTS				0	
6. OTHER (electricity & cryogens)				1,559,000	
TOTAL OTHER DIRECT COSTS				3,837,300	
H. TOTAL DIRECT COSTS (A THROUGH G)				16,787,500	
I. INDIRECT COSTS (SPECIFY) 41% except equipment					
TOTAL INDIRECT COSTS				5,810,200	
J. TOTAL DIRECT AND INDIRECT COSTS (H + I)				22,577,700	
K. RESIDUAL FUNDS (IF FOR FURTHER SUPPORT OF CURRENT PROJECTS GPM 252 AND 253)				0	
L. AMOUNT OF THIS REQUEST (J) OR (J MINUS K) (in 1985-86 dollars)				22,577,700	$

PI/PD TYPED NAME & SIGNATURE*: H.G. Blosser, S.M. Austin — DATE: 3/14/86

INST. REP. TYPED NAME & SIGNATURE*: — DATE: 3/14/86

Director Contract and Grant Administration

FOR NSF USE ONLY
INDIRECT COST RATE VERIFICATION
Date Checked | Date of Rate Sheet | Initials - DGC Program

*SIGNATURES REQUIRED ONLY FOR REVISED BUDGET (GPM 233)

NSF Form 1030 (4-83) Supersedes All Previous Editions

BUDGET EXPLANATION PAGES

This page contains additional detail for some items of the Summary Budget Sheets. In addition, there is a discussion of the mechanism used to account for inflation and enumeration of the inflation-corrected budgets.

BUDGET ITEMS We collect here Tables giving detail of the items from the summary budget.

D. Permanent Equipment: See Tables VI.1 and VI.2.

E. Travel

Table VII.1. 1986-87 Travel Expenses

ACTIVITY	COST(K$)
Program Advisory Committee	$ 9.2
Executive Committee	3.4
Recruiting	6.0
Seminar Speakers and Visitors	10.0
User Experiments	32.0
NSF visits, Government Panels etc.	5.5
Individual Scientists	55.0
Training, Vendor, etc.	7.2
TOTAL	$128.3

G. Other Direct Costs.

Table VII.2. Materials and Supplies

ITEM	COST(K$)
Cyclotron Maintenance	$ 55.0
Beamline Maintenance	10.0
Vacuum Systems Maintenance	40.0
Experimental Apparatus Maintenance	15.0
Electronics Maintenance	12.5
Cryogenic Refrigerator Maintenance	20.0
Radiation Safety Supplies	6.5
Machine Shop Supplies and Tools	8.0
Welding Shop Supplies	4.0
Electrical Supplies	5.5
Standard Assembly Parts	10.0
Library	5.0
User Magnetic Tapes	20.0
Graphic Supplies and Services	6.0
Drafting Supplies	11.5
Computer Supplies	12.0
Messenger Van	2.5
Office Supplies	17.0
Postage	20.0
Telephone	55.0
Office Services	25.0
Building	20.0
Detectors	25.0
Miscellaneous Supplies	8.0
TOTAL	$413.5

Table VII.3. Consultant Services

CATEGORY	COST(K$)
Program Advisory Committee	$ 7.5
Cryogenics	5.0
Vacuum	2.0
RF	2.0
Equipment R&D	10.0
Nuclear Science	3.0
Management	1.5
TOTAL	$31.0

Table VII.4. Electrical Consumption Projection

CATEGORY	1985-86	1986-87	1987-88	1988-89
K500 (MWH)	1320	1320	1320	1320
K800 (MWH)	700	3970	5500	6000
Compressors (MWH)	2110	2980	2980	2980
Misc. (MWH)	1950	2140	2360	2360
Total (MWH)	6080	10410	12160	12660
Total (K$ @$36.70/MWH)	223.2	382.1	446.3	464.6
MSU Subsidy	61.6	61.6	61.6	61.6
NSF Cost	161.7	320.6	384.7	403.1

Table VII.5 1986-87 Computer Maintenance

EQUIPMENT	COST(K$)
Analysis VAX 11/750 ($17.0)	$ 5.0
Test VAX 11/750 ($17.5)	5.0
Data #1 VAX 11/750	13.1
Data #2 VAX 11/750	16.6
General Use VAX 11/780	33.3
Micro-vax	1.9
Intergraph CAD System	73.7
FPS-164 High Speed Processor	33.5
Tape and Disk Drives	16.7
Non-contract Hardware Maintenance	23.0
Software Maintenance	13.2
Initial Maintenance Parts & Training	40.0
TOTAL	$275.0

Table VII.6. MSU Contribution to NSCL Operating Effort

ITEM	86-87		87-88		88-89		89-90	
	FTE	K$	FTE	K$	FTE	K$	FTE	K$
Purchasing/Acc'ting								
Professional	1.0	23.0	1.0	23.0	2.0	46.0	2.0	46.0
Secretarial	1.0	15.9	2.0	31.8	2.5	39.7	3.0	47.7
Technical								
Professional	0.0	0.0	4.0	92.0	9.0	207.0	13.0	299.0
Salary Total		38.9		146.8		292.7		392.7
Total Salary + Fringes		47.4		179.1		357.1		479.1
Electricity		61.6		61.6		61.6		61.6
Total Direct Costs		109.0		240.7		418.7		540.7
Indirect Costs		44.7		98.7		171.7		221.7
Total		153.7		339.4		590.4		762.4

TOTAL BUDGETS CORRECTED FOR INFLATION

For ease of understanding and interpretation, all budgets, including the Summary Budgets have been presented in 1985-86 dollars. Of course the effects of inflation must be dealt with and in this section we do so. For this purpose we have chosen to use the DOE inflators of October 1985. Over the three year term of the budget, these inflators predict an increase averaging about 5.6% per year which seems a reasonable estimate. The precise values are give in Table VII.7.

Table VII.7. Total budgets after accounting for inflation.

Year	Budget (1985-86 K$)	Inflation Factor	Budget(Current K$)
1986-87	6943.8	(5%)	7291.0
1987-88	7416.4	(5%)(5.8%)	8238.8
1988-89	8217.5	(5%)(5.8%)(6.1%)	9685.9

TOTAL REQUESTED AMOUNT: $25,215,700

VIII. NSCL STAFF

This section lists the senior members of the NSCL staff, including those supported by the NSCL Operating Grant, the Phase II Construction Grant and MSU funds. The Nuclear Science staff includes faculty members appointed in the tenure stream in the Departments of Physics and Chemistry and the NSCL, as well as four NSCL Continuing Appointment Faculty. The Professional Staff includes those appointed in the NSCL Continuing Appointment system and the MSU Specialist system. The group affiliations of the professional staff are noted following the key at the end of this section.

A. Nuclear Science Staff:

Physics, Chemistry and NSCL Faculty

*# Sam M. Austin, Professor, Ph.D., 1960, Wisconsin

*# Henry G. Blosser, Professor, Ph.D., 1954, Virginia

*Walter Benenson, Professor, Ph.D., 1962, Wisconsin

Boyd Alex Brown, Assoc. Professor (NSCL), Ph.D., 1974, Stony Brook

* Gerard M. Crawley, Professor, Ph.D., 1965, Princeton

* Aaron I. Galonsky, Professor, Ph.D., 1954, Wisconsin

* Claus Konrad Gelbke, Professor, Ph.D., 1972, Heidelberg

* Morton M. Gordon, Professor, Ph.D., 1950, Washington University

Leigh Harwood, Asst. Professor (NSCL), Ph.D., 1978, Florida State

* Edwin Kashy, Professor, Ph.D., 1959, Rice

William G. Lynch, Asst. Professor, Ph.D., 1980, Washington

Michael Maier, Assoc. Professor (NSCL), Ph.D., 1970, Munich

* William C. McHarris, Professor, Ph.D., 1965, Berkeley

David Morrissey, Asst. Professor, Ph.D., 1978, Berkeley

* Jerry A. Nolen, Professor, Ph.D., 1965, Princeton

* David K. Scott, Hannah Distinguished Professor, D.Phil., 1967, Oxford

John D. Stevenson, Asst. Professor, Ph.D., 1977, Berkeley

Gary Westfall, Assoc. Professor (NSCL), Ph.D., 1975, Texas

To be named: tenure stream professor(Physics)

To be named: tenure stream professor(Physics)

Staff Physicists

Narayanaswami Anantaraman (LP), Ph.D., 1973, Chicago

Richard Blue (LP), Ph.D., 1963, Wisconsin

Ronald Fox (C), M.S., 1981, Illinois

David Johnson (A), B.S., 1964, MSU

Helmut Laumer (O), Ph.D., 1971, MSU

Felix Marti (A), Ph.D., 1977, MSU

Reginald Ronningen (LP), Ph.D., 1975, Vanderbilt

John Yurkon (F), M.S., 1979, MSU

Senior Physicists

* Richard Au (C, E, Head), B.A., 1965, MSU

Paul Koblas (E), Ph.D., 1971, Oregon

* Peter Miller (O, Head), Ph.D., 1969, Princeton

Engineers

Lynn Foth (C), M.S., 1979, Michigan

Thomas Jones (E), B.S., 1981, MSU

John Kuchar (D), B.S., 1970, MSU

Christopher Magsig (F), B.S., 1984, Western Michigan

Albert McGilvra (E), B.S., 1983, Michigan

Leonard Morris (D), M.A., 1975, Western

James Moskalik (D), B.S., 1967, Western Michigan

William Nurnberger (E), M.S., 1967, Michigan

Staff Engineers

Jon DeKamp (F), B.S., 1982, MSU

John Vincent (E), B.S., 1983, MSU

IX. CURRENT AND PENDING GRANT SUPPORT

	Source	Title	Amount	Period	Location
I. PRINCIPAL INVESTIGATORS					
A. CURRENT SUPPORT					
AUSTIN, S.	NSF	1	$5,450,000	11/1/85-10/31/86	NSCL
	NSF	2	480,000	12/1/84-5/31/86	NSCL
	NSF	3	3,000,000	5/24/85-3/31/86	NSCL
BLOSSER, H.	NSF	1			
	NSF	2			
	NSF	3			NSCL
	HG	10	707,565	10/84-10/86	NSCL
B. PROPOSALS PENDING					
AUSTIN, S.	NSF	1a			NSCL
BLOSSER, H.	NSF	1a			
II. CO-PRINCIPAL INVESTIGATORS AND FACULTY ASSOCIATES					
A. CURRENT SUPPORT					
AU, R.	NSF	1			
BENENSON, W.	NSF	1			
BROWN, B.A.	NSF	1			
CRAWLEY, G.	NSF	1			
	NSF	4	17,450	9/15/85-2/29/88	NSCL/Argentina
	NSF	8	17,450	2/1/86-6/30/88	NSCL/Brazil
GALONSKY,A.	NSF	1			
	NSF	9	59,236	6/1/81-11/30/86	NSCL/Hungary
GELBKE, C.	NSF	1			
	NSF	5	46,000	4/1/84-3/31/87	NSCL/Grenoble/Caen (GANIL)
HARWOOD, L.	NSF	1			
GORDON, M.	NSF	1			
KASHY, E.	NSF	1			
LYNCH, WM.	NSF	1			
	NSF	6	25,000	5/1/85-5/1/86	NSCL
MAIER, M.	NSF	1			
MCHARRIS, WM.	NSF	1			
MILLER, P.	NSF	1			
MORRISSEY, D.	NSF	1			
NOLEN, J.	NSF	1			
SCOTT, D.	NSF	1			
	NSF	5			
STEVENSON,J.	NSF	1			
WESTFALL, G.	NSF	1			
B. PROPOSALS PENDING					
AU, R.	NSF	1a			
BENENSON,W.	NSF	1a			
BROWN, B.A.	NSF	1a			
CRAWLEY,G.	NSF	1a			
GALONSKY,A.	NSF	1a			
GELBKE,C.	NSF	1a			
	NSF	7	205,500	3/86-3/88	NSCL
GORDON, M.	NSF	1a			
HARWOOD, L.	NSF	1a			
KASHY, E.	NSF	1a			
LYNCH, WM.	NSF	1a			
	NSF	7	205,500	3/86-3/88	NSCL
MAIER, M.	NSF	1a			
MCHARRIS, WM.	NSF	1a			
MILLER, P.	NSF	1a			
MORRISSEY, D.	NSF	1a			
NOLEN, J.	NSF	1a			
SCOTT, D.	NSF	1a			
STEVENSON,J.	NSF	1a			
WESTFALL, G.	NSF	1a			

1) Cooperative Agreement, Operation of the National Superconducting Cyclotron Laboratory and an Associated Research Program (Physics)
1a) This proposal, NSCL Operating Proposal
2) Acquisition of a Nuclear Physics High Speed Computing Facility
3) Construction of a National Facility for Research with Heavy Ions Using Coupled Superconducting Cyclotrons
4) U.S.-Argentina Cooperative Research Nuclear Structure and Energy Dependence of Heavy Ion Reaction Mechanics
5) Heavy Ion Induced Reaction at Intermediate Energies Research at Grenoble & Caen.
6) President Young Investigator Award
7) High Resolution Hodoscope for the Measurement of Particle Correlations at Small Relative Momenta.
8) Energy Dependence of Heavy Ion Reaction Mechanics, U.S.-Latin American Cooperative Science Program (Brazil).
9) The Study of Neutron and Gamma-Ray Emission in Strongly-Damped Heavy-Ion Collisions, U.S.-Hungary Cooperative Science Program
10) Construction of Superconducting Cyclotron System for the Radiation Oncology Center of Harper Grace Hospitals.